UMTRI-2001-10

DEVELOPMENT AND REFINEMENT OF ABDOMINAL-RESPONSE CORRIDORS

FINAL REPORT

Project D2a
Development of a Reusable, Rate-Sensitive Abdomen

Warren N. Hardy
Lawrence W. Schneider

University of Michigan
Transportation Research Institute
Biosciences Division
2901 Baxter Road
Ann Arbor, MI 48109-2150

Submitted to
General Motors Corporation
Warren, Michigan

July 2001

Technical Report Documentation Page

1. Report No.	2. Government Accession No.	3. Recipient's Catalog No.

4. Title and Subtitle	5. Report Date
DEVELOPMENT AND REFINEMENT OF ABDOMINAL - RESPONSE CORRIDORS, Project D2a - Development of a Reusable, Rate-Sensitive Abdomen[1]	July 2001
	6. Performing Organization Code

7. Author(s)	8. Performing Organization Report No.
Warren N. Hardy and Lawrence W. Schneider	UMTRI-2001-10

9. Performing Organization Name and Address	10. Work Unit no. (TRAIS)
University of Michigan Transportation Research Institute 2901 Baxter Road Ann Arbor, Michigan 48109-2150 U.S.A.	11. Contract or Grant No.

12. Sponsoring Agency Name and Address	13. Type of Report and Period Covered
General Motors Corporation 30500 Mound Rd. Warren, MI 48090-9055	Final Report
	14. Sponsoring Agency Code

15. Supplementary Notes

[1]The work covered by this report was financed by General Motors (GM) pursuant to an agreement with the U.S. Department of Transportation.

16. Abstract

This study was conducted in support of the development of a new, reusable, biofidelic abdomen for the Hybrid III ATD in Project D2b. The goals were to resolve discrepancies and fill in some of the gaps with regard to the biomechanical response of the human abdomen to dynamic loading in the automotive environment. Three types of impact tests were conducted. Following a review and reanalysis of the data in the literature on abdominal impact response, rigid-bar tests were performed into the mid and upper abdomen of unembalmed instrumented human cadavers using different impactor speeds. Most tests were conducted using a free-back condition, but several tests were conducted using a fixed-back condition to examine the effects of body mass and spinal flexion on the response. Force-deflection corridors were developed and compared to those previously established by other researchers. The second type of test involved dynamic belt loading of the unembalmed cadaver abdomen at the lower and midabdomen regions. The results were used to establish new abdominal force-deflection corridors for belt loading. The third type of test conducted involved static deployment of passenger frontal-impact airbags into the closely positioned abdomen. Three airbag tests were conducted using three unembalmed cadavers. The deflection-time histories were used to guide the development of a repeatable high-speed surrogate airbag loading device that uses a low-mass cylinder to simulate close-proximity passenger airbag loading of the abdomen. This device was used to conduct out-of-position, airbag-loading tests into the cadaver abdomen and to develop force-deflection corridors for this type of abdomen loading.

17. Key Words	18. Distribution Statement
Abdominal response, ATD, Crash dummy, Impact response, Response corridors, Belt loading, Airbag loading	Unlimited

19. Security Classification (of this report)	20. Security Classi. (of this page)	21. No. of Pages	22. Price
None	None	88	

ACKNOWLEDGMENTS

This research was sponsored by the General Motors Corporation (GM) pursuant to an agreement between GM and the U.S. Department of Transportation. The authors are thankful for the opportunity and support provided for this project.

This work was conducted by the University of Michigan Transportation Research Institute, Biosciences Division, and was carried out in accordance with the practices outlined by the Anatomical Donations Program of the University of Michigan Medical School. Necropsy assistance and pathology analysis were provided by Dr. Kanu Virani, consulting forensic pathologist.

Thanks are also extended to members of the Biosciences Division: Brian Eby and James Whitley for fixture fabrication assistance, Thomas Jeffreys for specimen preparation assistance, Stewart Simonett for instrumentation assistance, Anthony King for data processing assistance, and to Leda Ricci for assistance in coordinating project activities.

CONTENTS

LIST OF TABLES

LIST OF FIGURES

INTRODUCTION AND OBJECTIVES

1.1 BACKGROUND

1.1.1 Rigid-Bar Loading

Review of Existing Rigid-Bar Loading Data

A review of the literature disclosed a number of discrepancies within the existing body of abdominal response data pertaining to rigid-bar impacts. The primary conflicts concern rate effects, loading response shape, and hysteresis characteristics. A reanalysis of the existing data provided possible explanations for some of these differences and helped guide the direction of this research effort. Four previous studies were of greatest interest: Cavanaugh et al. (1986), Nusholtz et al. (1994), Viano et al. (1989), and Stalnaker et al. (1985). Many aspects of these studies are summarized in SAE J1460-1 (1995).

Cavanaugh et al. (1986) conducted abdominal impacts using a 2.5-cm-diameter rigid bar attached to 31.5-kg and 63.5-kg linear impactors. Twelve unembalmed, repressurized human cadavers were tested in a free-back seated posture. The average specimen age, mass, and stature were 54.7 years, 70.3 kg, and 167 cm, respectively. The impacts were performed in two speed ranges, averaging 6.1 and 10.4 m/s, at the level of the third lumbar vertebra. Equal-stress/equal-velocity scaling was applied to the data. Stiffness was found to be proportional to impactor speed and mass, suggesting rate sensitivity of the response. Loading was found to be a simple ramping function while unloading was essentially a vertical line. Peak abdomen deflection occurred at approximately 66-percent compression. It was remarked that the results were heavily influenced by the scaling techniques.

Nusholtz et al. (1994) conducted impacts using an angled semicircular rigid-tube attached to an 18-kg pendulum. Six unembalmed, repressurized human cadavers were tested in a free-back seated posture. The average specimen age, mass, and stature were 54.4 years, 58.3 kg, and 172 cm, respectively. Impacts were performed in two speed ranges, averaging 6.0 and 10.0 m/s, at the level of the second lumbar vertebra. No scaling technique was applied, and no rate sensitivity was found. It was remarked that small sample size, biovariability, low pendulum mass, and multidimensional loading influenced the results.

Viano et al. (1989) conducted impacts using a 15.2-cm-diameter rigid-disk attached to a 23.4-kg pendulum. Unembalmed, repressurized human cadavers were tested in a free-back suspended posture (seated with arms above the head). Sixteen thoracic, fourteen abdominal (7.5 cm below the xiphoid), and fourteen pelvic tests were performed, with some cadavers being used in multiple tests. The average specimen age was 53.8 years and the average mass was 67.2 kg. Abdominal impacts in three speed ranges, averaging 4.5, 6.7, and 9.4 m/s were performed thirty degrees to the right or left of the midline through the center of gravity of the specimen. Equal-stress/equal-velocity scaling was applied to the data, which were also renormalized for velocity. A force plateau followed the initial stiffness response in these tests, and the unloading response suggested action of restorative forces, which contrasts the sudden unloading reported by Cavanaugh et al. (1986).

Stalnaker et al. (1985) compiled and analyzed data from three earlier studies. These studies included sixteen frontal impacts conducted by Beckman et al. (1971), seventeen right- and left-side impacts conducted by Stalnaker et al. (1971), and two side and seven frontal impacts conducted by Trollope et al. (1973). Typical specimens included vervets, rhesus monkeys, baboons, and squirrel monkeys ranging from 0.53 kg to 19.40 kg. The tests used rigid-bar impactors (1.27-, 2.54-, and 5.80-cm-diameter bars), and wedge-shaped impactors (5.72- x 7.62-cm and 7.62- x 7.62-cm face wedges). The primates were positioned in a free-back seated posture for upper, middle, and lower abdomen tests. The impact speeds ranged from 8.4 to 17.0 m/s. The force-deflection data were described in terms of a three-stage rise-plateau-rise response, which differs from the results of all other studies. Analysis of the data relied upon linear velocity scaling, and averaging of the data to approximate a human response. The averaging of the data assumed that there were no differences between species, impact region, direction, or pendulum shape.

The combined results of these studies leave many questions regarding abdominal response to impact loading unanswered. The Cavanaugh data strongly suggest the presence of rate effects, while the Nusholtz data do not show a rate effect. The loading-phase response of the Viano data is different from that of the Stalnaker data, which is different from both the Cavanaugh and Nusholtz datasets. The Viano data are characterized by a hysteresis response that suggests some restorative force, while other data suggest a rapid unloading of the abdomen with no restorative response (i.e., more energy absorption). In addition, impactor mass, impact location, impact direction, impactor shape, and subject species varied significantly between these different studies.

Reanalysis of Existing Rigid-Bar Loading Data

The existing body of rigid-bar abdominal-impact data was reanalyzed by first digitizing the published results of the referenced authors' investigations. For simplicity, only eight points were taken from each curve for this analysis. Several techniques were employed to bring the existing data to a common basis so that meaningful comparisons could be made. The Nusholtz cadaver data were split into high- and low-speed corridors, and equal-stress/equal-velocity scaling was applied. The Viano cadaver data were averaged within the 6.7- and 9.4-m/s ranges to yield two mean curves.

Because the Cavanaugh tests were limited to the midabdomen, the upper abdomen tests were eliminated from the Stalnaker primate data. Of the remaining tests, those conducted at 10 m/s, +/- 1.5 m/s were selected for analysis (seven tests). Again, equal-stress/equal-velocity scaling was applied. The data were averaged across all species to obtain the "human" response. Squirrel monkeys accounted for much of the data. The prescribed three loading-phase stages were generated using 9.6-percent and 27-percent compression break points, and the data were normalized to an abdominal depth of 289 mm. Velocity scaling was used to generate a 6-m/s curve.

The Cavanaugh corridors were plotted to overlay the other reanalyzed datasets. The response of the frangible abdomen of Rouhana et al. (1990) was also plotted against the midspeed corridor data. Figure 1a shows a comparison of the 10-m/s Cavanaugh corridor and reanalyzed data. Only the loading phases of these datasets are plotted. Although there are discrepancies within the data in terms of curve shape, there seems to be general agreement in terms of rate of loading. Figure 1b shows a comparison of the 6-m/s Cavanaugh corridor to the reanalyzed data sets. This shows discrepancies within the data in terms of curve shape and loading rate. With the exception of the Rouhana data, only the loading phases of these data are plotted.

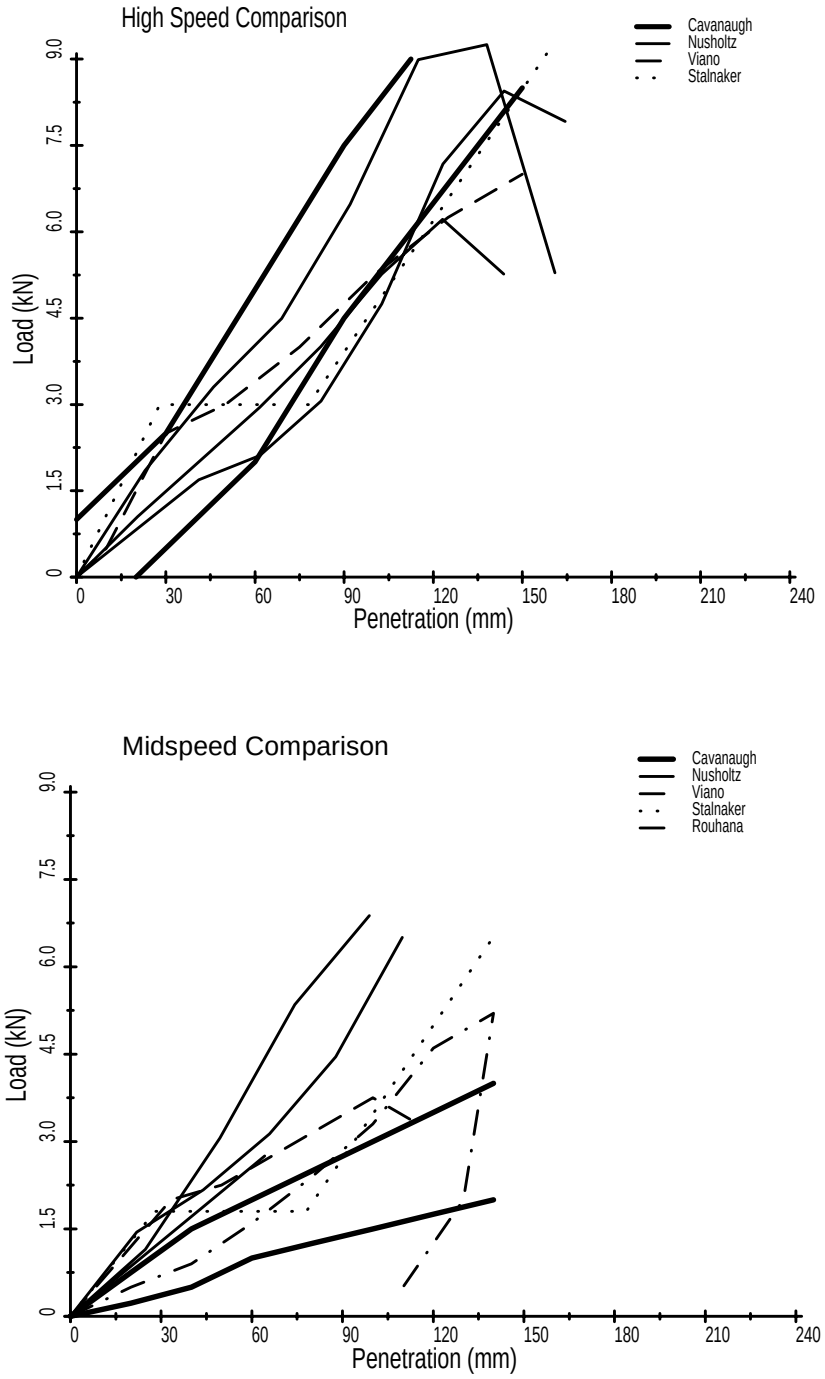

FIGURE 1. Reanalysis of existing rigid-bar abdominal impact data: High-speed data (10 m/s) showing reasonable agreement between studies (a); Midspeed data (6 m/s) showing differences in stiffness between the various studies (b). The Cavanaugh data suggest rate dependence, while the other data do not.

Reanalysis of the existing data suggested that observed rate effects, whether of a viscous or mass-recruitment nature, are dependent upon the relative impactor/subject masses involved. If the impactor mass is relatively small compared to the effective mass of the struck region of the subject, the response of the subject may not be indicative of the response that would be observed in an actual crash event. It is thought that because the impactor used in the Nusholtz tests was relatively low in mass and the impactor used in the Cavanaugh tests was of relatively high mass, the Nusholtz data do not show rate effects whereas the Cavanaugh data do show these effects.

Differences in the type of loading-phase response probably depend on impactor shape. Both the Nusholtz and Cavanaugh data resulted from tests using a round rigid-bar impactor, and the loading-phase responses are very similar ramp functions. The rigid-disk impacts conducted by Viano produced an initially steep loading followed by a plateau. This is probably due to the much larger impactor surface area involved in the tests, as compared to the Nusholtz or Cavanaugh tests. It is also possible that the wedge-shaped impactors used by Stalnaker contributed to the three-stage, rise-plateau-rise response, which also differs from the Nusholtz and Cavanaugh data. However, this three-stage response could also have been influenced by relative impactor/subject mass, inertial effects, and impact location.

Differences in hysteresis may depend on impact location. The Viano data exhibit a reduction in penetration as unloading occurs, while the other datasets suggest a rapid unloading of the abdomen with little rebound in abdominal penetration. The region of impact and the size of the impactor resulted in rib involvement in the Viano tests. This rib involvement may have contributed to restorative forces, which produced a return toward original specimen depth. The abdomen is rather incapable of providing this type of restorative force.

1.1.2 Belt Loading

Another goal of this study was to provide data on the response of the human cadaver abdomen to belt loading. Previous research efforts have used swine and swine cadaver models to gain insight into this area. Rouhana et al. (1989 and 1990) conducted fifteen impacts on swine cadavers using a controlled-stroke MTS machine. A yoke fixture was used to drive 50-mm seatbelt webbing into the abdomens of the swine cadavers using speeds of 0.2 m/s to 5.3 m/s at the level of L4. The swine cadavers averaged 43.6 kg, and were tested in a supine posture with the back supported. The belt material was initially in contact with the anterior of the abdomen, but did not wrap around the sides of the abdomen. Actuator force and deflection were measured, as was belt stretch.

The data from a study conducted by Miller et al. (1989) were also reviewed. This included results from twenty-five belt-loading tests to the abdomens of anesthetized swine averaging 46.1 kg. The loading was a haversine displacement-time (velocity-time) function. The data were separated into 3.7- and 6.3-m/s groups and normalized. Average abdomen stiffness in response to the belt loading was found to be 30 kN/m, and peak compression ranged between 6 and 70 percent. The load-penetration responses were characterized by a slightly convex ramp (occasionally concave), followed by an essentially vertical unloading. The swine cadaver and anesthetized swine data were compared to examine the scaling possibilities between human cadavers and living humans. The viscous response was touted as being applicable to loading rates between 3 and 30 m/s, while compression was a good injury predictor for rates below 3 m/s.

Rouhana's analysis of the swine data and available human data was used in the design of a frangible abdomen for use in the Hybrid III dummy. The frangible abdomen is a notched closed-cell foam insert. The notches are cut in a repeating triangular pattern such that the foam widens with increased abdominal depth. The frangible abdomen made assessment of injury due to submarining possible using the Hybrid III dummy. Both the presence of submarining and the probability of injury could be assessed using compression of the frangible abdomen as an index.

1.2 OBJECTIVES

The primary focus of this project was to determine the response of the human cadaver abdomen to various types of impact loading. Of interest were rigid-bar (steering-rim-like), seatbelt, and airbag loading responses. Of principal concern was the mechanical response of the abdomen, although the injuries produced in these tests were also of interest. In addition to enhancing the general knowledge base of abdominal response to impact loading, these data were used to generate response corridors for use in developing and evaluating a new, biofidelic abdomen for the Hybrid III anthropomorphic test devices (ATD).

The initial goal of this study was to resolve apparent discrepancies within the existing response data regarding rigid-bar loading of the abdomen. To do this, the discrepancies within the existing research had to be clearly defined. Therefore, the results of several previous research efforts were reanalyzed and brought to a common basis so that direct comparisons could be made.

A new series of rigid-bar loading tests was designed in an effort to clarify some of the discrepancies exposed by these comparisons, and to establish definitive response corridors. These tests included impacts to the upper and midabdomen regions (epigastric region), as well as tests at different impactor speeds. Most tests were conducted with the cadaver in a free-back condition, but some tests were conducted with a fixed-back mounting to investigate effects of spinal flexion on abdominal response.

It was also desired to confirm the swine-based belt-loading corridors developed by Miller and Rouhana with data from belt-loading tests conducted with unembalmed cadavers. To do this, a pneumatic device was fabricated to pull a length of belt webbing into the cadaver abdomen from behind in a prescribed manner, with the belt webbing placed on and above the pelvis. The peak seatbelt loading rate in these tests was approximately 3 m/s, and the penetration speed-time history was roughly haversine in shape.

The final goal of this study was to obtain data on the response of the human cadaver abdomen to close-proximity airbag loading, for which no data are currently available. Given the difficulty in assessing loads applied to the abdomen during airbag deployment, and problems associated with the repeatability of airbag systems, an airbag simulation device (surrogate airbag) was developed for this study. Other researchers have developed airbag simulators for use in head, neck, and thorax injury studies. Duma et al. (1997) designed a pneumatic inflator and folded airbag fabric device. Special valving was developed to produce rapid filling of the fabric that was similar to an actual airbag deployment. The surrogate airbag developed in this study does not employ folded airbag fabric, but uses a lightweight, thin-wall cylinder impactor. In this way, reliance on the airbag fold pattern, or a specific type of airbag fabric, is eliminated.

2.0 METHODS

The impact response of the human cadaver abdomen was investigated under three different conditions: (1) rigid-bar impacts, (2) seatbelt loading, and (3) close-proximity airbag loading. The rigid-bar loading employed a ballistic pendulum that was used to drive a 25.4-mm steel bar into the abdomen at two levels using different speeds. Both free- and fixed-back tests were conducted. These tests were designed to resolve the discrepancies within the existing data, and to add information regarding upper abdominal response. The seatbelt tests were designed to provide the response of the mid and lower abdomen to low-speed distributed belt loading. The airbag tests were designed to provide data on the penetration-time history of the abdomen to close-proximity loading by passenger airbags, and also to provide information on the types of injuries that can occur in this type of loading scenario. The penetration-time history information was used to design a surrogate airbag device to simulate close-proximity airbag loading of surrogate abdomens. This device was designed to be more repeatable than an actual airbag, and to allow measurement of reaction loads under high-speed, low-mass, distributed loading conditions.

2.1 RIGID-BAR TESTS

2.1.1 Free-Back Loading

The free-back rigid-bar impacts were conducted in an attempt to clarify issues raised by the results of other research efforts. This type of test approximates the interaction of an unrestrained occupant with a steering rim. Of greatest concern was the question of rate dependency of the abdomen. To help resolve this issue, a series of ballistic pendulum tests was conducted. Figure 2 illustrates the laboratory setup and test facility. The pendulum consists of a 48-kg cylindrical ballistic mass suspended by vinyl-jacketed stainless steel cables from a support structure that was designed to fit within an airlock testing area. This mass was selected because it is significantly larger than the effective mass of a typical abdomen, and because it represents the median of the masses used in the Cavanaugh experiments.

A 2.5-cm-diameter rigid-bar impactor is attached to the pendulum by means of a load cell. A pivoting fork provides the interface between the pendulum and pneumatic cannon. The ballistic mass is driven at its center of gravity along the tangent to the arc of its swing by the piston of the pneumatic cannon, which is supported by a sand-filled base that provides adjustment in position and attitude of the pneumatic cannon. An electromagnet interfaces with the rear of the pendulum and maintains contact between the cannon piston and pendulum yoke prior to firing. The impact bar was horizontal when in contact with the cadaver abdomen, and the pendulum traveled +/- 3 mm vertically during impact.

Many of the specimen preparation, positioning, and testing techniques were consistent among the different types of loading investigated in this study. Therefore, many of the techniques and procedures outlined with respect to the rigid-bar tests in the following discussion also pertain to the seatbelt and airbag tests described in subsequent sections. Additional considerations specific to the seatbelt and airbag tests are discussed in those sections, respectively.

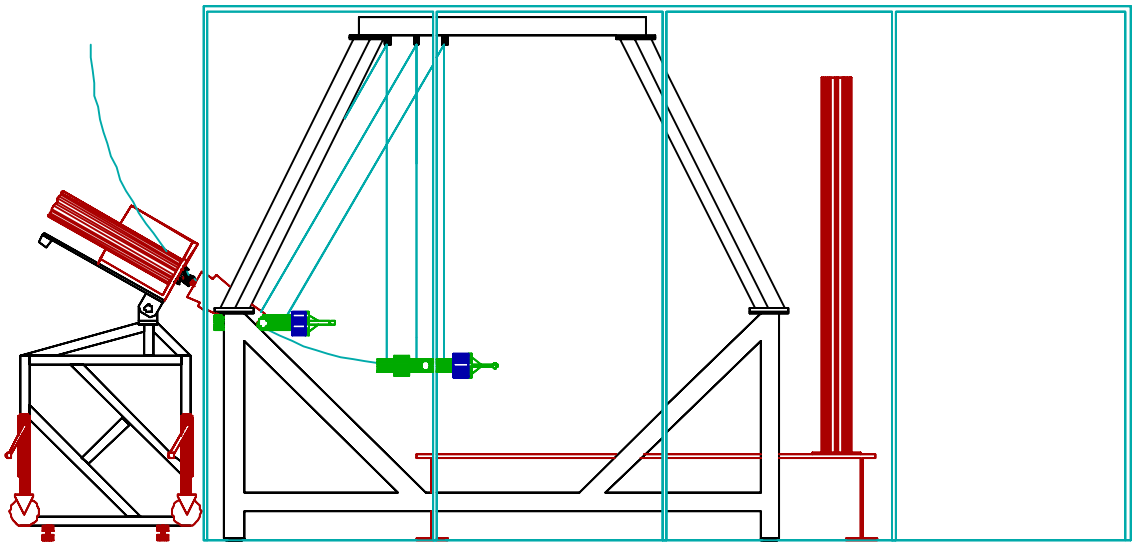

FIGURE 2. Schematic representation of the pneumatic cannon and short-cable, long-throw ballistic pendulum fixtures within the airlock test facility.

Specimen Preparation

Prior to acceptance, each cadaver underwent visual, serologic and radiographic screening to determine suitability. Foley catheters, barbs and clamps, and compression fittings were used for bilateral descending perfusion attachments to the carotid arteries and jugular veins. Access to the abdominal aorta was obtained through the right femoral artery. Similarly, access to the inferior vena cava was gained through the right femoral vein. The external iliac artery and vein were perfused on the left side through the left femoral artery and vein. Prior to the attachment of the perfusion system, the vascular system of the cadaver was flushed with approximately two liters of normal saline. The cadaver was allowed to reach room temperature and warm normal saline was pumped into the right common carotid artery using approximately 28 kPA. Blood and clots were allowed to exit from the right internal jugular vein, and clot removal was assisted by repeatedly inserting long angled forceps into the superior vena cava. Champion Millenium Co-Injectant Beta Factor was added to the saline to help destroy and remove blood clots.

Prior to testing, accelerometer mounts were fixed to T1, L3 (T11 for upper abdominal impacts), S1, and the body of the sternum via tapered Steinmann pins. Millar pressure catheters were positioned in the stomach, sigmoid colon, abdominal aorta, and urinary bladder. The Millar units were installed through 30-cc Foley catheters, so that the esophagus, rectum, femoral artery and urethra could be sealed and/or perfused. The bladder was first evacuated, and then received 250 cc of normal saline. Pretest x-rays were used to verify the instrumentation locations. The cadaver was shaved (head), diapered, and the mouth and nose were packed with gauze. The cadaver was dressed in leotards and tights, and the hands and heads were wrapped in stockinet material.

Specimen Positioning

For most tests, the cadaver was positioned in a seated, upright, free-back posture with the legs positioned forward on a curved plastic skid. The height of the skid was adjusted using plastic spacers. The hands were positioned in front of and above the head, to eliminate their direct involvement in the impact. Impact load and acceleration in the median plane were measured. Anteroposterior and inferosuperior acceleration measurements were made at the levels of the mount attachments. Dual-marker target masts were fixed to these locations to facilitate kinematic analysis using high-speed film. Overhead and lateral high-speed cameras were used to film the impact event at 1000 fps. A contact sensor triggered LED's visible in each camera field, and provided the data acquisition system with a synchronizing signal.

A safety harness with a ratchet-mechanism was fastened around the cadaver under the arms and scapulae. D rings on the harness were positioned above each shoulder and attached to adjustable tiedown assemblies via S hooks. A central ring was suspended by a swivel snap shackle that was actuated by a remote solenoid operated through a flexible cable. This shackle was attached to the top and center of the main support structure via a pulley and winch, allowing height adjustments. The harness also had a posterior ring to which the belt of a retractable lanyard was latched. This retractor mechanism was fastened to a rigid beam above the test platform. A cargo net was suspended from this beam using elastic straps and the bottom of the net was attached to the test platform using pear-shaped threaded chain connectors. This rigging was designed to control the cadaver after impact. Typical free-back, rigid-bar impact configurations are shown in Figure 3.

Specimen Testing

Prior to impact, the cadaver was given a few "full breaths" through a tracheostomy. The perfusion device was then activated, pumping 13.8-kPa heated, normal saline mixed with methylene blue stain into the arterial system. Fluid returned to the perfusion device through the venous system. The lights were turned on, the cameras started, and the cannon fired. The pendulum broke free of the electromagnet as computer sampling was triggered. The pendulum then passed through the beams of a laser speed trap mounted outside of the cadaver's knees. Approximately 10 ms prior to the pendulum contacting the abdomen of the cadaver, the shackle suspending the cadaver was released. For the midabdominal impacts, the rigid bar made initial contact with the umbilical region, approximately at the level of the umbilicus or L3. For the upper abdominal impacts, the rigid bar made initial contact with the epigastric region approximately at the level of T11. During impact the cadaver was propelled into the cargo net, and the retractable lanyard ensured that the cadaver remained in the net. Each cadaver was evaluated post-test for signs of abdominal injury during full necropsy.

Table 1 outlines the subjects and conditions used for the free-back rigid-bar tests. Eleven tests were conducted using ten cadavers. The first two tests involved a single cadaver and were used as proof-of-concept for the newly fabricated test facility. The remaining nine tests involved nine cadavers with an average age, stature, and mass of 78 years, 170 cm, and 68 kg, respectively. Six tests were conducted at the midabdominal level, with three of these in the 6-m/s range and three in the 9-m/s range. Three additional tests were conducted at the upper abdominal level, with two of these in the 6-m/s range and one in the 9-m/s range. The average impact speed for the 6-m/s range tests was 6.3 m/s, while the average speed for the 9-m/s range was 9.2 m/s. These values represent the initial rate of abdominal penetration, and were obtained from the slope of the first 15 ms (6-m/s range) and 7.5 ms (9-m/s range) of the penetration-time data.

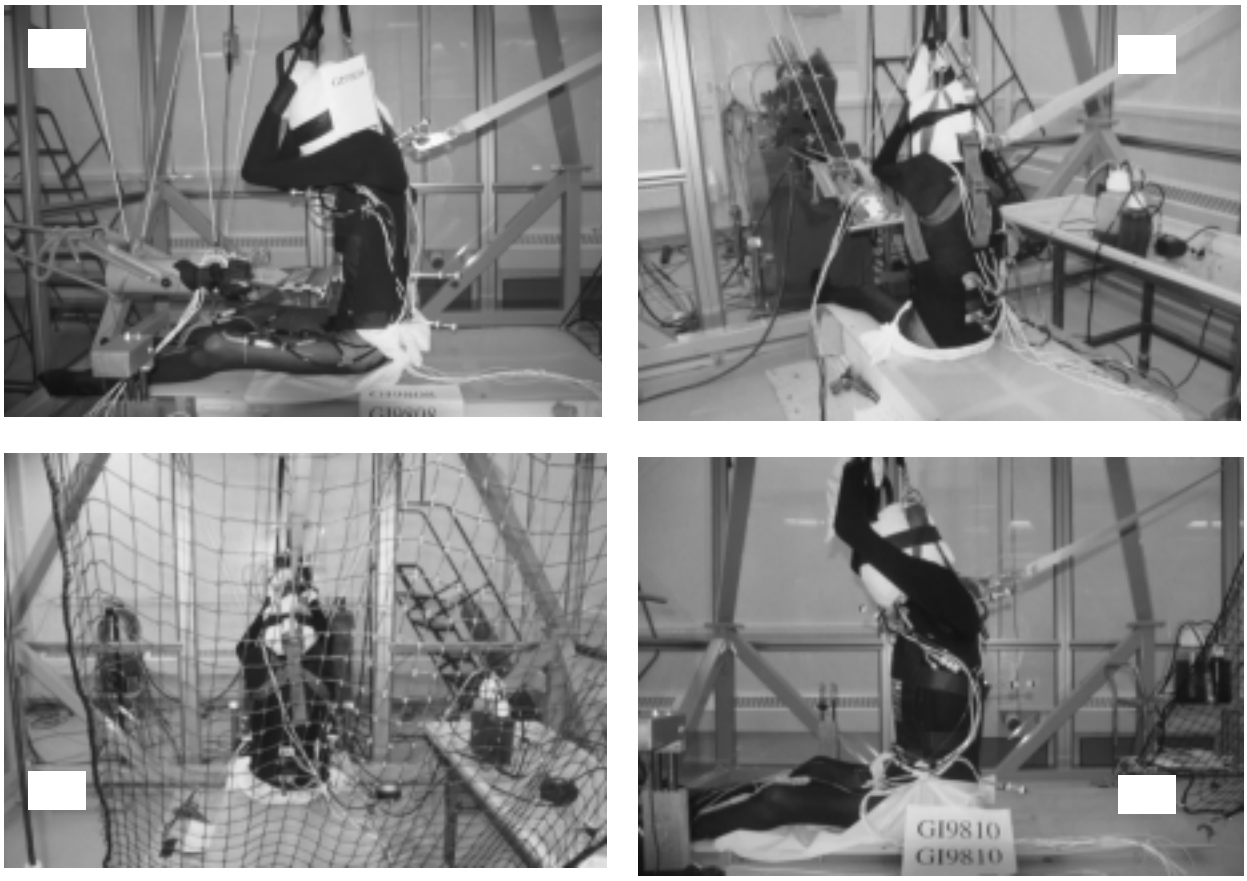

FIGURE 3. Aspects of the free-back rigid-bar loading tests: Midabdomen test setup showing cadaver position and pendulum contact location (a); Midabdomen test showing the pendulum in the set position, the Teflon skid, and the perfusion device (b); Midabdomen test showing the net, harness, and lanyard (c); Upper abdomen test showing the cadaver position (d).

TABLE 1
Free-Back Rigid-Bar Test Matrix of Subjects and Conditions

Test	Region	Speed (m/s)	Gender	Age	Stature (cm)	Mass (kg)	Cadaver
GI01	Mid	4.3	Female	73	175	36	28594
GI02	Upper	4.3					
GI03	Mid	6.3	Male	87	173	73	28682
GI04	Mid	6.6	Female	93	165	58	28764
GI05	Upper	6.0	Female	65	164	61	28800
GI06	Mid	6.1	Male	85	165	91	28838
GI07	Mid	9.1	Male	74	181	77	28879
GI08	Mid	9.0	Male	71	182	64	28889
GI09	Mid	9.6	Female	85	155	51	28942
GI10	Upper	8.9	Male	64	180	65	29084
GI11	Upper	6.2	Male	74	168	75	29115
				78	170	68	Average

2.1.2 Fixed-Back Loading

The role of the spine, whether in the recruitment of distributed masses or its own viscous characteristics, was not known. To investigate the response of the cadaver abdomen alone, a fixed-back test configuration was designed to eliminate the motion of the spine and the mass of the cadaver as a whole. For the fixed-back tests, a large male cadaver (175 cm, 88 kg, 80 yrs) was tested using rigid-bar loading. The free-back testing equipment was heavily modified to accommodate this type of test and special fixtures were fabricated to restrain the test specimen. The test platform was weighted to 18 kN, and rigidly attached to the base of the pneumatic cannon (another 18 kN). A set of flexible cables was installed on the ballistic pendulum. These cables were attached to an energy-absorption apparatus. Excess energy in the pendulum was dissipated by bending steel rods, as the pendulum motion was arrested after 200 mm of abdominal penetration.

Figure 4 shows elements of a typical fixed-back rigid-bar impact configuration. The test specimen was held in a seated posture using "u" clamps installed around the spine from behind. The clamps were in turn fastened to a rigid seatback. This obviated the need for spinal acceleration measurement and the associated mounts. Other specimen preparation considerations remained consistent with those used for the free-back tests. As shown in Table 2, the specimen was impacted seven times using a mixture of three different speeds: 3-, 6-, and 9-m/s ranges. The order of the tests was designed to minimize changes in the response due to previous testing, as well as disclose the changes that occurred. For instance, a 3-m/s test (GI12) was conducted first, followed by a 6-m/s test (GI13), and then another 3-m/s test (GI14). Beginning with the low-speed ranges helped minimize the damage to the cadaver for subsequent testing. Comparing the response from GI14 to GI12 helped determine the effect of test GI13, and multiple tests in general. Similarly, comparing test GI15 to GI13 helped disclose the effects of multiple testing, and helped to determine whether or not conducting 9-m/s tests would provide meaningful results.

2.2 SEATBELT TESTS

The seatbelt tests were conducted to determine the response of the human cadaver abdomen to low-speed distributed loading. The device used to achieve this loading was not designed to exactly replicate the belt path that would be experienced by a lap-belt-restrained automobile occupant, but was instead designed to maximize belt/abdomen interaction in a controlled, measurable, and repeatable fashion. Using standard seatbelt webbing (6-percent stretch), the cadavers were loaded about the midabdominal region, approximately at the level of the umbilicus. Some tests were run with the webbing in contact with the lower abdomen. The webbing was in contact with the anterior aspect of the abdomen, and fastened to a driving mechanism (ram) behind the cadaver. The ram consisted of a T-shaped apparatus connected to a pneumatic cylinder. The top of the T was positioned about 25 cm behind the cadaver, oriented right-to-left. The stem of the T was attached to a pneumatic cylinder, and was guided by Teflon bushings within a short length of square tubing. The seatbelt webbing was routed straight back from the sides of the cadaver (from a line tangent to the lateral-most aspects of the cadaver) to the ram. The webbing was attached to the ram via clamps whose position was adjusted right-to left. The ram was used to pull the webbing into the cadaver abdomens from behind. The device was designed to provide peak loading rate of approximately 3 m/s, and an approximately haversine penetration speed-time history. These specifications were determined from 13.4-m/s sled tests conducted by First Technology Safety Systems using a lap-and-shoulder- belt-restrained Hybrid III dummy with minimal belt slack and no knee bolster.

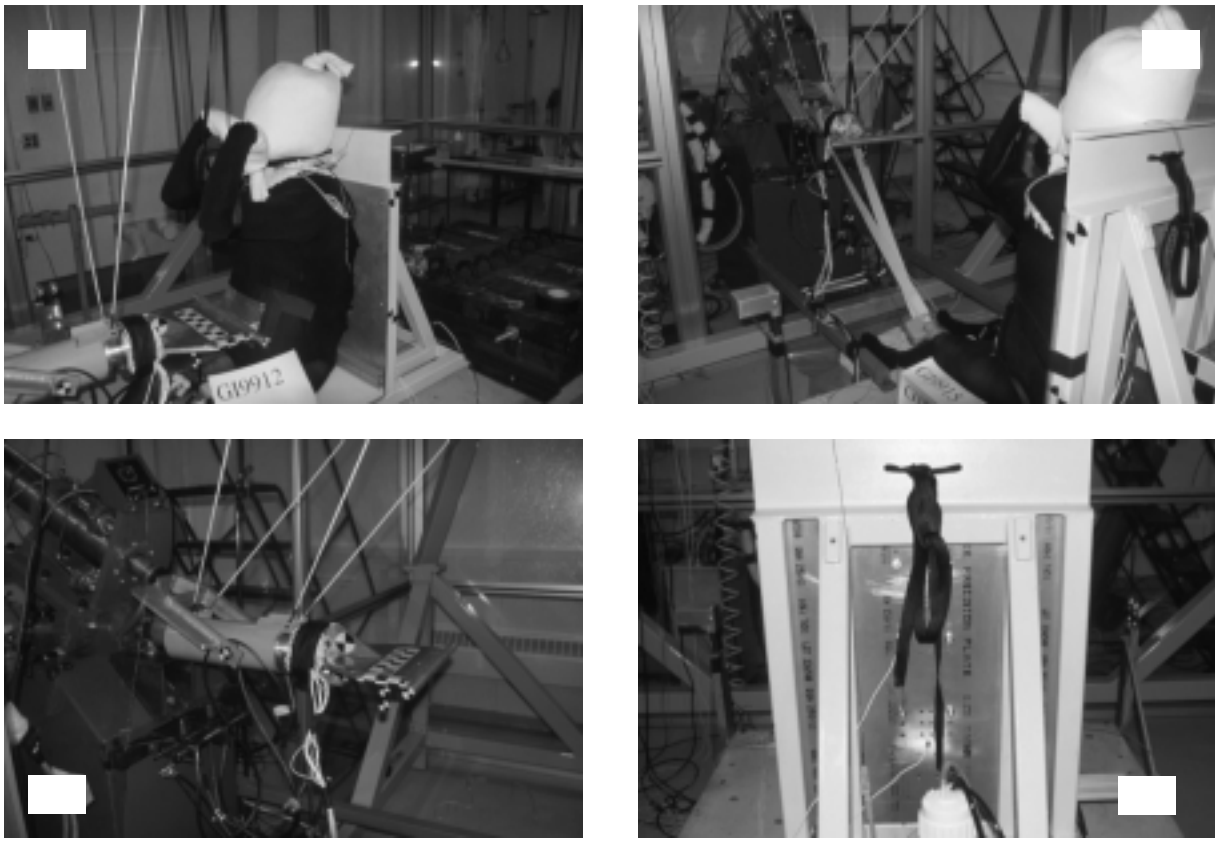

FIGURE 4. Aspects of the fixed-back rigid-bar loading tests: Midabdomen test setup showing cadaver position and pendulum contact location (a); Midabdomen test showing the pendulum in the set position (b); The ballistic pendulum in the set position against the pneumatic cannon, and the energy absorbing bar apparatus (c); The posterior aspect of the fixed-back fixture showing the "u" bolt attachments (d).

TABLE 2
Fixed-Back Rigid-Bar Test Matrix of Subjects and Conditions

Test	Region	Speed (m/s)	Gender	Age	Stature (cm)	Mass (kg)	Cadaver
GI12	Mid	3.03	Male	80	175	88.4	29425
GI13	Mid	6.30					
GI14	Mid	3.15					
GI15	Mid	6.27					
GI16	Mid	9.43					
GI17	Mid	6.30					
GI18	Mid	9.42					

The cadavers were seated upright with the legs outstretched, supported by a Teflon skid, with the hands positioned above the head. Three string potentiometers were used to measure the displacement of the webbing and a laser tracked the displacement of L3 relative to the ram. A linear potentiometer and an accelerometer measured the motion of the ram, and an inductive transducer provided a measure of the speed of the ram. The difference between the ram displacement and the motion of the spine with respect to the ram provided displacement of the spine with respect to the laboratory. The difference between the motion of the seatbelt and the displacement of the spine with respect to the laboratory provided penetration of the belt into the abdomen. Two seatbelt load cells and an inertia compensated load cell in the T mechanism measured the forces developed in the webbing. A long mercury strain gage was used to estimate belt stretch. The harness device suspending the cadavers was released just at the start of impact. The release was not complete, but allowed two feet of slack in the suspension mechanism. Other specimen preparation and testing considerations remained consistent with those used for the free-back rigid-bar tests.

Figure 5 shows typical mid and lower abdomen belt loading configurations. Table 3 outlines the matrix of subjects and conditions. Three cadavers were used in six tests. Each cadaver was tested twice. The average subject age, stature, and mass were 81 years, 165 cm, and 59 kg, respectively. The first cadaver was tested twice with the belt about the midabdomen. The first test was a free-back condition, while the second test was fixed back, using a simple two-rung back support. The remaining two cadavers were each tested in the midabdomen first, and subsequently in the lower abdomen. Because the loading mechanism was pneumatic, the accumulator pressure was adjusted slightly depending on the subject mass. The haversine penetration speed profile was achieved by varying inlet and outlet valve timing.

2.3 AIRBAG TESTS

2.3.1 Passenger Airbag Loading

Airbag out-of-position deployment tests were conducted to characterize the penetration-time history of the abdomen under these loading conditions for use in the design of a surrogate airbag loading device. In addition, these tests provided information on abdominal injuries under this type of high-speed loading.

Two hollow carbon/composite shafts were inserted through the abdomen. Each shaft was fitted with a small disk having numerous holes about its circumference. These disks were sutured to the abdominal dermis on opposite sides of the umbilicus and passed through mounts attached to the spine at L3. Targets mounted to the shafts and the spine facilitated measurement of abdominal penetration via high-speed film. The cadavers were suspended such that the center of the horizontally fired airbag module was aligned with the umbilicus (L3/L4). The legs were spread out in front of the cadaver, and the buttocks were approximately 20 cm from the top surface of the deck of the test fixture. A load cell mounted between the airbag module and the rest of the fixture measured the reaction forces developed during the deployments. Aspects of these test configurations are shown in Figure 6. Other specimen preparation and testing considerations remained consistent with those used for the free-back rigid-bar tests.

Table 4 outlines the test subjects and conditions used in these tests. Three static deployments of passenger airbags were conducted into three cadaver abdomens. The first test involved a relatively aggressive passenger airbag with the module door attached. The

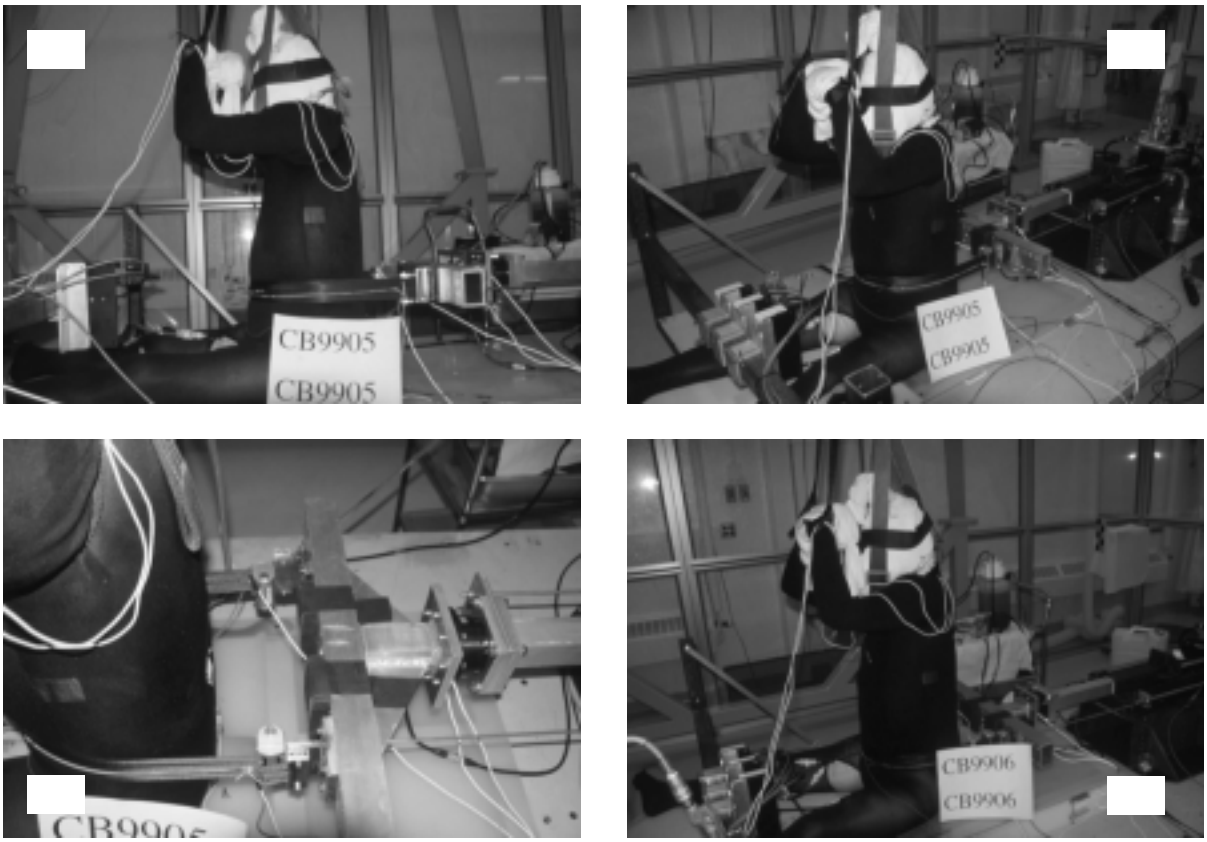

FIGURE 5. Aspects of the seatbelt loading tests: Lateral perspective of a midabdomen seatbelt test showing the cadaver position and belt location (a); Oblique perspective of a midabdomen test showing the string potentiometer configuration and the ram mechanism (b); Close-up of the ram showing the transducer locations (c); Oblique perspective of a representative lower abdomen belt test (d).

TABLE 3
Seatbelt Loading Text Matrix of Subjects and Conditions

Test	Region	Type	Gender	Age	Stature (cm)	Mass (kg)	Cadaver
CB01	Mid	Free	Female	77	168	53	29311
CB02	Mid	Fixed					
CB03	Mid	Free	Male	78	170	52	29116
CB04	Lower	Free					
CB05	Mid	Free	Male	88	156	72	29131
CB06	Lower	Free					
				81	165	59	Average

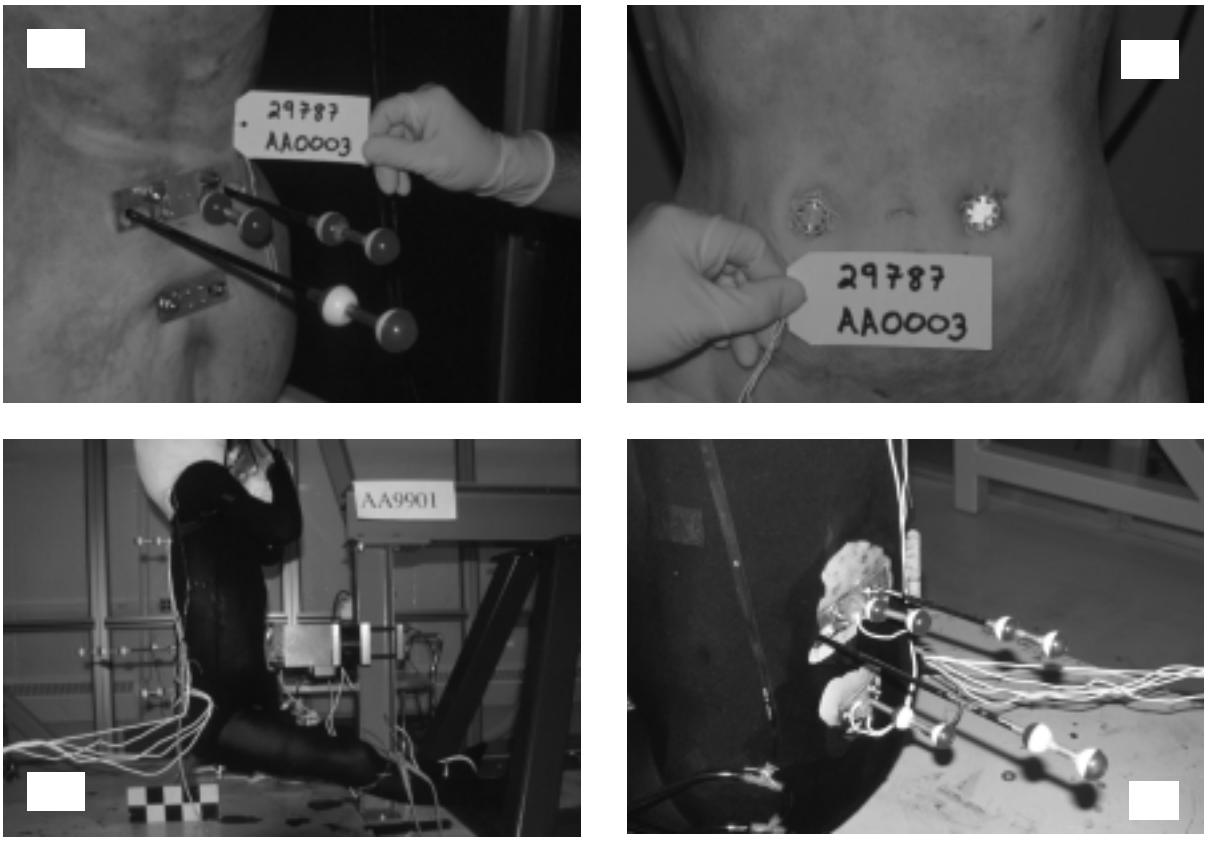

FIGURE 6. Aspects of the passenger airbag loading tests: Typical installation of the dorsal film target components during preparation (a); Ventral disks sutured to the skin, attached to the composite tubes running through the specimen (b); A lateral perspective showing the cadaver position and airbag location for an out-of-position deployment with the abdomen in contact with the module door (c); Typical target and accelerometer configuration on a specimen positioned for deployment (d).

TABLE 4
Airbag Loading Text Matrix of Subjects and Conditions

Test	Airbag	Configuration and Spacing	Gender	Age	Stature (cm)	Mass (kg)	Cadaver
AA1	More Aggressive	Door/0 cm (4 cm)	Male	83	160	73	29613
AA2	Less Aggressive	No door/0 cm	Male	81	166	64	29739
AA3	Less Aggressive	No door/5 cm	Female	79	169	64	29787
				81	165	67	Average

door was initially in contact with the cadaver abdomen, creating an approximately 4-cm gap between the airbag fabric and the cadaver. The second test involved a redesigned, less aggressive, passenger airbag with the module door removed. In this case, the airbag fabric was initially in contact with the cadaver. The third test was run in a similar fashion, but there was an initial 5-cm gap between the airbag fabric and the cadaver. In all cases, the airbag was never withdrawn from its canister prior to a test, and the airbag fold was not disturbed.

2.3.2 Surrogate Airbag Loading

In an effort to design a more controlled and repeatable experiment capable of mimicking the conditions of passenger airbag punch-out loading, an airbag simulator was designed to penetrate the cadaver and dummy abdomen without contacting the ribs or pelvis of a Hybrid III dummy. This device is a low-mass (approximately 1 kg), high-speed (up to 18 m/s) impactor capable of delivering relatively distributed loads to the abdomen similar in area to those expected in the early stages of an OOP airbag deployment. The device includes a pneumatic firing mechanism and a lightweight aluminum impactor constructed of welded thin-wall tubing. The face of the impactor is the sidewall of a 7.6-cm-diameter tube that is 20-cm long. The ends of the cylinder are fitted with rounded caps to help eliminate edge loading of the abdomen as penetration increases. The cylinder is attached to a 5-cm-diameter shaft that is 30-cm long. An accelerometer mounted within the head of the device and a pressure transducer mounted at the end of the shaft (piston face) are used to calculate contact load. A solenoid valve actuates a pneumatic cylinder that drives the main ball valve of the device. A large muffler constantly vents the drive pressure to the atmosphere, acting like a low-pass filter on the lengthy plenum created by the main cylinder, valves, and pneumatic connections. The device operates at 225 psi with the valve open for 60 ms. Contact with the abdomen occurs approximately 7.6 cm from the end of the surrogate airbag travel. At the end of travel, the pressure driving the surrogate airbag is rapidly exhausted through vents. The main bearing of the device is allowed to float in an effort to reduce potential damage caused by moments that could develop as the device penetrates a specimen.

The passenger airbag OOP tests determine the levels of peak penetration and rate of penetration needed to provide an accurate simulation. Using this information, a number of preliminary tests were conducted to develop and tune the surrogate airbag device. The device was deployed into various urethane and silicone pads, and cardboard honeycomb. Different pressures and valve timings were investigated. Each preliminary test was conducted with the struck object held stationary. This was done for two reasons: first, the fixed condition made comparison of reaction load and calculated contact forces easier. This comparison was necessary to prove that accurate contact interaction forces could be determined using the surrogate airbag device. This comparison could only be made when using lightweight cardboard honeycomb to avoid mass-recruitment effects. Second, the cadaver specimens moved very little during the initial part of the OOP deployments. Because of this, a fixed-back condition could be used to help compensate for the relatively small amount of energy possessed by the surrogate airbag. A positive side effect of this is that abdominal penetration measurement was simplified. Only the motion of the surrogate airbag device need be measured. This measurement was accomplished using a high-speed, high-resolution laser displacement device.

The surrogate airbag tests employed the same fixture used to position the cadaver in the fixed-back rigid-bar tests. However, instead of “u” clamps fixed around the spine, a single strap was wrapped around L3 through incisions made in the back of the cadaver. This strap was tightened against the seating fixture using a ratcheting mechanism. The

legs of the cadaver were outstretched, and the abdomen exposed. The arms were suspended above the cadaver, out of the way of the surrogate airbag device. The surrogate device contacted the abdomen approximately at the level of the umbilicus, such that contact with the ribs and pelvis was avoided. Measurement of abdominal contact was facilitated by several thin wires. Allowance was made for change in abdominal depth after the startup of perfusion. Figure 7 illustrates various aspects of the surrogate airbag device and representative cadaver positioning. Other specimen preparation and testing considerations remained consistent with those used for the free-back rigid-bar tests.

Table 5 summarizes the test subjects and conditions. Three cadavers were used in six tests. The first four tests were performed using one cadaver. The first three of these tests were used to optimize the performance of the surrogate airbag device by adjusting the test setup. The first test was a free-back condition, while the second test used the same two-rung back support used in the fixed-back seatbelt test. The third test used the same rigid seat support used in the fixed-back rigid-bar tests. The fourth test was a repeat of the third, with a minor adjustment in possible peak abdominal penetration. The subsequent two tests were conducted in a similar fashion using two cadavers. The average cadaver age, stature, and mass were 75 years, 171 cm, and 72 kg, respectively.

2.4 TEST CONTROL

2.4.1 Facilities and Fixtures

All tests were conducted within an Airlock test facility. The Airlock is a sealed enclosure made from interlocking aluminum-framed vinyl panels. The Airlock is a negative pressure area, as it has a high volume, reverse HEPA filter unit which exhausts through the ceiling. This exhaust is carried outside of the building via a roof-mounted blower. The Airlock houses a square tubing superstructure and a steel platform test fixture. The superstructure supports netting, cadaver harnesses and release mechanisms, as well as items such as winches and a portable x-ray head. Lateral and overhead Photosonics cameras were also located outside of the Airlock, and were accompanied by approximately 40 kW of lighting. These AC cameras were typically operated at their maximum frame rate, which is 1000 fps. Instrumentation connections were made through an acrylic patch panel built into one side of the Airlock. A steel platform was used to support cadavers and associated fixtures.

2.4.2 Signal Conditioning and Data Acquisition

Pacific Instruments Model 8250 amplifiers were used for signal conditioning. These amplifiers provide 0-15 Volt remote-sensing variable excitation to bridge transducers and variable gain from 1-2500, with a common-mode rejection ratio of 120 dB at 60 Hz and gain of 1000. These amplifiers also provide a bandwidth of 100 kHz, 50-MOhm input impedance, and 100 uV quiescent noise plus 0.001% of peak-to-peak signal. Automatic balancing and bipolar shunt calibration capabilities were employed as well. The 8250 amplifiers come equipped with switchable two-pole low-pass Bessel filters, which have undergone in-house modifications to perform antialiasing filtering. The 10-kHz filter setting has been altered to fit a second-order Butterworth profile with a cut-off frequency (-3 dB point) of 3850 Hz. Use of these filters requires digital post processing to meet SAE J211 specifications. However, with the filter's high cut-off frequency and low-attenuation rate, any SAE channel class can be achieved by using a 4th-order Butterworth FFT phaseless filter.

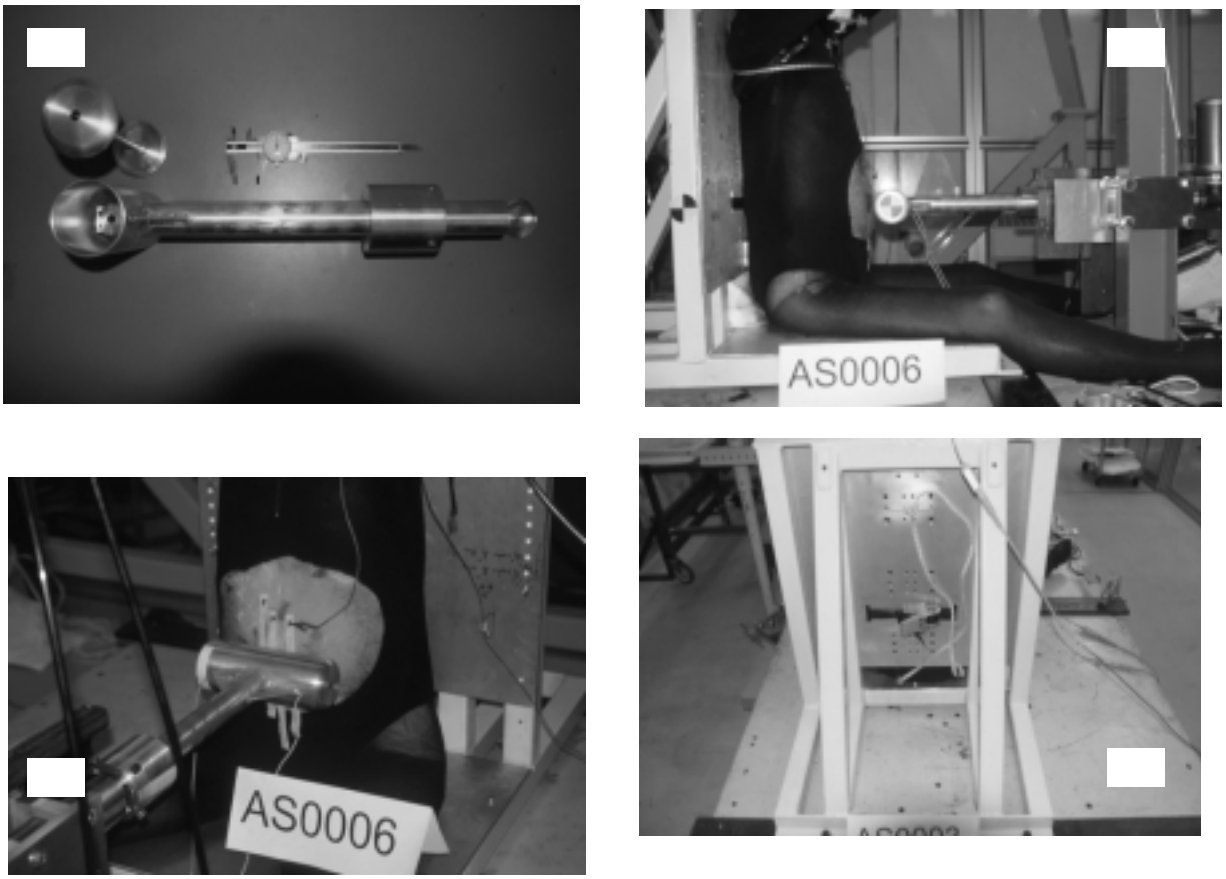

FIGURE 7. Aspects of the surrogate airbag testing: Key components of the surrogate airbag during the development state (a); A lateral perspective of the completed surrogate airbag showing the cadaver position and the surrogate airbag contact location (b); The fine wires used to measure contact (c); Posterior perspective of the modified fixed-back testing fixture, showing the ratchet and strap mechanism (d).

TABLE 5
Surrogate Airbag Loading Test Matrix of Subjects and Conditions

Test	Peak Penetration (mm)	Configuration	Gender	Age	Stature (cm)	Mass (kg)	Cadaver
AS1	83	Free back	Female	68	163	57	29490
AS2	76	Fixed back					
AS3	73	Fixed back					
AS4	76	Fixed back					
AS5	76	Fixed back	Male	86	173	79	29566
AS6	76	Fixed back	Male	72	178	81	29491
				75	171	72	Average

A Data Translation analog-to-digital conversion and digital i/o board was used in a Windows95-based Pentium computer to acquire data. This board is able to sample sixteen single-ended inputs in real time. Since there is no simultaneous sample-and-hold circuitry on this board, there is a slight skew of the data channels. However, because the board burst samples at 1 MHz, the skew between adjacent channels is 1 usec, and the maximum skew between the first and last channel is 15 usec. The board was generally operated at a 10 kHz sampling rate. Analog data backup was achieved using a tape drive and multiplexors. The tape drive is a Honeywell Model 96 reel-to-reel unit. It has six direct channels and eight FM channels. The multiplexors mix eight channels of frequency modulated data onto one channel, which is then recorded on a direct-record channel. When necessary, the data were retrieved from the tape using a Schlumberger Model 4167 dual discriminator FM demultiplexor.

2.4.3 Event Sequencing

An in-house-designed sequencing unit was used to coordinate the impact events. This is a ten-channel unit that has front panel programmable delay and duration, as well as trigger channel source selection. The timing modules can by configured for AC or DC switching. The pneumatic cannon, airbags, lights, cameras, release mechanisms, and computer sampling are all triggered using this unit. A separate timing mark generator is used to mark the high-speed film at regular intervals and a solid-state and LED-based system marks both the high-speed film and the digitized data to provide time-zero synchronization.

2.5 DATA PROCESSING

2.5.1 Film Analysis

Analysis of the 16-mm high-speed film was conducted using a NAC Film Motion analyzer. This analyzer is equipped with a sparker/digitizer that is interfaced to a PC. This system was used to digitize the locations of reference points and cadaver target bobbers in two perspectives. A timing generator was used to place LED marks every 1 ms along the perforation border. These marks were used to determine the actual film speeds during the airbag deployments. The solid-state circuit was used to drive LEDs placed in front of each camera lens. This provided an optical indication of the time of contact, and was used for synchronization. Because the high-speed cameras were operating at about 1000 frames-per-second, the film alignment cannot be guaranteed to be less than 1 ms. However, it is likely closer to 0.5 ms. Both lateral and overhead camera perspectives were filmed. The results of analysis from both views were sometimes compared to provide confidence in the data. The film was primarily used to determine abdominal penetration.

2.5.2 Data Analysis

All of the digital data collected using PC-based hardware was processed and stored using Unix-based workstations. All of the data were processed using in-house programs or scripts written in the C language. These programs were executed on a Sun Microsystems Sparc20. All of the data were stored on an SGI Irix 5.3 machine. Backup of the data was accomplished via a DAT recorder. A number of the processing techniques require some explanation.

Filtering and Scaling

The data from the rigid-bar, seatbelt, and airbag loading tests were treated separately, but in a similar fashion. All of the signal polarities were adjusted in accordance with the SAE J211 standard. The digital post-processing filter used was a phaseless Fast-Fourier Transform (FFT) filter with pre- and post-zero padding. The filter profile corresponded to a 4th-order Butterworth low-pass filter. The filter cut-off frequencies were varied depending on the nature of each signal and suggested SAE channel class (cc). The conversion between SAE channel class and Butterworth profile is a multiplicative factor of 1.65. For example, for a signal requiring an SAE cc1k Hz filter the cut-off frequency was set to 1650 Hz.

The load- and penetration-time histories are presented as SAE channel class (cc) 180 Hz for the rigid-bar and seatbelt tests. The load-time histories for the airbag tests are presented as SAE cc 1000 Hz, but the penetration-time histories are SAE cc 180 Hz. For comparison to the Cavanaugh corridors, the load-penetration data are filtered at SAE cc 60 Hz, and equal-stress/equal-velocity scaled using 76 kg as the reference mass.

Equal-stress/equal-velocity scaling is a volumetric scaling, which assumes geometric similitude between subjects. The modulus of elasticity and the density of each subject are presumed consistent. Mass is used as an indication of relative size between subjects. To obtain the appropriate scale factors for each subject, first the chosen representative mass is divided by the subject mass. To make the density relationships dimensionally correct, length must be multiplied by the mass ratio raised to the one-third power. Likewise, to maintain the modulus of elasticity, the force must be multiplied by the square of length scale factor.

Viscous Criterion

The main V*C algorithm components are velocity of penetration (V) and compression (C). Compression is calculated based upon measured abdominal penetration and initial abdomen depth. Penetration velocity is found by differentiation of penetration. The Viscous Criterion was calculated using two different approaches. In the first, more-traditional approach, penetration is filtered using an Infinite Impulse Response (IIR) phaseless filter prior to differentiation. In this case, a forward/backward finite-difference filter was used. The filter profile corresponds to a 4th-order Butterworth low-pass filter having a cutoff frequency of 100 Hz. After differentiation, the data represent velocity (speed) and are again filtered using the same digital filter. The filtered velocity is then multiplied by the filtered penetration at each point in time. The V*C is found by multiplying this quantity by an external factor and dividing it by the initial abdomen depth. For cadaver tests, an external factor is not relevant and was not applied. Individually measured abdominal depths were used. In the second, alternate approach, penetration was filtered using an SAE channel-class 180 Hz phaseless filter, but the velocity is not filtered further. The specifications provided by the SAE J1727 standard (penetration filtered at SAE channel-class 600, with no subsequent filtering of the velocity) are not indicated for use with cadaver data obtained from high-speed film, as significant noise in the data results in very large, short duration, localized penetration speeds after differentiation. These large speeds are oscillatory artifacts that confound the V*C results. Therefore, lower filter frequencies provide a more realistic estimate of V*C in this case.

Corridor Generation

The new load-penetration corridors were generated in a similar manner for all types of testing. Separate load-penetration corridors were developed for each case using the newly acquired data. The data were equal-stress/equal velocity scaled using 78 kg, the mass of a Hybrid III 50th-percentile-male dummy (upper limit of dummy mass, plus shoes and clothing) as the reference mass. For development of these corridors the penetration data were filtered at SAE cc 60 Hz. The load data were brought to a common basis with respect to penetration using cubic spline interpolation. This resulted in load values for each fixed, regular penetration increment, for all tests. For a given type of test, the aligned load values were averaged for each penetration increment, and the standard deviation was calculated. A corridor upper bound is the average load plus one standard deviation, and a lower bound is the average minus one standard deviation. Using this approach, the penetration data are not averaged. Calculation stops at the point of maximum penetration of the test that reaches this peak first. Piecewise continuous linear approximations to corridor upper and lower bounds were established qualitatively, and represent the final corridors. These corridors are meant to encompass the data as tightly as possible while providing practical slope and intercept values.

Spine Accelerations

The spine acceleration measurements have not been analyzed as part of this investigation. It is anticipated that these accelerations would be examined as part of future analyses. However, the peak anterioposterior spine accelerations opposite the impact region are provided for each type of test, for completeness.

3.0 RESULTS

3.1 FREE-BACK RIGID-BAR TESTS

Eleven free-back rigid-bar pendulum impacts were conducted using ten cadavers. The first two tests were used to check the test setup and no response data were collected. Of the remaining nine tests, six were impacts to the midabdomen, with three high-speed and three midspeed tests. The other three tests were impacts to the upper abdomen, including one high-speed and two midspeed tests.

3.1.1 Load and Penetration Measurement

For the free-back rigid-bar tests, inertia compensation of a pendulum-mounted load cell provided load measurement. The motions of the pendulum and spine targets were tracked using 1000-fps 16-mm film. Different scale factors were applied depending upon the distance of the tracked object from the camera, e.g., the spine targets were farther from the camera than the end of the impact bar, so a larger factor was applied to the spine target motion. The dual target masts on the spine mounts were used to vector back to the point of attachment at the spine. This method helped compensate for fluctuations of the targets and bending of the spine during impact. This method cannot compensate for slight differences in vertical position between the impact bar and spine mounts. If a spine mount tended to roll above or below the bar during impact, the penetration would be slightly overestimated.

To provide confidence in the load results, the inertia compensated loads were compared to the product of the pendulum mass and pendulum acceleration. To provide confidence in the penetration results, the difference between double integrated pendulum and spine accelerations was compared to the film data. The data are in excellent agreement, particularly for the first 30 ms. A typical comparison of double integrated acceleration differences and film data is shown in Figure 8. For one of the rigid-bar tests, film was not available, so the accelerations were used to determine penetration.

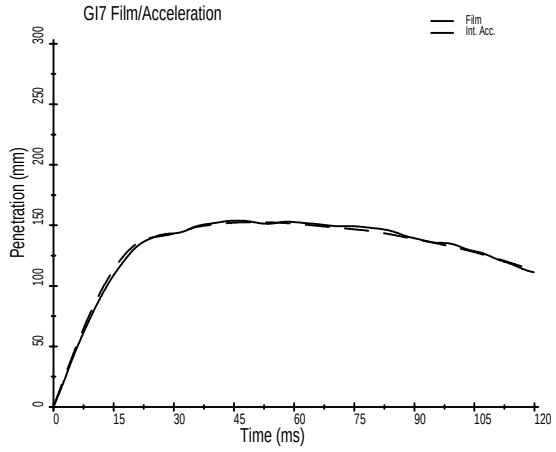

FIGURE 8. Typical comparison of abdominal penetration determined from film analysis and the difference between double integrated spine and pendulum acceleration.

3.1.2 Load and Penetration Data

Figure 9 shows the load-time histories and the penetration-time histories for the free-back rigid-bar tests. When comparing the high-speed (9-m/s range) midabdomen tests to the midspeed (6-m/s range) midabdomen tests, a few observations can be made. First, the loads for the high-speed tests reach peaks that are roughly twice those of the midspeed test loads, and they reach these peaks in approximately half the time. Second, the high-speed test loads exhibit a more pronounced two-peak response. Third, the peak abdomen penetration of the high-speed tests is generally less than that seen in the midspeed tests. These last two points are related. The rapid load increase of the high-speed tests is accompanied by greater whole-body motion for a given penetration than that which occurred in the midspeed tests. This greater whole-body motion limits the penetration of the pendulum into the abdomen. As the body is accelerated with the pendulum, the load drops slightly. As the body slows after accelerating from initial contact, the load either increases again or plateaus. This occurs near 30 ms, and an associated small increase in penetration depth can be seen at this point. Overall, this effect is probably related to the viscous nature of the abdomen, and its reduced compressibility at higher speeds.

Upper Abdomen Data

The upper abdomen load-time response is distinctly different from that of the midabdomen due to loading of the ribcage that is not present in the midabdomen tests. Both high and midspeed tests produced similar results. The initial load increase is quite rapid, followed by a significantly more gradual rise to the peak load. This subsequent rise is relatively noisy, probably because of rib fracture as well as compression of abdominal and thoracic contents. Test GI5 is a special case, where the cadaver skeleton was extremely osteoporotic. Because of this, the initial sharp load increase is absent as the ribs give way easily. After rib compression, the load levels reach those of test GI11, the other midspeed upper abdomen test. However, the penetration experienced during test GI5 is roughly 20-percent greater than that in test GI11. In contrast to the midabdomen tests, the difference in peak penetration between the high and midspeed upper abdomen tests (GI10 and GI11) is minor. This is probably related to influence of the ribs and time of fracture. Again, the greater the whole-body motion for a given penetration, the lower the peak penetration ultimately achieved.

3.1.3 Load-Penetration Responses

Figure 10 shows the load-penetration responses for the free-back rigid-bar impacts in the left column, and the filtered and scaled (76 kg) load-penetration responses compared to the Cavanaugh corridors in the right column. The 6-m/s range responses show peak loads between 4.1 and 4.3 kN, and peak penetrations between 178 and 209 mm. In general, the responses are characterized by a ramp to peak load (constant stiffness) followed by a sudden drop in load with little change in penetration. The responses for the 9-m/s tests show peak loads between 6.3 and 8.1 kN, and peak penetrations between 145 and 159 mm. Unlike the midspeed tests, the response is not a simple ramp to peak load, but is more complex. Two of the tests, GI7 and GI9, exhibit a rise-plateau-rise response very similar to that described by Stalnaker et al. (1985). Test GI9 does not quite fit this description, but does show two or three different slopes. It is possible that this type of response is influenced by rib involvement. The high-speed tests resulted in far greater rib fractures than did the midspeed tests, suggesting greater rib involvement. It is also possible that the influence of the ribs in test GI7 and GI8 was different than that in test

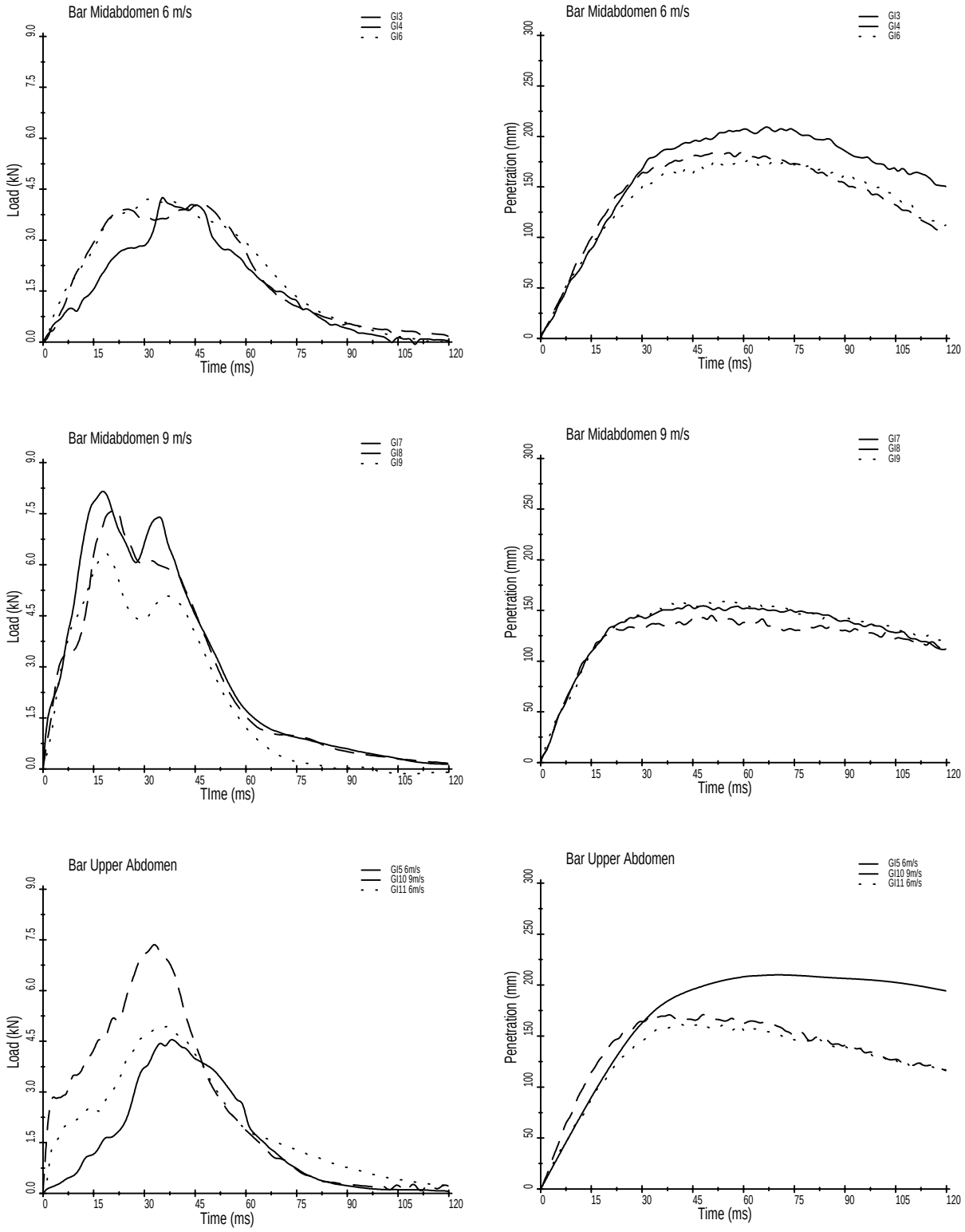

FIGURE 9. Load (LEFT COLUMN) and penetration (RIGHT COLUMN) data for all free-back rigid-bar impacts. The midabdomen tests are separated by speed, and upper abdomen tests are grouped together.

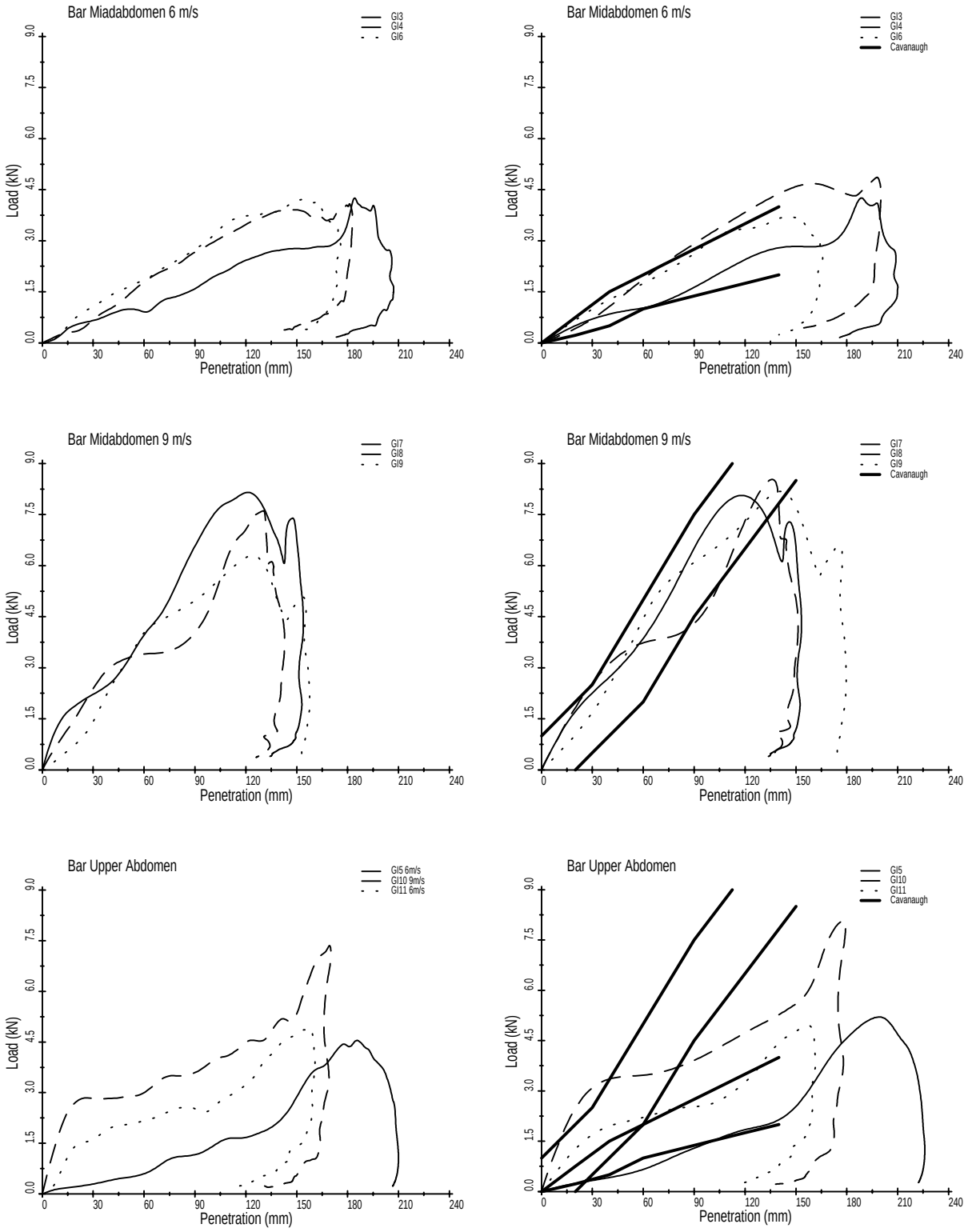

Figure 10. Load-penetration responses for all free-back rigid-bar tests. The data, scaled and filtered per Cavanaugh et al. (1986), are compared to the Cavanaugh corridors in the right-hand column.

GI9. The cadavers used for tests GI7 and GI8 were approximately midsize males of about 70 years, while the cadaver used for test GI9 was a small female of 85 years. The small "notch" near the end of these load-penetration responses represents the mechanism of the body slowing after initial acceleration (Figure 10, Bar Midabdomen 9 m/s). This effect could be due to recruitment of mass from other portions of the body such as the extremities, or influence of the harness release apparatus. After this notch, the load returns to zero while the penetration remains essentially constant.

Response of the Upper Abdomen

The upper abdomen load-penetration responses show very similar shapes for both the high and midspeed tests, with the exception of test GI5. There is a sharp rise followed by a very gradual rise or plateau followed by another steep rise. The high-speed test, GI10, shows a rise of force near the end of penetration, indicating bottoming of the impactor. These tests tend to exhibit somewhat less hysteresis than the midabdomen tests. That is, the penetration tends to decrease slightly as the load decreases. This effect is less noticeable in the midabdomen tests, and may be related to small restorative forces exerted by the ribs, even though many are fractured, during the upper abdomen tests.

3.1.4 Comparison to Cavanaugh Data

The comparison of these data to the Cavanaugh corridors is quite good for both mid and high-speed tests. This is particularly true in light of the fact that the Cavanaugh corridors (approximations shown here) were generated using plus-or-minus one standard deviation of average load plotted against average penetration and, as such, do not represent upper and lower bounds of the entire data set. These data convincingly illustrate the rate sensitivity of the human cadaver abdomen when subjected to rigid-bar impacts at different speeds using a 48-kg pendulum. However, the contributions of mass recruitment, tissue viscosity, and spine stiffness to this rate sensitivity remain unknown.

Comparison of the upper abdomen response to the Cavanaugh corridors shows that the initial stiffness of the midspeed test is about the same as that in the high-speed Cavanaugh data. The high-speed test is about twice as stiff initially as the high-speed Cavanaugh data. Due to the difference in impact location, these data do not follow the shape of either Cavanaugh corridor. The stiffness of the midspeed upper abdomen test GI5 (severe osteoporosis) is below that of the midspeed Cavanaugh corridor.

3.1.5 Development of New Response Corridors

Figure 11 shows scaled (78-kg) load-penetration responses. The scaling has the effect of spreading the peak penetrations slightly. Had a perfect mapping to a common basis been attained, a single curve would have resulted. The better a model approximates the physical situation, the tighter the scaled data will be clustered. Given the closeness of the original, unscaled data, it is not clear that equal-stress/equal-velocity scaling is the best approach. The assumption of geometric similitude between subjects for these tests is probably not entirely valid. Abdominal breadth and depth vary depending on aspects of initial subject posture, and are not necessarily perfectly proportional to mass. However, this classic approach was selected in an initial attempt to normalize these data, until eventually replaced by a more complete model representation of the human cadaver abdomen. Given that, the stiffness of the scaled data changed little from that of the original. These scaled data were used to generate additional abdominal response corridors.

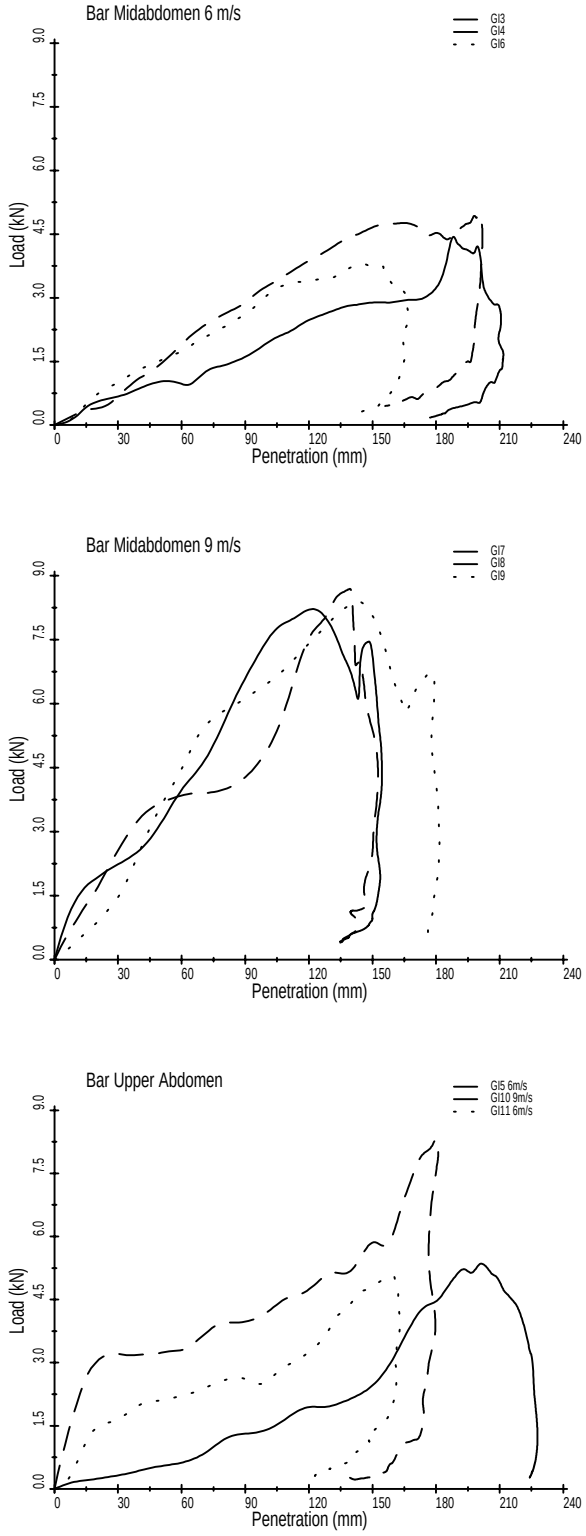

FIGURE 11. Equal-stress/equal-velocity normalized free-back rigid-bar load-penetration responses.

Figure 12 shows the newly developed free-back rigid-bar impact response corridors for the human cadaver abdomen in two speed ranges. Each of these corridors was developed using three cadaver tests. Although these are relatively small numbers of tests, the large degree of similarity between the tests helps reinforce confidence in the data and suggests that a reasonable general representation has been obtained. The midspeed corridor is defined by two piecewise continuous linear approximations of the standard deviations. The lower bound has a slope of 19 kN/m, and the upper bound has a slope of 35 kN/m (27 kN/m average). Similarly, the high-speed corridor has a low-bound slope of 50 kN/m, and an upper bound slope of 75 kN/m (63 kN/m average). This suggests approximately two times greater stiffness for the high-speed corridor.

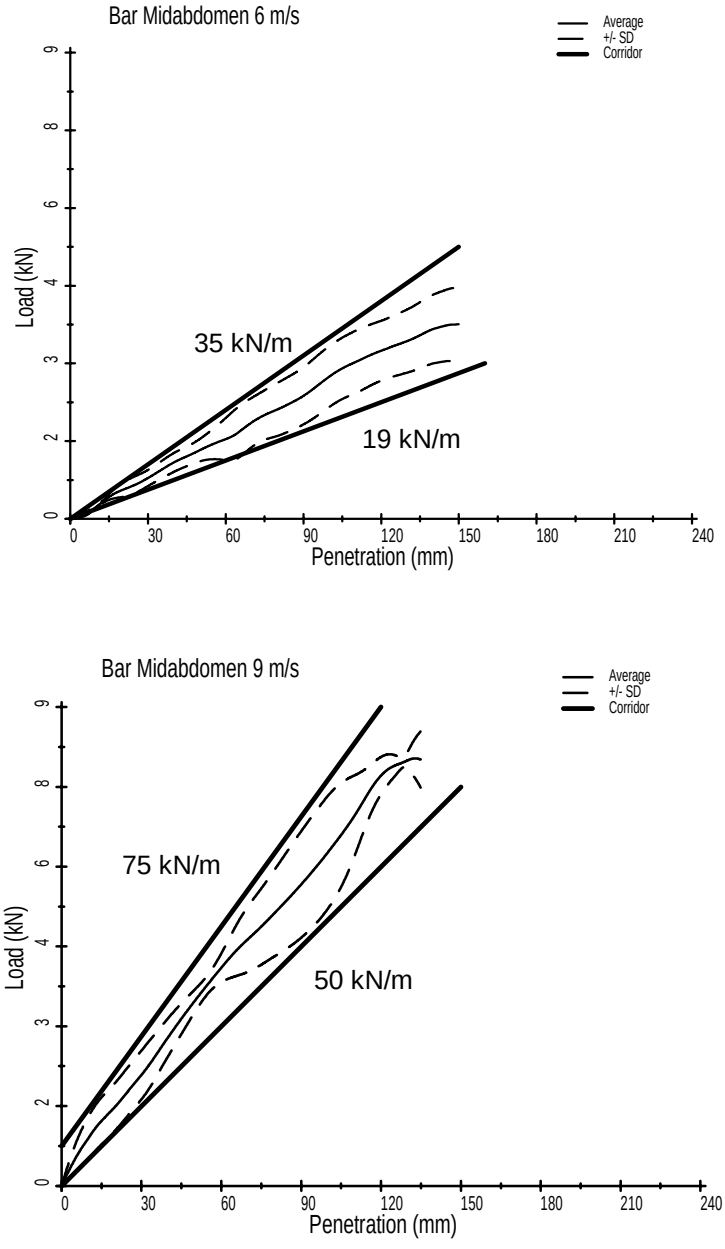

FIGURE 12. Newly developed 6-m/s and 9-m/s range load-penetration response corridors for free-back rigid-bar pendulum impacts to the human cadaver abdomen.

3.1.6 Injury-Related Findings

The autopsy results from the free-back rigid-bar tests are cataloged in Appendix A. The most common injuries were multiple rib fractures, followed in descending order by lacerations of the liver, spleen, and diaphragm. There was one case of intestinal injury: a laceration of the cecum. The upper abdomen impacts resulted in the most serious spleen injuries, followed by the high-speed midabdomen impacts, then the midspeed midabdomen impacts. Figure 13 shows some of the typical injuries observed during autopsy resulting from the rigid-bar tests. Figure 13a shows a liver laceration experienced by cadaver 28682 during the midspeed midabdomen test GI3. Figure 13b shows a torn diaphragm experienced by cadaver 28838 during the midspeed midabdomen test GI6. Figure 13c shows a splenic tear experienced by cadaver 29084 during the high-speed upper abdomen test GI10.

Injury Predictors

Table 6 summarizes the maximum impact speed, load (SAE cc 180 Hz), penetration (SAE cc 180 Hz), compression, load*compression, viscous response, absorbed energy (area under the load-penetration curves), and peak anteroposterior spine acceleration opposite the level of impact for the free-back rigid-bar tests. The MAIS level is also provided. No clear relationship or distinction between the response parameters and MAIS is evident.

TABLE 6
Free-Back Rigid-Bar Test Results: Peak Values

Test	Region	Speed (m/s)	Load (N)	Penetration (mm)	Comp. (%)	Comp. * Load (N)	V*C (m/s) cc180	V*C (m/s) fir100	Energy (J)	L3/*T11* Acc. (g)	MAIS
GI03	Mid	6.3	4251	209	68	2900	3.5	2.5	378	66.8	4
GI04	Mid	6.6	4084	184	63	2567	2.9	2.3	405	37.0	4
GI05	Upper	6.0	4548	210	84	3822	2.7	2.6	379	31.5	4
GI06	Mid	6.1	4207	178	58	2453	4.9	1.7	423	30.1	3
GI07	Mid	9.1	8150	155	62	5085	3.2	2.3	739	50.3	3
GI08	Mid	9.0	7613	145	61	4659	3.9	3.1	532	133.1	4
GI09	Mid	9.6	6319	159	75	4754	4.2	3.2	597	82.0	5
GI10	Upper	8.9	7356	172	60	4437	2.9	2.3	603	40.0	5
GI11	Upper	6.2	4934	163	56	2752	2.7	1.8	373	16.6	5

3.2 FIXED-BACK RIGID-BAR TESTS

Seven fixed-back tests were conducted using a single cadaver, at three different speeds, with two tests at roughly 3.1 m/s, three at 6.3 m/s, and two at 9.4 m/s. The load and penetration measurement techniques were similar to those used for the free-back tests. The tests are listed in each legend in the order in which they were conducted.

3.2.1 Load and Penetration Data

Figure 14 shows the load-time histories and the penetration-time histories for the fixed-back rigid-bar tests. The different speeds are grouped by the curves' shade of gray. A fine horizontal line is displayed in the penetration plot at 200 mm because the stroke of the pendulum was arrested between 200 and 225 mm of penetration. Only the response data before 200-mm penetration is considered. The load-time histories are characterized

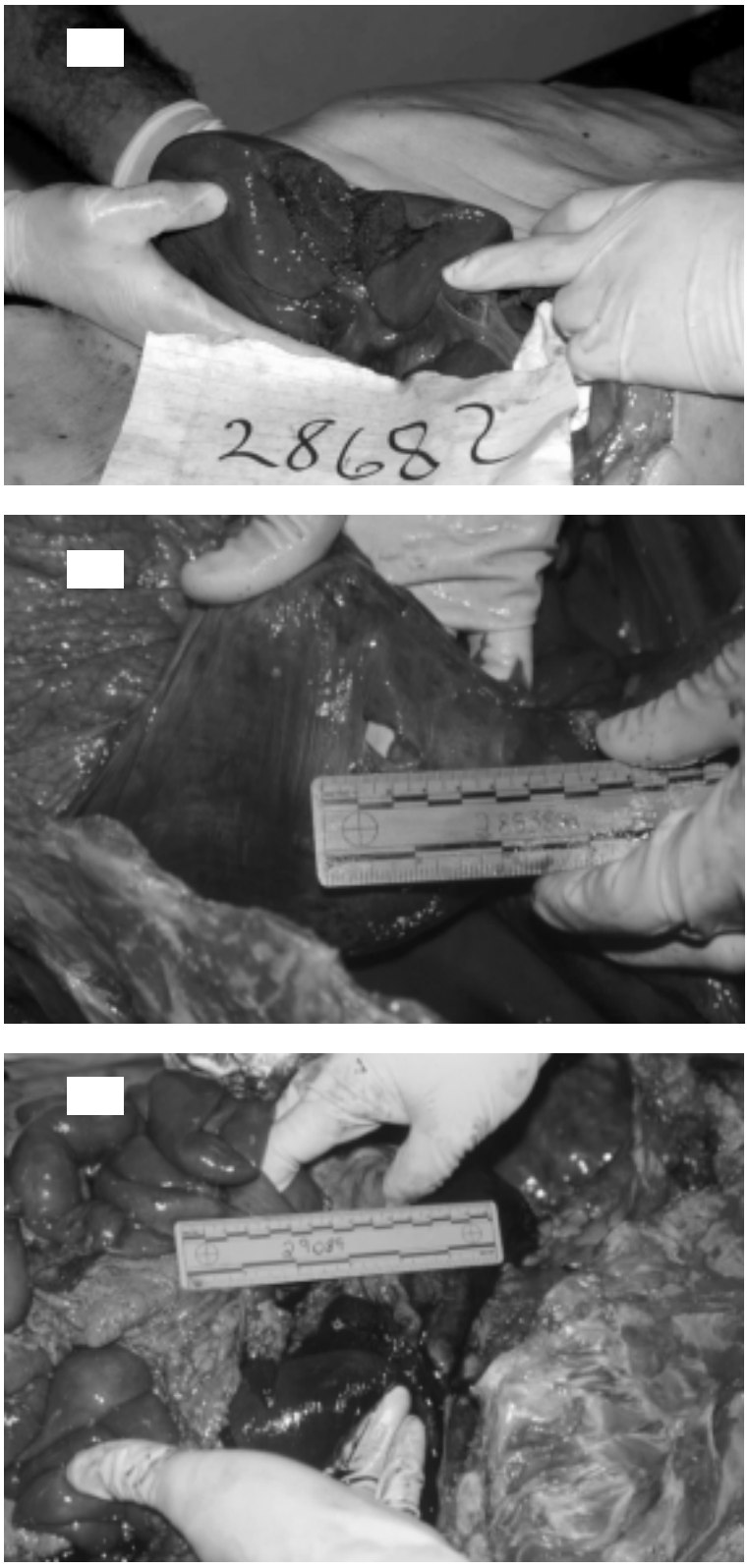

FIGURE 13. Typical injuries from free-back rigid-bar tests: (a) Liver laceration (CAD 28682/GI3); (b) Torn diaphragm (CAD 28838/GI6); (c) Splenic tear (CAD 29084/GI10).

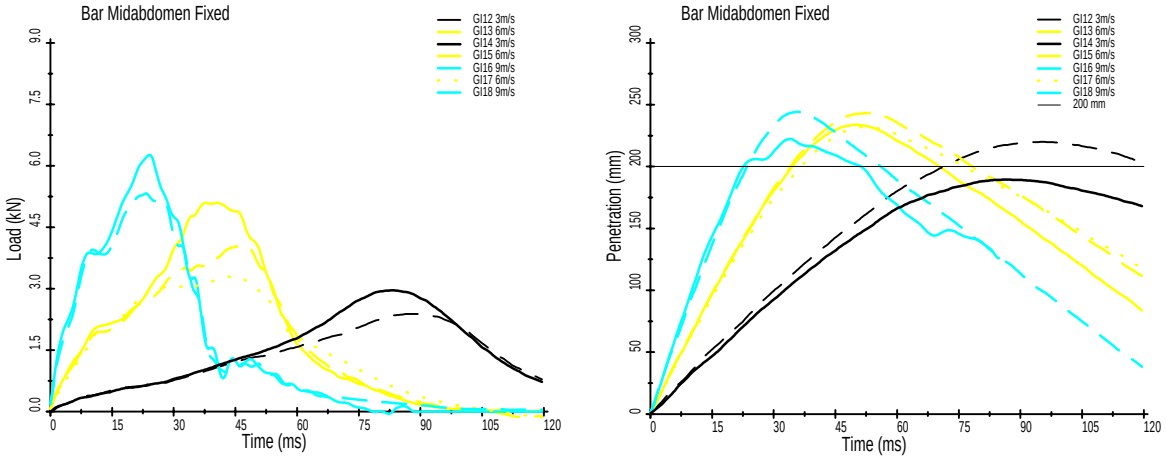

Figure 14. Load (LEFT) and penetration (RIGHT) data for all fixed-back rigid-bar impacts. The horizontal line on the penetration plot shows the point at which arrest of the pendulum began.

by a single peak, even for the high-speed tests. This differs from the free-back tests, and supports the hypothesis that subsequent recruitment of additional mass slows the cadaver slightly in the free-back condition. The reduction in peak load due to sequential testing is evident in the fixed-back data. However, the initial rise in load remains relatively unaffected from one test to the next, as does the slope of the penetration-time curves.

This suggests that multiple tests can be performed on a single large male cadaver without significant change in the impact response between tests when the primary purpose of the tests is the mechanical response, as opposed to injury response. This holds true only when energy levels are controlled such that the specimen is not grossly damaged. Importantly, however, no soft-tissue injuries were found upon autopsy of this cadaver.

3.2.2 Load-Penetration Responses

Figure 15 shows the load-penetration responses of the fixed-back rigid-bar tests. The first set of curves is unscaled data. The second set of curves is scaled (76 kg), SAE cc 60 Hz data compared to the Cavanaugh corridors. The third set of curves is also scaled (78 kg) data. The most important point that these data illustrate is that the human cadaver abdomen is rate sensitive. These fixed-back tests eliminated the flexion and motion of the spine and mass of the whole from the abdominal response. With these factors eliminated, the abdomen still shows rate sensitivity. The relative influences of local mass recruitment and tissue viscosity are unknown, however. These data also show that the initial stiffness of the abdomen does not change much from the free- to fixed-back condition. The fixed-back data match the first part of the Cavanaugh corridors quite well. Subsequently, the curves fall below the Cavanaugh corridors. This is probably because of the missing whole-body acceleration component. During the free-back tests, the reaction loads experienced by the pendulum result from compressing abdominal tissue and accelerating the body. During the fixed-back tests, the reaction loads result from compressing abdominal tissue only. It is reasonable to assume that the motion of a free-back specimen would begin at a force level below that at which the fixed-back curves begin to fall below the corridor.

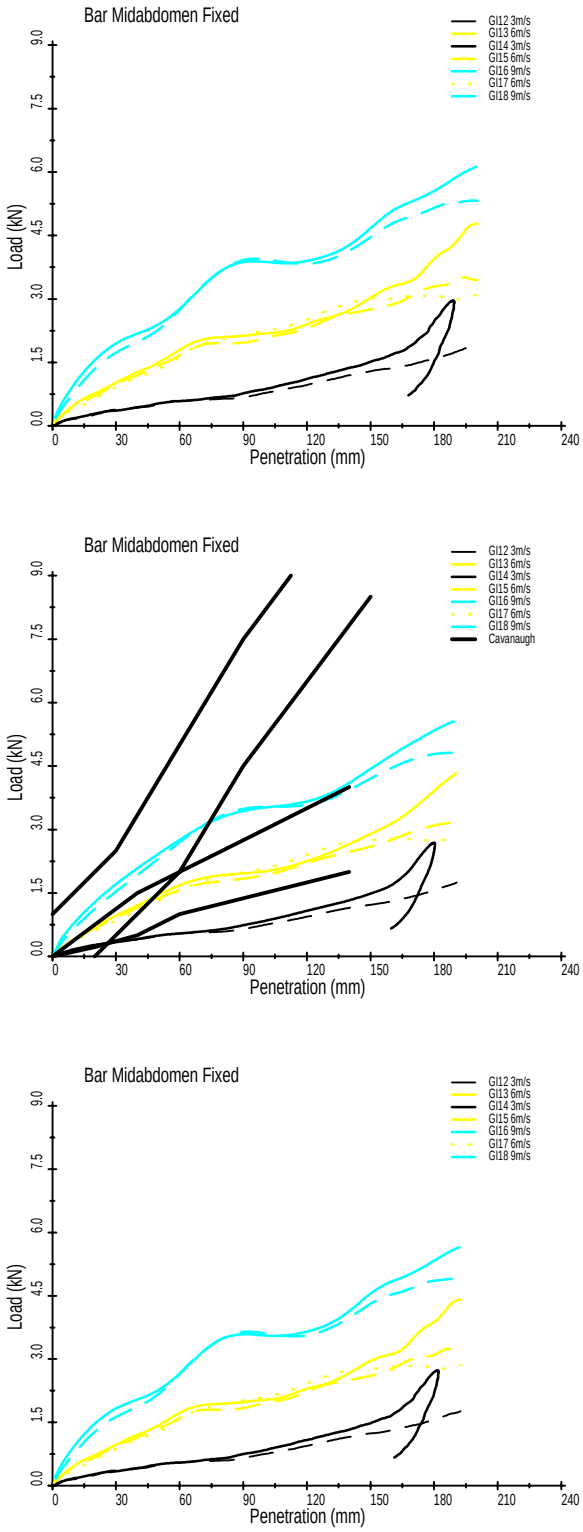

FIGURE 15. Load-penetration responses for all fixed-back rigid-bar tests. Original data (TOP), scaled and filtered per Cavanaugh et al. (1986) and compared to the Cavanaugh corridors (MIDDLE), equal-stress/equal-velocity scaled [78 kg] data (BOTTOM).

3.2.3 Comparison to Stalnaker Data

In addition to falling below the Cavanaugh corridors, the fixed back data also tend to exhibit a rise-plateau-rise response similar to that described by Stalnaker et al. (1985). This characteristic becomes more pronounced as the impact speed increases, which corresponds to increased rib involvement. There was considerable compression of the upper abdomen and lower thorax during the high-speed fixed-back tests. This is in keeping with the effects observed during the upper abdomen free-back tests, and some of the high-speed free-back midabdomen tests.

Alternately, this response could be related to mass effects. Other than fixed-back conditions, tests in which the mass of the cadaver is quite large (heavy individual) or somehow constrained (e.g., delay in release mechanism activation) might produce this type of three-stage response. In the aforementioned case, the mass of the striking object should be significantly greater than the local effective mass of the struck region of the cadaver. Otherwise, results similar to those of Nusholtz would likely be obtained. A possible scenario could be the following. The initial response of the abdomen of the heavy or constrained specimen would be similar to those of the light or free specimen, approximately to the point where the free specimen is set in motion. At this point, the response of the free specimen would reflect the addition of a whole-body inertial component (or gradually increasing percentage thereof). Therefore, the stiffness of the free specimen would continue to increase, whereas the stiffness of the "less-free" specimen would start to drop off, or plateau, as only compression of abdominal tissues occurs. Eventually, the tissues are compressed to the point that stiffness again increases, even in the absence of whole-body motion.

3.2.4 Low-Speed (3-m/s) Response

Of the scaled (78 kg) load-penetration responses, those in the 3-m/s range are of primary interest. The two 3-m/s range tests, GI12 and GI14, were averaged to obtain an estimate of the human cadaver response to low-speed rigid-bar loading. Because there are only two tests using a single cadaver, a response corridor could not be developed. However, the average response shown in Figure 16 suggests that the stiffness of the abdomen in this speed range is approximately 10 kN/m. Given the mass (88 kg) and size (350-mm initial abdominal depth) of the cadaver, it is unlikely that there would be much difference between the free- and fixed-back response at 3 m/s.

3.2.5 Injury-Related Findings

The autopsy results for the fixed-back rigid-bar tests are cataloged in Appendix A. No injuries to the abdominal organs were observed. The only injuries consisted of multiple rib fractures and a postmortem contusion (dried liquefied fat) of the anterior abdominal wall.

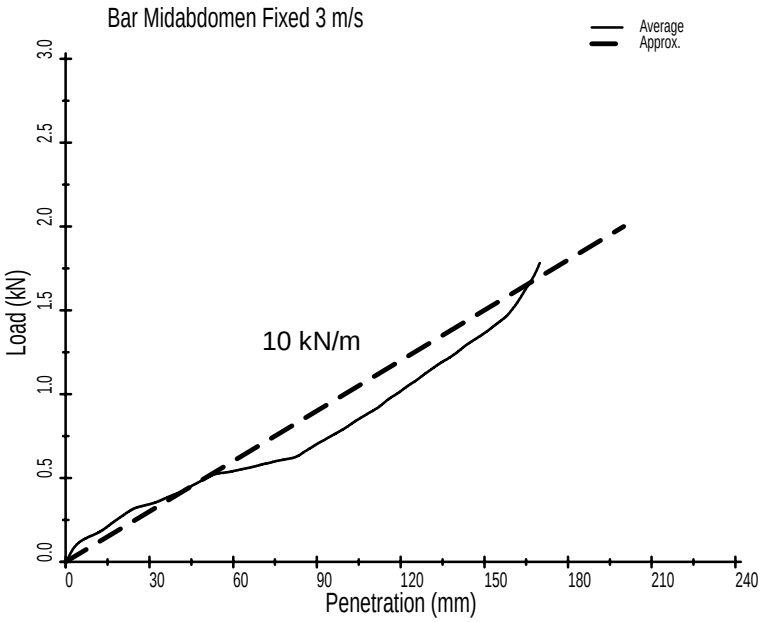

FIGURE 16. Fixed-back rigid-bar scaled load-penetration response for 3-m/s impact (averaged responses from GI12 and GI14). This response is likely to be representative of the abdominal response for the free-back condition as well.

3.3 SEATBELT TESTS

Six seatbelt loading tests were conducted using three cadavers. Each cadaver was tested twice. The first cadaver was subjected to a free- and a fixed-back test, both at the midabdomen level. The subsequent cadavers experienced a midabdomen test followed by a lower abdomen test. The penetration speeds averaged 3.5, +/- 1.0 m/s.

3.3.1 Load and Penetration Measurement

For the seatbelt tests, the load was determined using inertia compensation of output from a load cell in the ram of the seatbelt apparatus and by summation of loads measured by seatbelt load cells at each belt anchor point. Comparison of results from these two techniques provided confidence in the data, and showed that the belt maintained its original configuration, straight back from the sides of the cadaver, during the tests. Had the belt deviated from this position, agreement between the two load calculation methods would have been poor. Figure 17 shows the various components of the load calculation for both methods, and compares the calculated results for a typical test. The comparison was at least this good for all other tests.

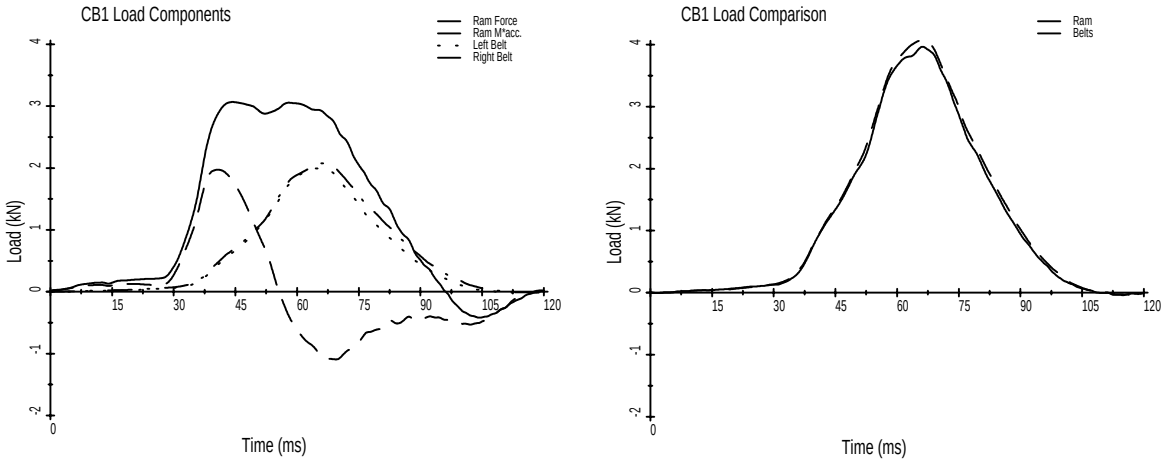

FIGURE 17. The various components involved in two methods for calculating seatbelt load (LEFT) and comparison of the results of the two methods (RIGHT), for test CB1.

Abdominal penetration was determined from three different components: (1) motion of the ram with respect to the laboratory, (2) motion of the spine with respect to the ram, and (3) motion of the belt with respect to the laboratory. Figure 18 shows these various components and the calculated penetration for a typical test. The first plot shows the difference between the ram motion and the spine with respect to the ram motion resulting in the spine motion with respect to the laboratory. The second curve shows calculation of abdominal penetration by taking the difference between the belt motion and the spine motion.

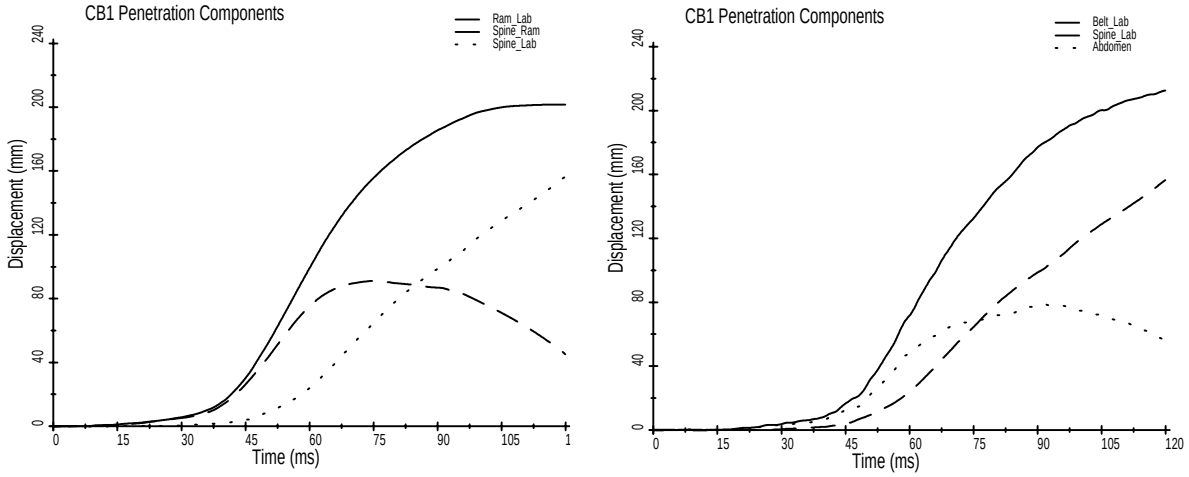

FIGURE 18. Determination of spine motion with respect to the laboratory during seatbelt loading (LEFT) and calculation of abdominal penetration from belt and spine motion (RIGHT) for test CB1.

3.3.2 Load, Penetration, and Penetration Speed Data

Figure 19 shows the load-time, penetration-time, and penetration speed-time histories from the three midabdomen seatbelt tests performed on different cadavers. The load-time histories are largely haversine in nature, as are the penetration-speed curves. Penetration speed is determined by differentiating the abdominal penetration data. The penetration speeds are approximately 3 m/s.

Fixed-Back Condition

Figure 20 compares a fixed-back midabdomen test (CB2) to a free-back test (CB1) performed on the same cadaver. The fixed-back comparison shows little change in the initial load and penetration response from the free-back condition. However, because the body is constrained, the peak load is much larger and the peak penetration is reached much sooner than in the free-back test. For the fixed-back test, the point at which the load and penetration decrease corresponds to the simple rung structure supporting the back giving way. The penetration speeds for these two tests were similar.

Abdomen Test Data

Figure 20 also compares results from two sets of lower abdomen tests to midabdomen tests. The pairs of midabdomen and lower abdomen tests were conducted using two cadavers, with each cadaver subjected to one of each type of test. The different types of test are grouped by line type in the plots, and the different cadavers are grouped by shade of gray. In general, the loads developed during the lower abdomen tests are greater than those seen in the midabdomen responses. For the first set of tests, CB3 and CB4, the penetration is less for the lower abdomen test. For the second set of tests, CB5 and CB6, the penetrations are greater for the lower abdomen test. However, the cadaver used for CB5 and CB6 (29131) had considerably more tissue in the lower abdomen region in front of the pelvis than did the cadaver used for CB3 and CB4 (29116). Like the trend seen in the rigid-bar tests, the tests in which the whole body moved more for a given penetration early in the event ultimately resulted in smaller peak abdominal penetrations. Differences between mid and lower abdomen geometry for cadaver 29131 resulted in the belt initially penetrating the lower abdomen at a higher rate, producing a shorter-duration load peak (CB6). The belt interacted with a greater amount of abdominal tissue sooner in the event during the midabdomen test CB5, resulting in greater whole-body motion initially and less penetration than were observed during CB6.

3.3.3 Load-Penetration Responses

Figure 21 shows the load-penetration responses for the belt loading tests. Comparison of the three midabdomen tests shows a large degree of similarity between the results, particularly concerning initial stiffness. The peak loads range from 3.1 to 4.1 kN, and the peak penetrations range from 75 to 95 mm. The fixed-back test produced a rather large peak load (6 kN), but the peak penetration (90 mm) was only 11 mm greater than that of the free-back test on the same cadaver. However, the initial stiffness responses are nearly identical for these two tests. Comparison of results for the lower abdomen tests to those of the midabdomen tests shows a very tight grouping of initial stiffness, although the responses subsequently diverge. The differences in peak penetration are greater than the differences in peak load. The peak loads range from 4.1 to 4.5 kN, and the peak penetrations range from 56 to 114 mm for the lower abdomen belt tests.

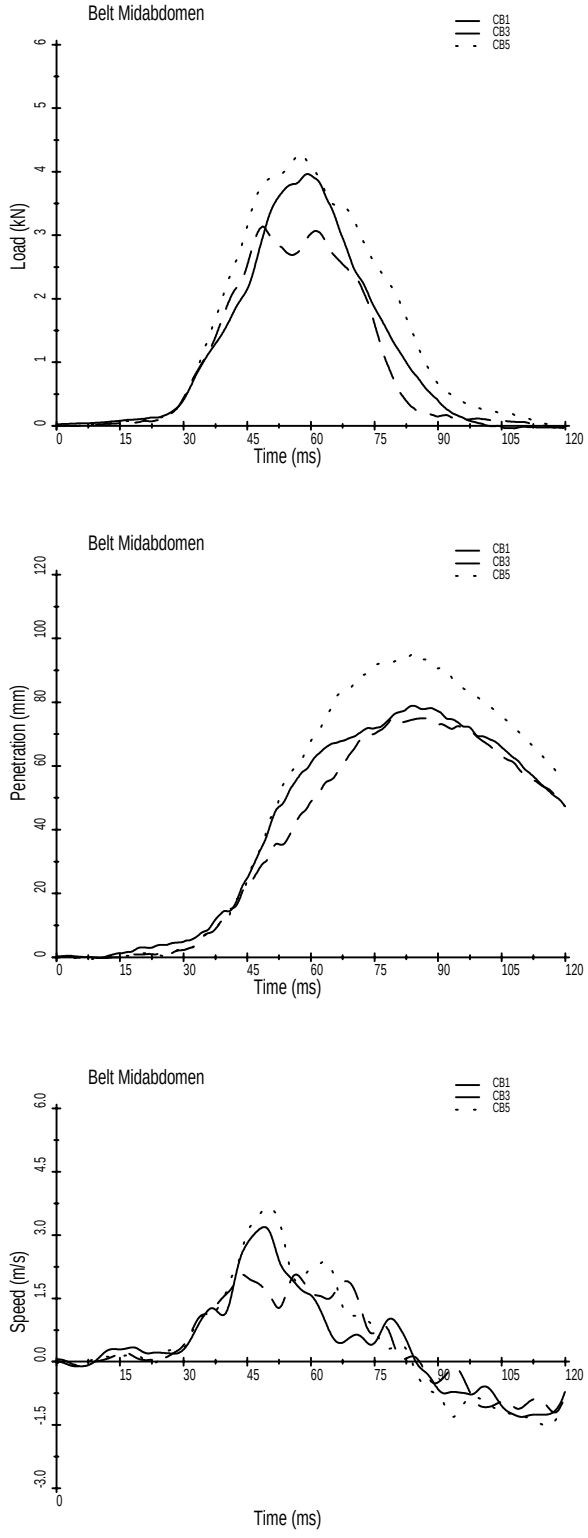

FIGURE 19. Load (TOP), penetration (MIDDLE), and penetration-speed (BOTTOM) data from the three midabdomen seatbelt tests performed on three different cadavers.

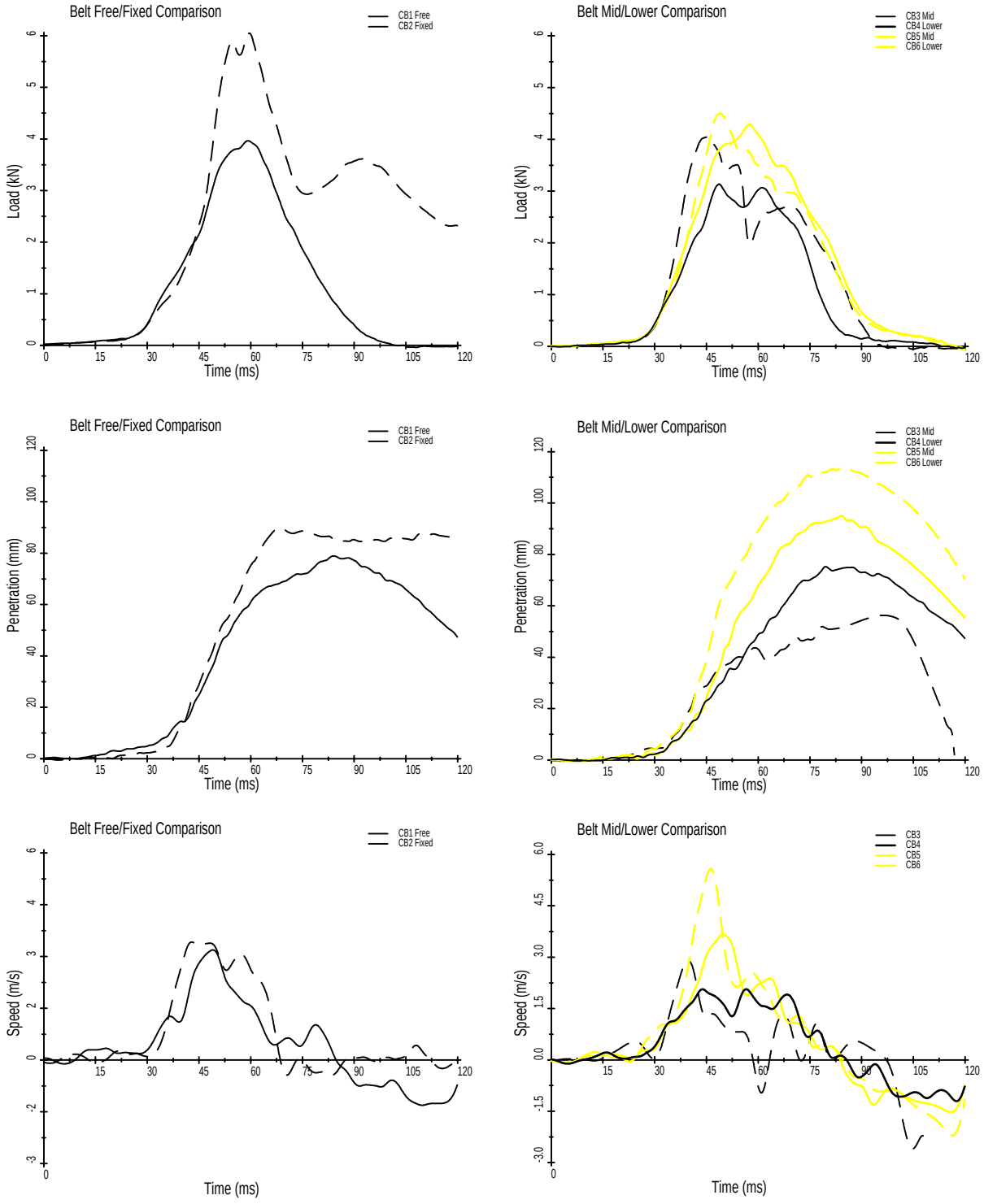

FIGURE 20. Comparison (LEFT) of load (TOP), penetration (MIDDLE), and penetration-speed (BOTTOM) data from fixed-back midabdomen test (CB2) to a free-back test (CB1), which were both performed on the same cadaver. Comparison (RIGHT) of load (TOP), penetration (MIDDLE), and penetration-speed (BOTTOM) data from two lower abdomen tests to two midabdomen tests. The midabdomen and lower abdomen tests were conducted using two cadavers, with each cadaver subjected to one of each type of test.

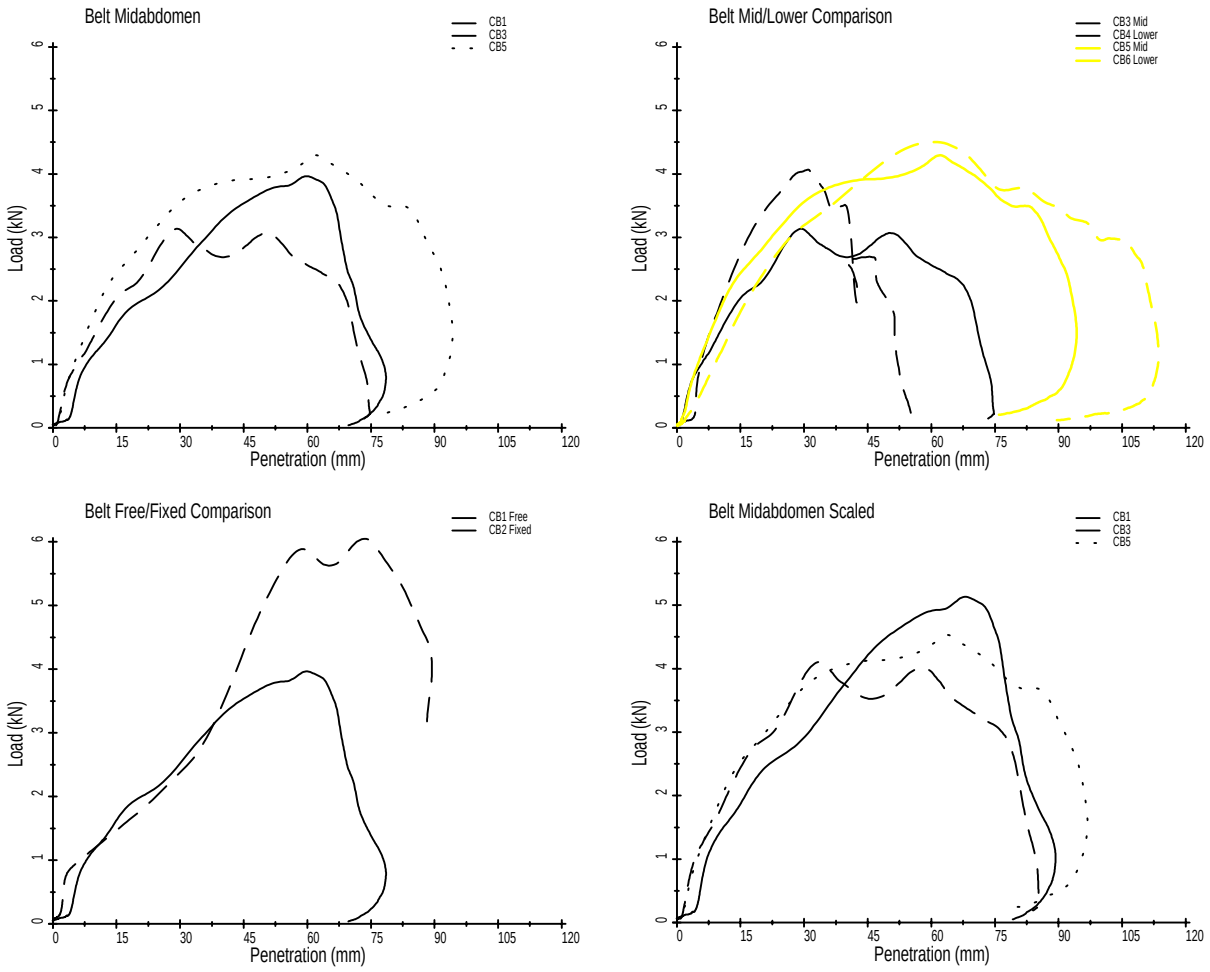

FIGURE 21. Load-penetration responses for the midabdomen belt-loading tests (UPPER LEFT); comparison of the lower abdomen to midabdomen responses (UPPER RIGHT); comparison of the fixed-back response to the free-back response for one cadaver (LOWER LEFT); and the equal-stress/equal-velocity scaled load-penetration responses for midabdomen belt loading (LOWER RIGHT).

Figure 21 also shows the equal-stress/equal-velocity scaled (78 kg) load-penetration responses for midabdomen belt loading. In this case, scaling resulted in a closer grouping of the curves. The initial stiffness results from circumferential loading of the front and sides of the abdomen by a relatively broad surface. This means that the lateral aspects of the abdomen have a significant influence in this response. Having the belt wrapped around the sides limits the lateral motion of abdominal tissue, and therefore reduces penetration of the belt into the anterior abdomen. This, combined with the distributed nature of the loading, produces large initial stiffness.

3.3.4 Development of New Response Corridor

Figure 22 shows the newly developed free-back seatbelt response corridor for the human cadaver abdomen loaded at the level of the umbilicus, and the average speed of penetration plotted with respect to penetration. The speed/penetration plot defines the performance required of a belt-loading device to produce this type of load-penetration response. This corridor was developed using three cadaver tests. Although this is a relatively small number of tests, the large degree of similarity between the tests provides confidence in the data and suggests that a reasonable general representation has been obtained. This corridor is defined by two piecewise continuous linear approximations of the standard deviations. Each approximation has three segments. The slope (stiffness) of each segment of the upper bound is the same as that of the corresponding lower bound. The loading stiffness is 120 kN/m. The subsequent stiffness is significantly lower (25 kN/m), and the unloading is opposite the loading (-120 kN/m). The penetration speed profile needed to produce this result is a 3-m/s peak haversine over 90 mm of abdominal penetration.

3.3.5 Comparison to Miller and Cavanaugh Data

Figure 23 compares the fixed-back and lower abdomen responses to the new midabdomen belt-loading corridor. Although each of the curves exceeds the boundaries of the corridor, the initial responses are quite similar. Figure 24 compares the new belt-loading corridor to a plus-and-minus one standard deviation corridor adapted from the results of Miller (1989) and to the high-speed Cavanaugh rigid-bar corridor. The initial response characteristics of the corridor developed from the results of this study suggest stiffness four times that of the Miller data (120 kN/m vs. 30 kN/m). This is most likely due to the difference in the way the belt interfaced with the abdomen in these two studies. For the Miller investigation, only the center of a length of belt webbing was in contact with the abdomen initially, and webbing contact increased throughout the course of a test. Therefore, there was essentially no constraint of the lateral aspects of the abdomen. In the present study, the webbing was wrapped around abdomen, engaging the lateral aspects of the abdomen, from the start of each test. In the Miller tests, the abdomen was able to “escape” the belt by deforming to the side. In these tests, the abdomen was unable to deform in this way, creating a much stiffer response. In comparison to rigid-bar tests, although the belt penetrates into the abdomen relatively slowly (3 m/s) compared to the impactor used in the Cavanaugh study (10 m/s), the belt-loading response is stiffer initially. This is due to the distributed nature of the belt loading, and again to the influence of the sides of the abdomen during the belt tests.

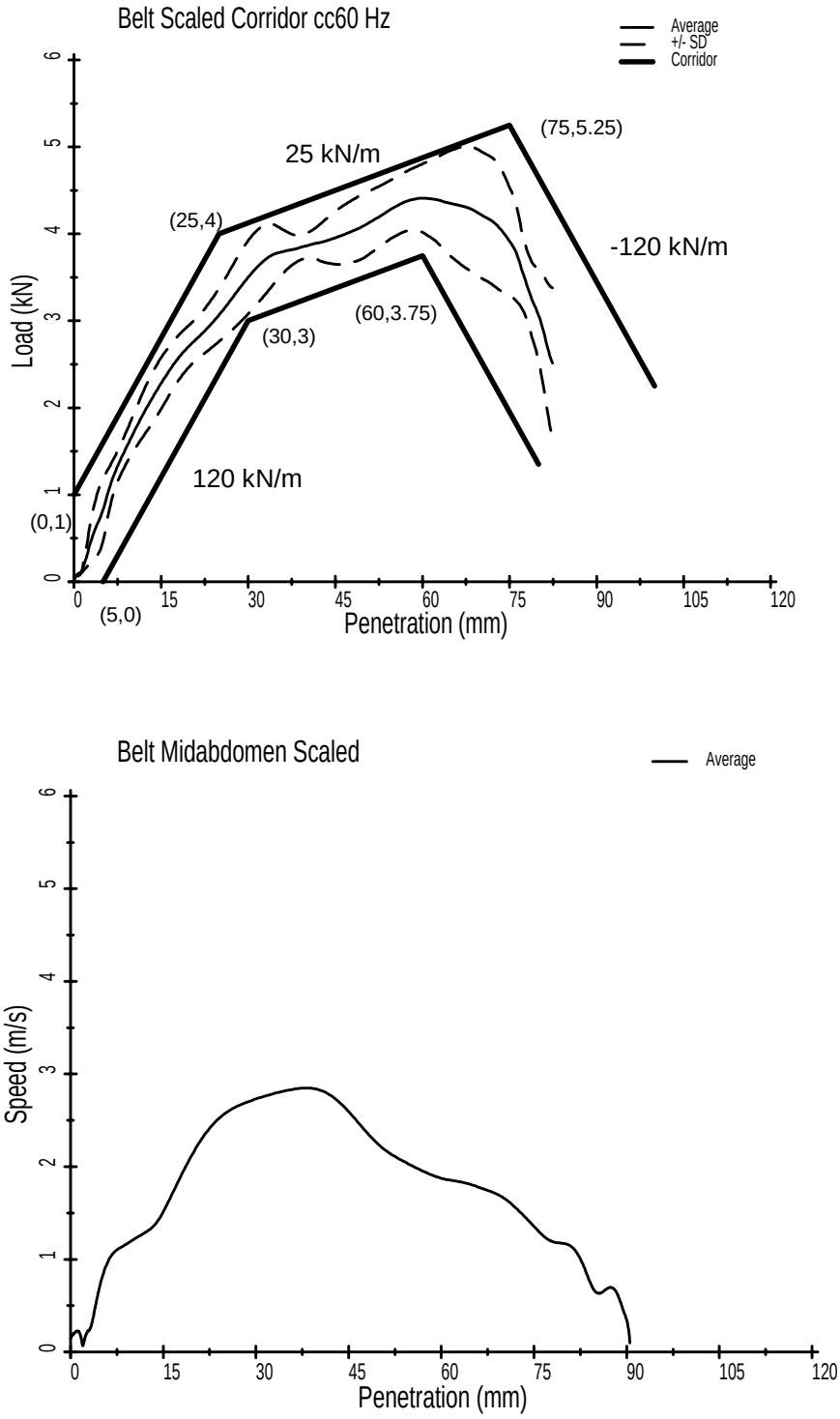

FIGURE 22. Newly developed free-back seatbelt response corridor for the human cadaver abdomen loaded at the level of the umbilicus (TOP), and the average speed of penetration with respect to penetration, which defines the input required to produce this type of response (BOTTOM).

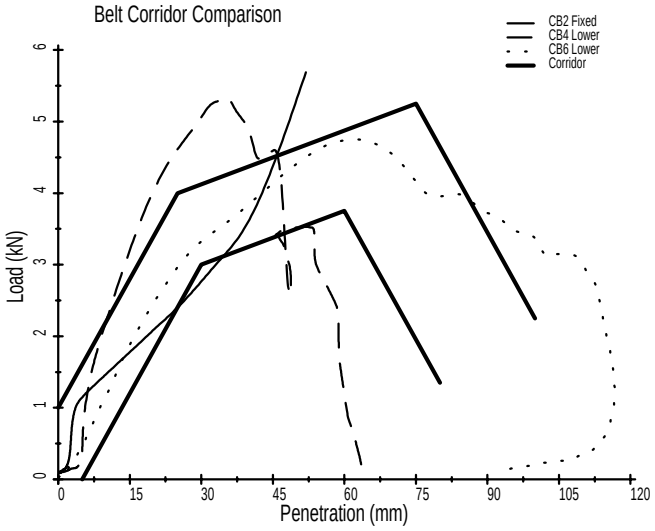

FIGURE 23. Comparison of the fixed-back and lower abdomen responses to the midabdomen corridor.

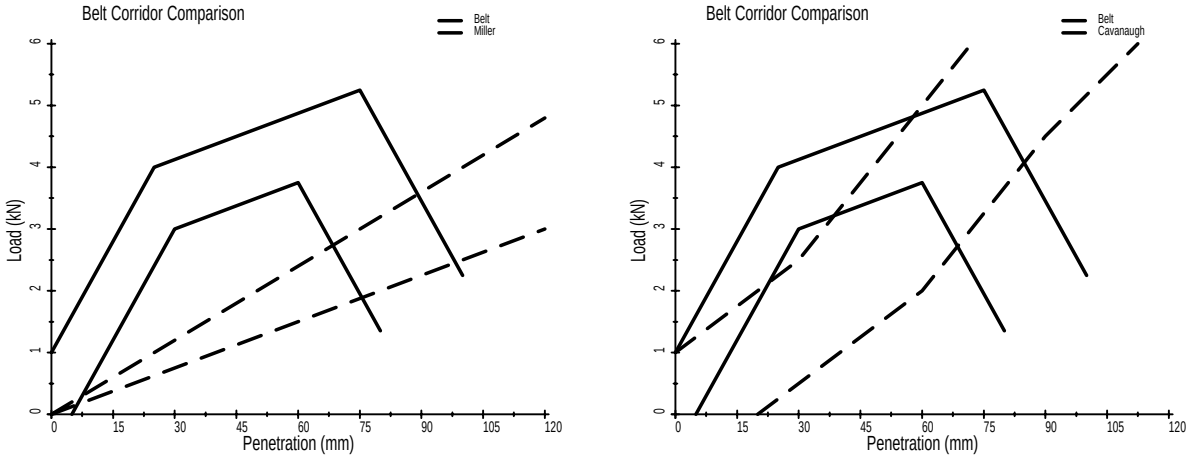

FIGURE 24. Comparison of the new belt-loading corridor to a plus-and-minus one standard deviation corridor (LEFT) adapted from the results of Miller (1989) and to the high-speed Cavanaugh rigid-bar corridor (RIGHT).

3.3.6 Injury-Related Findings

The autopsy results obtained from the seatbelt tests are cataloged in Appendix B. No injuries to the abdominal organs were found. Multiple rib fractures were observed in the small-female cadaver used for the fixed-back test. Fewer rib fractures were observed in a male cadaver suffering from severe osteoporosis. It is unlikely that many, if any, rib fractures would have been found in the absence of osteoporosis and if the fixed-back test was not performed.

Table 7 summarizes the maximum impact speed, load (SAE cc 180 Hz), penetration (SAE cc 180 Hz), compression, load*compression, viscous response and peak anteroposterior spine acceleration opposite the level of impact for the seatbelt loading tests. The MAIS level is also provided. No clear relationship or distinction between the response parameters and MAIS is evident.

TABLE 7
Seatbelt Test Results: Peak Values

Test	Region	Type	Speed (m/s)	Load (N)	Penetration (mm)	Comp. (%)	Comp. * Load (N)	V*C (m/s) cc180	V*C (m/s) fir100	L4/*S2* Acc. (g)	MAIS
CB1	Mid	Free	3.2	3965	79	33	1298	0.7	0.5	-	4
CB2	Mid	Fixed	3.4	6050	90	29	1757	1.1	0.9	-	4
CB3	Mid	Free	2.1	3136	75	36	1124	0.8	0.5	14.0	3
CB4	Lower	Free	2.9	4067	56	26	1041	0.6	0.3	*38.9*	3
CB5	Mid	Free	3.7	4295	95	33	1422	0.9	0.6	9.4	0
CB6	Lower	Free	5.6	4501	114	37	1681	1.2	0.9	*27.5*	0

3.4 AIRBAG TESTS

Three cadavers were used in three close-proximity passenger airbag tests. The penetration speeds ranged from 10.7 to 12.9 m/s for these tests. Three additional cadavers were used in six surrogate airbag tests. The first cadaver was tested four times, while the second and third cadavers were tested only once. The penetration speeds from the three usable surrogate airbag tests averaged 13.2, +/- 0.3 m/s.

3.4.1 Surrogate Airbag Load Measurement

The penetration-time histories obtained from the passenger airbag tests were used to develop the surrogate airbag device. Contact loads could not be measured during the passenger airbag tests, but were measured during the surrogate airbag tests. The surrogate airbag tests were used to develop load-penetration corridors for the early stages of airbag-like loading. Acceleration of the surrogate airbag device and the pressure driving the device were used to calculate contact interaction loads. Since pressure was measured at the device's rapidly accelerated piston face, a special acceleration resistant pressure transducer was used. To calculate load, the surrogate airbag mass multiplied by acceleration was added to the driving pressure multiplied by the area of the piston face. Figure 25 shows these load components from a cardboard honeycomb test as well as the outputs from two reaction load cells. The calculated interaction load is then compared to the sum of the reaction loads. Unless the struck object had zero mass, this comparison could never be exact. With this in mind, the comparison is quite good, illustrating the efficacy of this approach.

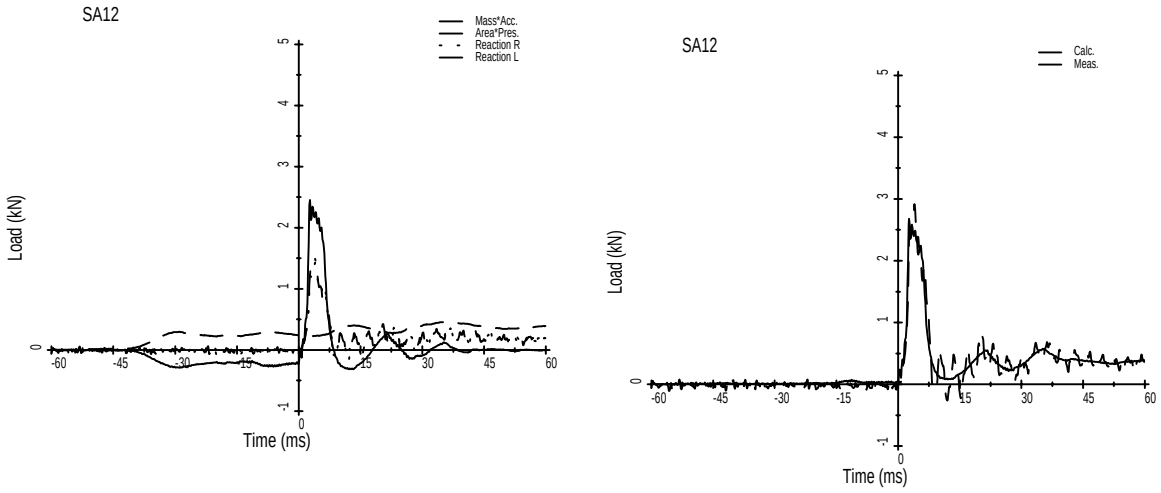

FIGURE 25. Components used in the calculation of surrogate airbag load and reaction load. The surrogate airbag mass multiplied by acceleration was added to the driving pressure multiplied by the area of the piston face (LEFT). The calculated interaction load (cardboard honeycomb impact) is then compared to the sum of the reaction loads measured by two load cells (RIGHT).

3.4.2 Surrogate Airbag Repeatability

One of objectives of the surrogate airbag design was to provide a controllable and repeatable method of simulating the punch out phase of a midmount passenger airbag loading the cadaver abdomen. Penetration was the parameter controlled to provide this simulation. Figure 26 shows the displacement-time history of the surrogate airbag device for two impacts of silicone padding. The tests are two impacts conducted one after the other during the design of the surrogate airbag. These tests illustrate the repeatable way in which the surrogate airbag performs.

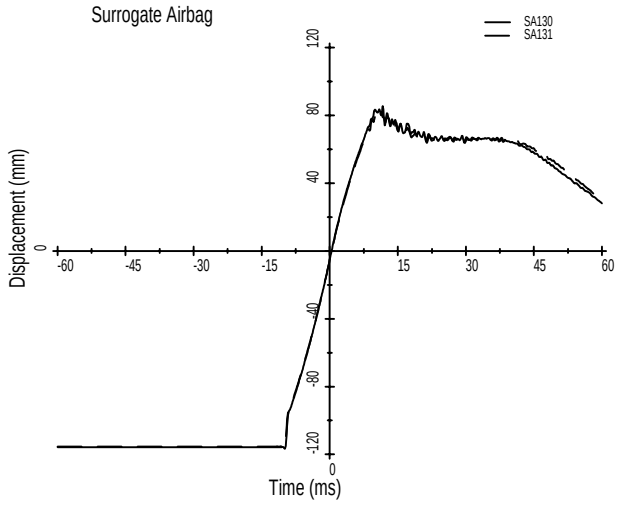

FIGURE 26. Displacement-time history of the surrogate airbag device for two impacts of silicone padding, illustrating the repeatability of the device.

3.4.3 Passenger and Surrogate Airbag Penetration Data

Figure 27 shows the penetration-time histories of the actual passenger airbag (AA) and airbag surrogate (AS) tests. The results of the airbag tests are shown in the first plot. The largest penetration obtained from any of the airbag tests is 76 mm (AA2). This was from a test using a next-generation midmount passenger airbag with the module door removed. The cadaver abdomen was in direct contact with the airbag fabric prior to deployment. The smallest penetration was obtained using the same airbag with the cadaver 50 mm from contact with the fabric prior to deployment (AA3). The most extreme of these cases was selected as a design goal for the surrogate airbag. Therefore, the surrogate airbag was designed to penetrate at least 76 mm into the cadaver abdomen. The results of the surrogate airbag tests are shown in the second plot. Since the first three tests of the first cadaver were used to further refine the performance of the surrogate airbag, only AS4-AS6 are presented. Since the device was designed to exhaust the driving pressure after 76 mm of penetration, the laser tracking the surrogate airbag impactor was occasionally disrupted after this point, causing the oscillations shown in the traces. This is of little consequence as only the first 76 mm are of importance. The third plot compares the average of the surrogate airbag penetration-time histories to the airbag penetration-time histories. The 76-mm limit is also shown. This plot shows that the surrogate airbag simulated the actions of the actual passenger airbags quite well. Because the driving pressure was exhausted after 76 mm, the contact interaction load could not be calculated beyond this point, even though the surrogate airbag impactor continued to penetrate the abdomen.

3.4.4 Passenger and Surrogate Airbag Penetration Speed Data

Figure 28 shows the penetration speed-time histories of the airbag and surrogate airbag tests. The results of the airbag tests are shown in the first plot. The peak penetration speed obtained from any of the airbag tests was 12.9 m/s (AA2). The lowest penetration speed obtained is 10.7 m/s. Therefore, the surrogate airbag device was designed to penetrate the cadaver abdomen at peak speed of approximately 13 m/s.

The results of the surrogate airbag tests are shown in the second plot. The laser lost accurate tracking for a portion of test AS4. This is indicated by the shaded section of curve. The third plot compares the average surrogate airbag penetration speed to the passenger airbag penetration speeds. This plot illustrates the large degree to which the surrogate device simulates the close-proximity airbag loading. One difference, however, is that the peak penetration speed occurs at contact for the surrogate airbag, but after contact for the actual airbags. This is because the surrogate device is at peak speed at the time of contact, while the deploying airbags were still inflating and building speed at the time of contact.

Although there are some differences in the penetration-speed profiles of the passenger and surrogate airbag tests, these differences are thought to be negligible. A far greater factor in the injury response of the cadavers is likely to be the large surface area attained by the passenger airbags after the initial punch-out phase, as opposed to the small contact area maintained by the surrogate airbag. This would be difficult to ascertain considering the time of injury cannot be determined during any of the airbag tests.

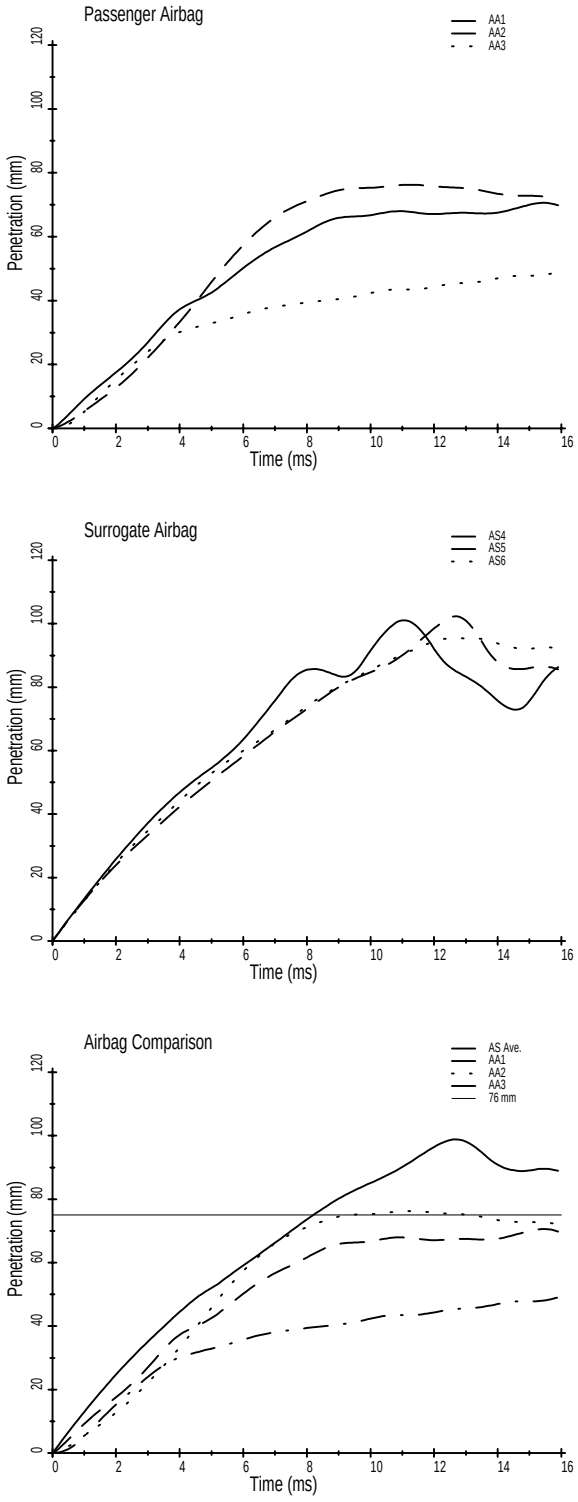

FIGURE 27. Penetration-time histories of the passenger airbag tests (TOP), the surrogate airbag tests (MIDDLE), and a comparison between the average response of the surrogate airbag tests and the individual passenger airbag tests (BOTTOM). Because of pressure release, surrogate load could not be calculated for penetration greater than 76 mm.

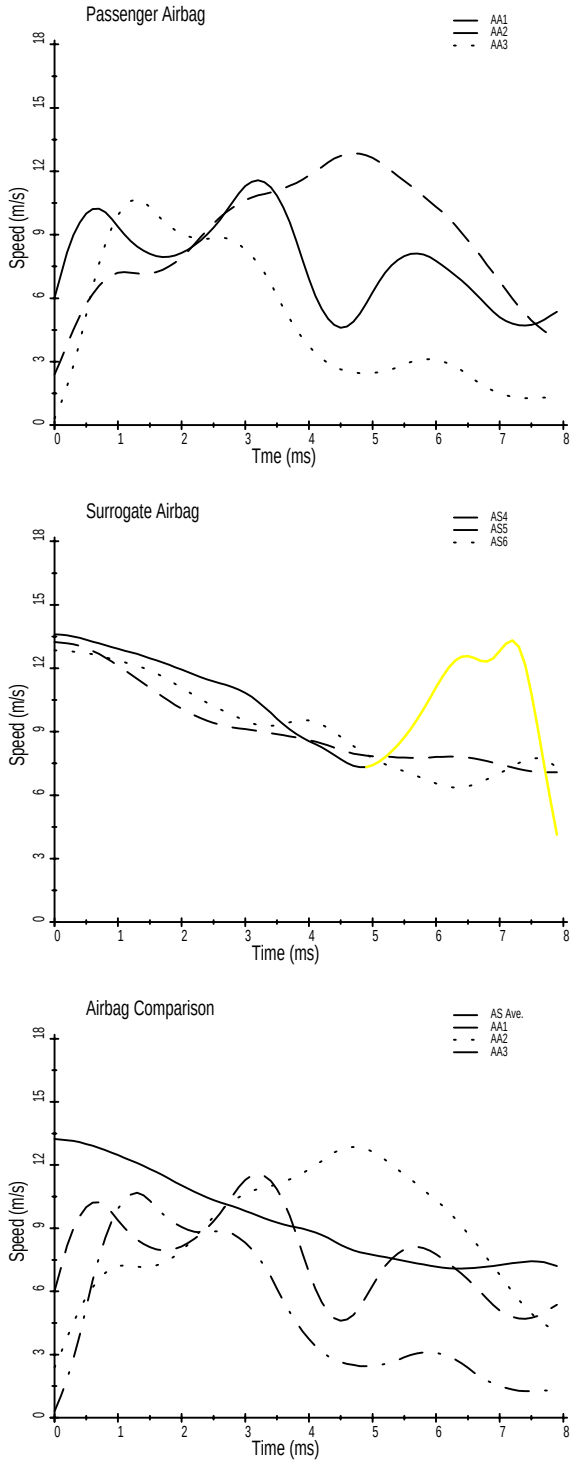

FIGURE 28. Penetration speed-time histories from the passenger airbag tests (TOP) and surrogate airbag tests (MIDDLE). The BOTTOM plot compares the average surrogate airbag penetration speed to the penetration speeds from the individual passenger airbag tests, illustrating the degree to which the surrogate airbag simulated the passenger airbags.

3.4.5 Surrogate Airbag Load-Penetration Responses

Figure 29 shows the load-time histories, the load-penetration responses and the scaled (78 kg) load-penetration responses for the surrogate airbag tests. The load-time histories are characterized by an initial very fast, very steep rise, followed by a slightly oscillatory decay. The entire event transpires in less than eight milliseconds, but the most important part takes less than two milliseconds. The load-penetration responses look very similar to the load-time histories. The peak loads range between 3.8 and 4.6 kN. The penetrations are limited by the design of the surrogate airbag device. The equal-stress/equal-velocity scaling causes the data to separate slightly, as in the case of the rigid-bar data. However, given the closeness of the original data, this is not a dramatic effect.

3.4.6 Surrogate Airbag Response Corridor

Figure 30 shows the load-penetration corridor generated for the response of the human cadaver abdomen to airbag-like loading. Again, the corridor results from piecewise linear approximations of the plus-and-minus standard deviations of the data. As previously described, the load data were first brought to a common basis by interpolation with respect to penetration. The initial stiffness is the most important part of this corridor. As such, the lower oscillations of the response were sacrificed in the generation of the corridor in an effort to preserve the initial stiffness and produce a relatively simple corridor. The lower bound of the initial stiffness is 500 kN/m, and the upper bound is 2000 kN/m. The descending slope of the lower bound is –75 kN/m, while the two upper bound descending slopes are –100 and –50 kN/m.

3.4.7 Comparison to Cavanaugh Data

Figure 31 shows the newly developed surrogate airbag response corridor compared to the high-speed Cavanaugh rigid-bar loading corridor. The initial stiffness of the surrogate airbag corridor is significantly larger than that of the Cavanaugh data.

3.4.8 Injury-Related Findings

The autopsy findings for the airbag and surrogate airbag tests are cataloged in Appendix C. The airbag tests resulted in injuries to the ribs, colon, liver, mesentery, peritoneum, and diaphragm. The surrogate airbag tests resulted in far fewer injuries, but still produced liver lacerations. Figure 32 shows some of the more interesting injuries generated by the airbag tests. Figure 32a shows a tear of the transverse colon serosa experienced by cadaver 29613 during airbag test AA1. In this test, the abdomen was in contact with the module doors prior to deployment, but there was a 4-cm gap between the doors and the airbag fabric due to the design of the airbag. Figure 32b shows peritoneal tears experienced by the same cadaver. These injuries are similar to those that might be expected from an underwater blast. Figure 32c shows a liver laceration experienced by cadaver 29739 during test AA2. This test involved a next-generation airbag, but the module doors were removed, placing the cadaver abdomen in direct contact with the airbag fabric prior to deployment. The injuries sustained by this cadaver were slightly less complicated than those sustained by cadaver 29613. The reduction of injury using the next-generation airbag would probably have been more pronounced had test AA2 also had a 4-cm gap between the airbag fabric and the abdomen. Test AA3, which involved a next-generation airbag and 5-m spacing between the airbag fabric and the abdomen, resulted in fewer injuries than the contact case, AA2. The surrogate airbag tests resulted in relatively few injuries. This is because only the initial stages of punch-out loading are simulated by this device. Cadaver 29490, a smaller female, sustained multiple liver lacerations over the course of four impacts. Cadaver 29566 sustained no abdominal trauma, while cadaver 29491 experienced mild liver damage.

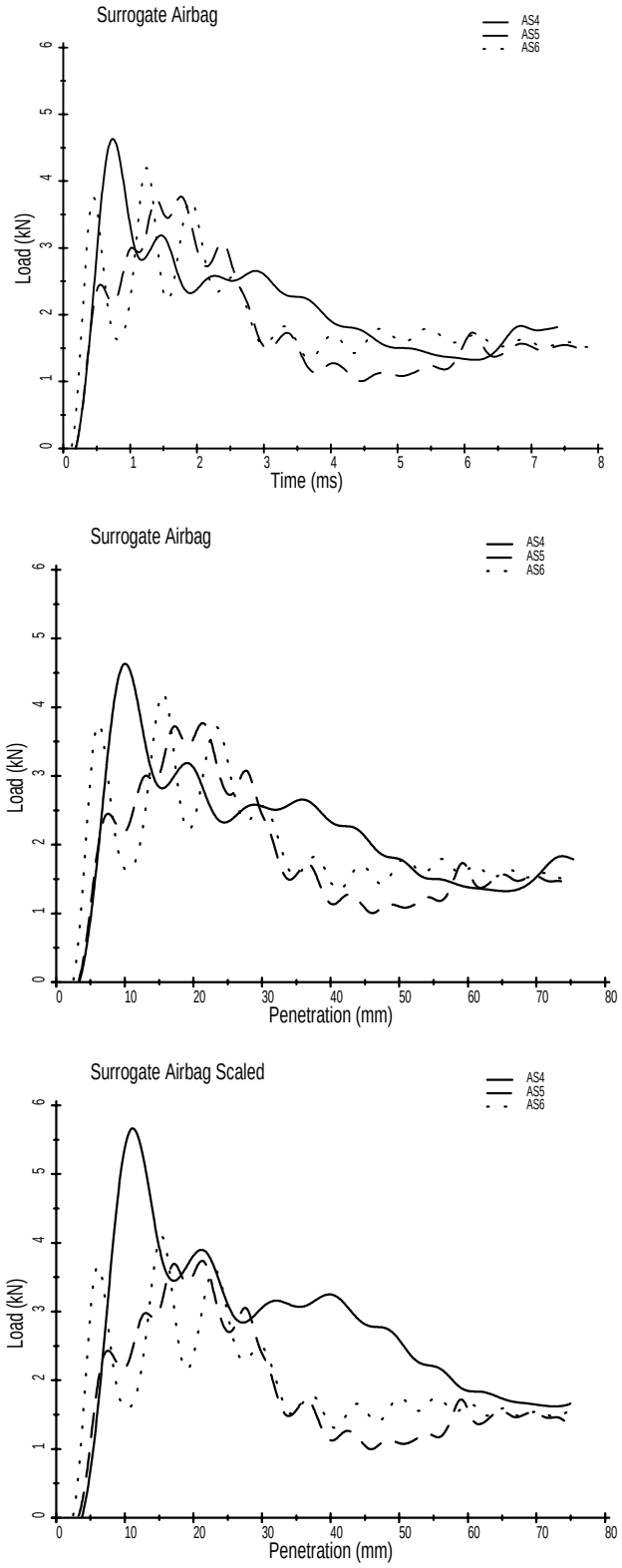

FIGURE 29. Surrogate airbag load-time histories (TOP), load penetration responses (MIDDLE), and equal-stress/equal-velocity normalized [78 kg] load-penetration responses (BOTTOM).

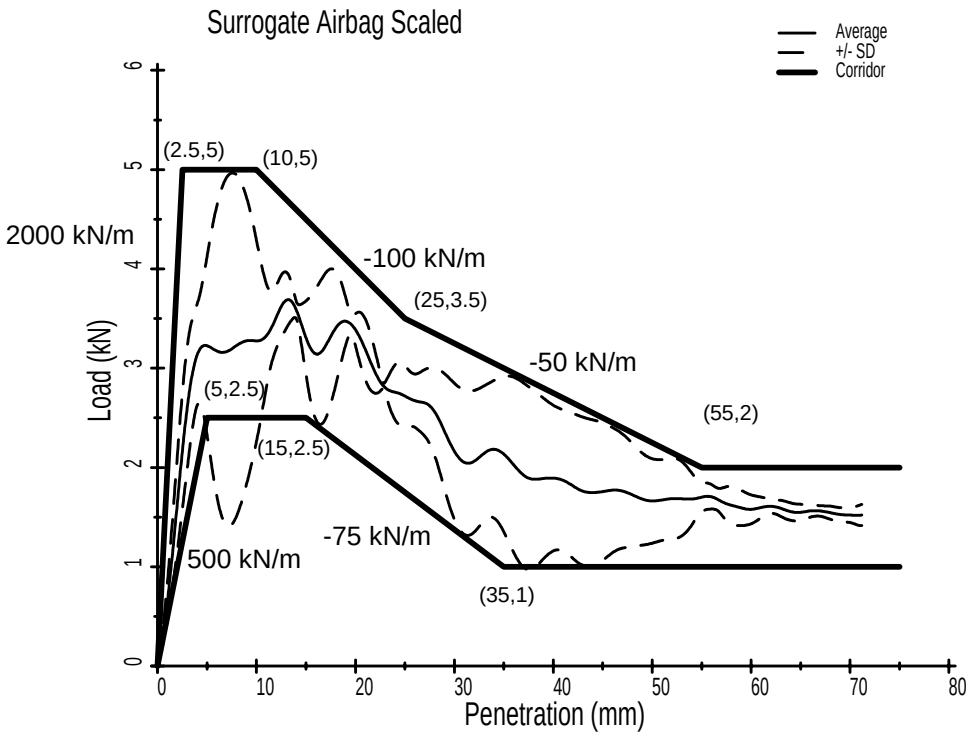

FIGURE 30. The load penetration corridor generated for the response of the human cadaver abdomen to airbag-like loading.

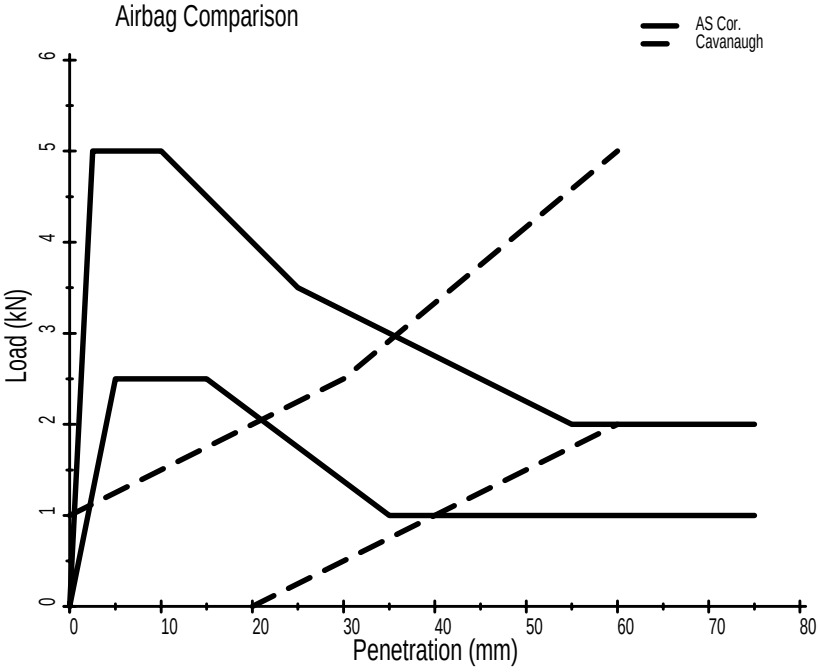

FIGURE 31. The newly developed surrogate airbag response corridor compared to the high-speed Cavanaugh rigid-bar loading corridor.

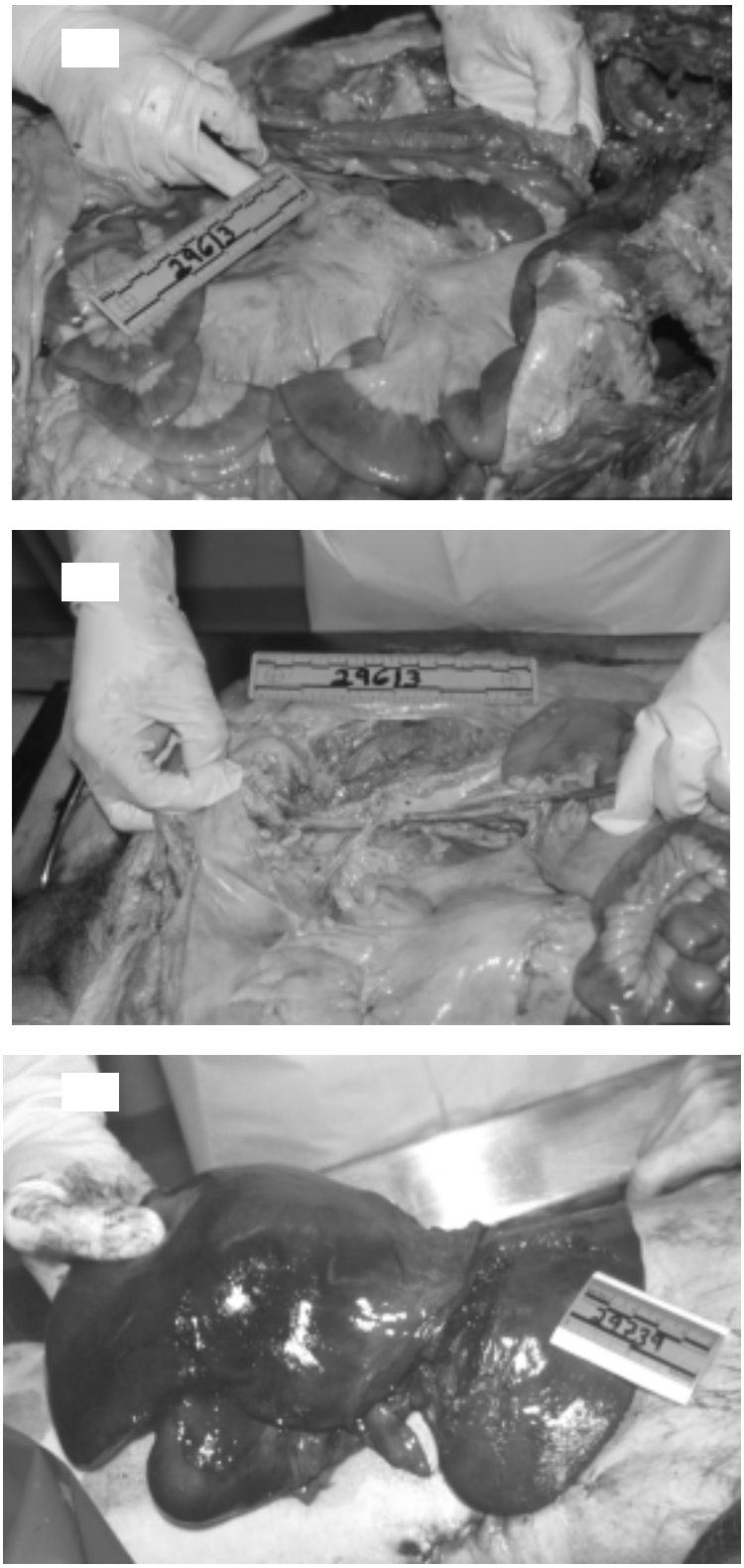

FIGURE 32. Some of the more interesting injuries generated by the passenger airbag tests: (a) tear of the transverse colon serosa (CAD 29613/AA2); (b) peritoneal tears (CAD 29613/AA1); (c) liver laceration (CAD 29739/AA2).

Table 8 summarizes the maximum impact speed, load (SAE cc 1k Hz), penetration (SAE cc 180 Hz), compression, load*compression, viscous response and peak anteroposterior spine acceleration opposite the level of impact for the airbag and surrogate airbag tests. It was not possible to measure load during the passenger airbag tests. The MAIS level is also provided. No clear relationship between the response parameters and MAIS is evident.

TABLE 8
Airbag Test Results: Maximum Values

Test	Airbag	Speed (m/s)	Load (N)	Penetration (mm)	Comp. (%)	Comp. * Load (N)	V*C (m/s) cc180 fir100		L4 Acc. (g)	MAIS
AA1	Passenger	11.6	-	73	32	-	1.7	1.5	72.5	4
AA2	Passenger	12.9	-	76	32	-	2.5	2.2	76.0	4
AA3	Passenger	10.7	-	50	24	-	0.9	0.7	93.5	3
AS4	Surrogate	13.6	4633	101	38	1752	5.0	2.4	-	2
AS5	Surrogate	13.2	3769	102	33	1258	2.7	1.7	-	1
AS6	Surrogate	12.9	4197	95	32	1347	1.9	1.7	-	2

4.0 DISCUSSION

This study investigated the frontal impact response of the human cadaver abdomen to different types of loading. Rigid-bar (steering rim), seatbelt, and airbag loading tests were conducted. Load-penetration response corridors were developed for each type of loading, and compared to the available existing data. In addition, testing apparatus and methods that could be used for standardized testing have been developed.

Twenty cadavers were used in thirty-three tests. Eleven free-back rigid-bar tests were conducted using ten cadavers. The first cadaver was impacted twice as proof of concept for the newly developed laboratory fixtures and the results were not presented. The remaining nine cadavers were each tested once. Response of the mid and upper abdomen was tested using two different speeds. An additional cadaver was used for seven fixed-back rigid-bar tests. Six seatbelt tests were conducted using three cadavers, each cadaver being tested twice. The first cadaver was tested about the midabdomen in both free- and fixed-back configurations, while the other two cadavers were tested about the mid and lower abdomen. Response to midmount passenger airbag deployment was investigated in three tests using three cadavers. The penetration-time histories from these tests were used to design a simplified, repeatable surrogate airbag device. This device was used in six tests using three cadavers. The first cadaver was tested four times, but the subsequent cadavers were each tested once. The stiffness of the resulting corridors increased from the 3-m/s midabdomen bar tests (10 kN/m), to the 6-m/s midabdomen bar tests (21 kN/m), to the 6-m/s midabdomen bar tests (63 kN/m), to the 3-m/s seatbelt tests (120 kN/m), to the 13-m/s surrogate airbag tests (1250 kN/m). The upper abdomen tests fell between the 6 and 9-m/s bar tests, their responses being characterized by more than a single stiffness.

4.1 IMPACT RESPONSE CONSIDERATIONS

The test methods used in this study represent approximations or simulations of real-world events. The test methods were designed to provide simplified, easily controlled and measured, repeatable events containing key aspects of real-world impact inputs and injury outcomes. Aside from providing insight into the response of the human cadaver abdomen to various types of loading, these tests provide information applicable to the design of other human surrogates such as the Hybrid III dummy, and to the design of standard testing techniques.

4.1.1 General Issues

Efficacy of Cadaver Model

All of the cadavers were tested after rigor mortis had passed. None of the cadavers was embalmed. All of the cadavers were tested fresh except for those frozen for use in the surrogate airbag tests. This was acceptable because the passenger airbag tests were used to determine injury response, and little injury was expected from the relatively low energy surrogate airbag tests. A number of researchers have used animals to investigate abdominal impact and injury response using an *in vivo* model. A cadaver model cannot produce the same mechanical or injury response of living tissue (muscle tone, circulation, respiration), but has the advantage of anatomic similarity. The influence of muscle tone is not known, but is assumed to be small for high-energy tests. The effects of circulation and respiration can be somewhat simulated using appropriate perfusion and ventilation

techniques. These experiments paid particular attention to the temperature of the specimens and the level of perfusion. The cadavers were brought to near-physiologic temperature using heated normal saline pumped into the arterial system slightly above physiologic pressures. The lungs were inflated using compressed air just prior to impact. The types of abdominal injuries obtained in the cadaver model will not be identical to those a human would experience, but are close approximations. The injuries seen in this study are generally commensurate with the available field data.

Rationale for Multiple-Impact Testing

Some cadavers in this study were tested more than once. This is not highly significant in this study because the primary focus was mechanical response rather than injury response. Any change in mechanical response between tests is not as crucial as the inability to attribute a given injury to a specific input. However, relatively few cadavers were tested more than once. The fixed-back rigid-bar tests showed that the mechanical response of the abdomen of a large male cadaver changes little between tests when excess energy is managed appropriately. The results of these tests provided enough confidence to conduct two belt tests, one free- and one fixed-back, in the midabdomen region of one cadaver. The similarity between the initial responses obtained from both of these tests indicated that conducting two belt tests in different regions of each of the remaining cadavers would be acceptable practice. It is unlikely that the mechanical response of the subsequent tests was affected much by the initial tests on each cadaver. The same holds true for the multiple surrogate airbag tests conducted on one cadaver; the impact response changed little between tests. It should be noted, however, that more injuries were observed in the cadaver that experienced the multiple surrogate airbag tests than in those that experienced a single surrogate airbag test.

4.1.2 Rigid-Bar Tests

The free-back rigid-bar tests clearly illustrate the rate dependent nature of the human cadaver abdomen. It is not known whether this response is due to mass recruitment or tissue viscosity, or both. The mass of the impactor (48 kg) being substantially greater than the effective mass of a typical abdomen probably helped disclose this response.

The results of this study agree well with the stiffness of the Cavanaugh corridors for rigid-bar loading of the midabdomen. The average stiffness of the lower speed tests was 27 kN/m (Cavanaugh, 21 kN/m), and the average stiffness of the high-speed tests was 63 kN/m (Cavanaugh, 70 kN/m). The lower speed tests of this study were faster than those of the Cavanaugh study, and the high-speed tests were conducted approximately 1 m/s slower. These differences in speed could account for the slight differences in stiffness between the two studies, e.g. a linear velocity scaling of the high-speed data from this study using the speeds from the two studies results in a stiffness of 70 kN/m, which is the same as that of the high-speed Cavanaugh data.

Elimination of the action of the spine and the role of the mass of the body as a whole during the fixed-back tests disclosed the rate dependent nature of abdominal tissues themselves. In fact, the load-penetration responses of the fixed-back tests matched the Cavanaugh corridors for initial loading. It is hypothesized that eliminating the inertial component of whole-body motion, e.g. removing a large mass-times-acceleration component, results in the load-penetration responses for fixed-back tests falling below the corridors for free-back tests.

For the midabdominal impacts in this study, the rigid bar struck the cadaver approximately at the level of the umbilicus or L3. For the upper abdominal impacts, the rigid bar struck the cadaver approximately at the level of T11. These tests were conducted in the AP direction. By comparison, the Viano tests were conducted with the specimen rotated thirty degrees. Therefore, the 15-cm-diameter flat disk struck the cadaver lateral to the abdomen, but through the center of gravity of the cadaver. The center of the disk initially contacted a point 7.5 cm below the xiphoid process. The Stalnaker data involved a variety of different test conditions. These data resulted from tests of different species (vervet, rhesus, and squirrel monkeys), in different impact locations (midabdomen, right side, left side), using different impactors (8x2-cm flat and 3x3-cm wedge).

A few of the tests in this study produced load-penetration responses shaped like those described by Stalnaker (rise-plateau-raise). This is also true of the Cavanaugh study. The tests from this study that produced this type of result were either high-speed, fixed-back, or upper abdomen impacts. It is hypothesized that the greater rib engagement observed in these tests contributed to this response shape. It is possible that the various-shaped impactors used in the Stalnaker study were large enough to involve a substantial portion of the rib cage, especially the ribs of the very small subjects used such as vervets and squirrel monkeys.

The upper abdomen tests, which involved substantial rib engagement, showed greater initial stiffness in both speed ranges (6 and 9 m/s) than did the counterpart midabdomen tests. In addition, there was less hysteresis observed in the upper abdomen response. Both the greater initial stiffness and subsequent greater restorative forces are likely related to the action of the ribs. The initial stiffness of the Viano data is likely related to rib engagement (impact regions positioned to contact ribs) and a broad impact surface (150-mm-diameter disk).

4.1.3 Seatbelt Tests

The seatbelt tests of this study produced an average initial stiffness of 120 kN/m. This is four times greater than the results of Miller (1989), and probably results from differences in the way the tests were conducted as well as differences in the test subjects. This study used a haversine penetration speed with respect to penetration, whereas the Miller study used a haversine penetration-time input. The Miller study used a yoke device to load the anterior of the abdomens of swine. The webbing material was initially in contact with a portion of the anterior surface of the abdomen, and the contact area increased as the penetration increased. The sides of the abdomen were not particularly constrained, although the backs of the animals were supported with a “V”-shaped fixture. In this study, the webbing was wrapped around the anterior and lateral aspects of cadaver abdomens. The contact area was quite large from the beginning of each test, and changed little throughout the tests. Also, the webbing restricted lateral motion of the sides of the abdomen, resulting in an additional stiffness increase. The Miller study investigated penetration speeds as high as 7 m/s and compressions as large as 70 percent, and some tests did produce injury in the swine. Typical penetration speed for this study was 3 m/s, although one test reached 5 m/s briefly. Compression typically did not exceed 30 percent.

The belt loading mechanism used in this study was designed for low-speed distributed loading by webbing material. The geometry of the belt was designed to optimize belt/abdomen interaction, and to minimize “roping” of the belt. This allowed accurate and repeatable measurement of the event. The webbing material was changed between

tests even though the Mercury strain gage showed minimal belt stretch occurred during the tests. Although submarining was not explicitly simulated, a good general loading of the abdominal contents was achieved. These tests provide insight into the belt-loading response of both the mid and lower abdomen of the human cadaver. In addition, a simplified and controllable method of testing the response of other human surrogates to belt loading has been developed and specified.

In the rigid-bar tests, the fixed-back condition resulted in load-penetration responses that eventually became less stiff than the free-back responses. The opposite is true for the belt tests. This is likely related to the constraint of the sides of the abdomen and the distributed loading during the belt tests. Either this combination resulted in very large stiffness (and limited compression) that dominated inertial effects in the fixed-back belt test, or increased lateral motion of abdominal tissues during the fixed-back rigid-bar tests played a role in the stiffness decrease compared to the free-back condition. The first hypothesis is most likely, as the initial stiffness of these belt tests was roughly twice that of the higher-speed rigid-bar tests, and the whole-body accelerations experienced during the belt tests were comparatively low.

4.1.4 Airbag Testing

Two types of midmount passenger airbags were used in three different deployment scenarios to create a generic penetration-time response of the human cadaver abdomen to airbag loading. All of the tests produced injury. Tests using a next-generation airbag and increased space between the airbag and abdomen prior to deployment produced fewer injuries. Because these airbags produced significant injury, they were good choices for use in developing a generic airbag response.

The generic penetration-time response was used to develop the surrogate airbag device. This device was designed to deliver low-mass, high-speed, distributed loading to the abdomen in an effort to simulate the punch-out phase of midmount airbag deployment. Initially, the airbag fabric unfurls in a tightly gathered roll and engagement of the airbag is largely limited to abdominal tissues. After continued inflation, the ribs and pelvis become involved. Only interaction with the abdominal tissues was of interest, so the surrogate airbag was designed to avoid contact with structures other than abdominal tissues. It was also desired to eliminate the dependence of the device on any specific airbag fabric, gas, or fold pattern. This device also facilitates the measurement of contact interaction load, which is not yet possible when using actual airbags. This approach resulted in a controllable, repeatable device that could be adapted for standardized testing.

The surrogate airbag response corridors exhibit an initial stiffness of approximately 1250 kN/m. This is roughly ten times that of the response from the belt tests. The surrogate airbag response looks very much like an impulse response. An impulse input is impossible to achieve, as it is characterized by infinitely large amplitude of infinitesimal duration. However, the surrogate airbag device does deliver an impulse-like input. This response could potentially be combined with system identification techniques to provide a better understanding and possibly a model of the gross response of the human cadaver abdomen. Some airbag-like injuries were obtained using this device, although they were relatively minor compared to those generated by the actual passenger airbag.

Appendix D contains a discussion of a possible method for compensating reaction loads measured during airbag interaction tests to obtain a better estimate of the actual contact interaction forces experienced by a subject. This method subtracts the unloaded (“free”)

response reaction load from the reaction load measured during subject interaction. Although the method still requires validation, comparison of this technique applied to test AA2 with the surrogate airbag corridor shows surprising similarity.

4.1.5 Data Normalization

The scaling method used in this study is the classic equal-stress/equal-velocity scaling described previously. This is a simple geometric similitude scaling based on ratios of mass. This may not be the most appropriate treatment for this data. The load-penetration responses show that the data were fairly tightly clustered prior to scaling for each type of test. However, the scaling was done to as an initial approach to bringing the data to a common basis and to compare the data from this study to the results of others. The data were scaled using 78 kg as the reference mass for application to dummy design. (The Hybrid III 50th-percentile male dummy has a total mass of about 78 kg.) The Cavanaugh data were scaled using this technique, but using 76 kg as the reference mass. The differences between the 76- and 78-kg scaled data are negligible.

The scaling method presented by Mertz et al. (1984) was not used. The Mertz method is a variation on equal-stress/equal-velocity scaling. The basic tenets of equal-stress/equal-velocity scaling are preserved by this method (constant density and modulus of elasticity), but the response of the subjects is mapped to a spring-mass model for calculation of the scaling factors for each response parameter. It is likely that the abdomen response should be characterized by a model containing viscous elements.

One procedure used by Mertz and others that may have application to further analysis of this data is the determination of effective mass of the struck tissue using the impulse-momentum technique. The effective struck mass is then used for scaling rather than the whole-body mass. The appropriate acceleration measurements were made during this study to facilitate this procedure. Further investigation, modeling, and mapping of the response data of this study are anticipated, but are beyond the scope of this report.

4.2 INJURY RESPONSE CONSIDERATIONS

Although the focus of this study primarily concerns the mechanical response of the human cadaver abdomen to various impact conditions, it is necessary to present the responses in some context relative to injury. In addition, the injury responses must be available even if the most appropriate model of the abdomen or most appropriate injury predictor has not been determined.

Because the most appropriate model of, and hence scaling for, the response of the abdomen has not been determined, and the potential predictors of injury were tabulated without being scaled by any method. However, the data needed for various methods of scaling have been cataloged in this report. The ASA injury predictor described by Cavanaugh et al. (1997) has not been evaluated, but is likely to be a component of subsequent analyses.

4.2.1 Laboratory Investigations

In a study of *in vivo* preparations of excised primate livers, Melvin et al. (1973) suggested that loading rate and pressure are important to injury. The various pressures measured throughout these tests have yet to be examined. Although there is no clear delineation of injury outcome with respect to various measured response parameters within specific

groups of tests, some trends emerge if all types of testing are considered together. For instance, injury levels are definitely higher for more severe impacts. This relates generally well to almost all of the calculated injury predictors (not scaled), especially when simply trying to separate serious injuries from mild injuries. No scaling or logistic regression analyses were performed in this cursory examination. This is because the appropriate model and mapping of the abdominal response is first needed so as to provide the most appropriate scaling of the data. It may be best to combine the data from this study with the data from other studies for this purpose. Initially, it would be easiest to combine these results with those of Cavanaugh et al. (1986). The preponderance of MAIS 4 outcomes from this current study additionally confounds the comparison of injury predictors to injury outcome. It is likely that AIS levels for the thorax and abdomen will be separated in future analyses, as rib fractures tended to be a dominant influence. In addition, the degree of AIS separation may extend to the level of individual abdominal organs. All of the data needed for independent coding of this nature are cataloged in the appendices of this report.

Ridella and Viano (1990) state that the viscous response (V*C) provides consistent prediction of abdominal injury above a certain speed. Slower speeds are better represented by compression, e.g. crushing injury. A method was developed for determining the transition speed at which V*C became more predictive of injury than compression. This speed was said to fall between 2.1 and 4.5 m/s. The results of this current study suggest that it is possible to achieve high V*C with little injury, and vice versa. The V*C levels for the surrogate airbag tests are generally higher than the V*C levels for the passenger airbag tests, yet the passenger airbag tests generated considerably more, as well as more serious, injuries. It would seem that the mechanism of loading might also play a role in injury outcome, requiring different approaches for different conditions. However, part of this result may be attributable to the low filter frequencies used in the calculation of V*C, which might not be appropriate for higher speed, short duration events.

Rouhana et al. (1986) tested the abdominal loading response of rabbits using a pneumatic impactor. The impact load was limited to either 1.0 or 1.5 kN using a Hexcel interface on the front of the impactor for some tests. The impact loads, penetration speeds (hence viscous response), and vascular pressures were all reduced in the force-limited impacts. However, the probability of injury did not change. It was noted that above 5 m/s, compression alone is not an adequate injury predictor, and speed must be considered as well. It was also noted that 1.0 kN was probably still too high to provide injury reduction. In a study of rigid-bar impacts to the abdomens of fixed-back swine, Miller (1989) concluded the Fmax, Cmax, and Fmax*Cmax were all reasonable predictors of injury greater than or equal to AIS 4 for lower speed tests. The results of this current study indicate that peak load may not be the best indicator of injury, and that the best predictor probably depends on the type of loading, and tissue, in question. For instance, the seatbelt tests produced no injuries to the abdominal organs, yet resulted in peak loads equal of those seen during the lower speed rigid-bar impacts, which did produce injuries to the abdominal organs. In this comparison, either Fmax*Cmax or V*C would be better predictors of injury. Both types of test generated rib fractures.

4.2.2 Field Investigations

In a review of NCSS data from January 1977 to November 1979, Bondy (1980) found abdominal injures to account for 2.6 percent of all injuries. However, abdominal injuries represented 14.6 percent of all severe injuries (AIS 3,4,5) found in towaway crashes. Severe injuries in turn accounted for 32 percent of all injuries to the abdomen. Liver

injuries were the most frequent, followed by an almost equal distribution of spleen and kidney injuries, and then injuries to the digestive system. For liver injuries for which a cause could be determined, 54 percent resulted from contact with the steering assembly and 11 percent resulted from contact with interior side structures. Similarly, 44 percent of spleen injuries resulted from contact with the steering assembly, as did 29 percent of kidney injuries. Kidney injuries were nearly equally induced by contact with interior side structures (26 percent) as by the steering assembly, but far fewer spleen injuries were caused by interior side structures (13 percent). Together, liver, spleen, and kidney injuries represented 74 percent of all abdominal injuries.

More recently, Elhagediab and Rouhana (1998) obtained results similar to those of Bondy in regard to injury incidence and location of injury. They examined NASS data collected from 1988 to 1994, and found injuries to the liver to be most prevalent, followed by the spleen and digestive system. However, injuries to the kidney were found less frequently (4 percent) than in the Bondy study (14 percent). When grouping all abdominal injuries together, the Bondy study found 51 percent of the injuries to have resulted from interaction with the steering rim, 48 percent due to interaction with other elements of the vehicle interior, and 1 percent from seatbelt interaction. In contrast, the Elhagediab and Rouhana numbers suggest 68 percent of all abdominal injuries result from contact with the steering rim, 14 percent from contact with vehicle interior components, and 14 percent were attributed to seatbelt interaction. This larger number of injuries associated with seatbelts was attributed to the increase in the use of seatbelts during the time between the two studies. It was also pointed out that the data did not reflect the serious head, neck, and chest injuries that were avoided by seatbelt use. However, in review of other studies, the authors stated that improper belt use was found to be a concern, and that it is a problem that could be addressed by education of belt wearers. The need for a biofidelic Hybrid III abdominal insert, one capable of measuring load and penetration, was emphasized.

In a study by Leung et al. (1982) it was found that the shoulder belt complicates submarining, and therefore abdominal injury, in only 10 percent of cases. This was attributed by the authors to poor belt geometry or improper slack conditions. It was noted that most cases of submarining were associated with impacts greater than 50 kph. To assess the potential for submarining using the Hybrid III dummy, a set of iliac crest pelvic force transducers was developed. A threshold of 800 N was suggested.

Asbun et al. (1990) reviewed 1400 cases of seatbelt-restrained occupants involved in motor-vehicle crashes. Only eight of these occupants were found to have sustained seatbelt-related injuries. The most common injuries were mesenteric tears, followed by ischemic loops of bowel. Ruptures of the digestive tract (ileum, jejunum, sigmoid colon) were found, as was the occasional splenic tear. One case involved rupture of the rectis abdominus muscle. In all cases, the injuries were said to present a clinical challenge, as they were difficult to diagnose because of few outward signs.

Many injuries commensurate with real-world crashes were observed during the rigid-bar tests. No kidney injuries were seen, but many impacts result from side impact, and perfusion of the kidneys is difficult. No injuries to the abdominal organs resulted from the seatbelt tests (several rib fractures were obtained), but belt injuries are seen relatively rarely in the field. It is unlikely that a single existing injury predictor will produce the best estimate of injury probability. It may be that a combination of predictors or an entirely new predictor is needed. Miller (1989) and Cavanaugh et al. (1986) made similar observations.

4.3 APPLICATION CONSIDERATIONS

The results of this study have direct application to the design and development of improvements to the Hybrid III dummy. These results further the understanding of the response of the human cadaver abdomen to various loading conditions and should be useful for improving the kinematics of the Hybrid III dummy. Although these experiments were limited to frontal impact, efforts to improve frontal dummy performance using these data may aid in improving side-impact performance, as it is reasonable to assume that an abdomen that performs mechanically similarly to these frontal tests might also perform as a human cadaver abdomen would in side impact.

The absence of an acceptable model for the human cadaver abdomen notwithstanding, and similarly the best method of injury prediction yet to be determined, any surrogate matching the responses of these tests should be considered a good representation of the human cadaver abdomen. In addition, these data should also prove useful in computer modeling applications. Finally, the devices and methods that have been developed and described as part of this study could be easily adapted to standardized forms of evaluating and calibrating human surrogates.

REFERENCES

Asbun, HJ; Irani, H; Roe, EJ; Bloch, JH (1990) Intra-abdominal seatbelt injury. *Journal of Trauma*, 30:2, 189-193.

Augenstein, JS; Digges, KH; Lombardo, LV; Perdeck, EB; Stratton, JE; Quigley, CV; Malliaris, AC; Byers, PM; Nunez, DB; Zych, GA; Andron, JL; Craythorne, AK; Young, PE (1995) Chest and abdominal injuries suffered by restraint occupants. *Advances in Occupant Protection Technologies for the Mid-Nineties*, pp. 37-44. SAE Paper No. 950657. Society of Automotive Engineers, Warrendale, PA.

Beckman, DL; McElhaney, JH; Roberts, VL; Stalnaker, RL (1971) *Impact Tolerance – Abdominal Injury.* NTIS No. PB204171.

Bondy, N (1980) Abdominal injuries in the national crash severity study. *National Center for Statistics and Analysis Collected Technical Studies, Vol. II: Accident data Analysis of Occupant Injuries and Crash Characteristics*, pp. 50-80. National Highway Traffic Safety Administration, Washington, DC.

Cavanaugh, JM; Nyquist, GW; Goldberg SJ; King, AI (1986) Lower abdominal tolerance and response. *Proceedings of the 30th Stapp Car Crash Conference*, pp. 41-63. Society of Automotive Engineers, Warrendale, PA.

Cavanaugh, JM; Zhu, Y; Huang, Y; King, AI (1993) Injury and response of the thorax in side impact cadaveric tests. *Proceedings of the 37th Stapp Car Crash Conference*, pp. 199-221. Society of Automotive Engineers, Warrendale, PA.

Duma, S.M.., Rudd, R.W., Kress, T.A., and Porta, D.J. (1997) *A pneumatic airbag deployment system for experimental testing.* SAE Paper No. 970124. Society of Automotive Engineers, Warrendale, PA.

Elhagediab, AM; Rouhana, SW (1998) Patterns of abdominal injury in frontal automotive crashes. *Proceedings of the 16th International Technical Conference on Experimental Safety Vehicles*, pp. 327-337. National Highway Traffic Safety Administration, Washington, DC.

Eppinger, RH (1976) Prediction of thoracic injury using measurable experimental parameters. *Proceedings of the 6th International Technical Conference on Experimental Safety Vehicles*, pp. 770-780. National Highway Traffic Safety Administration, Washington, DC.

Hill, JR; Mackey, GM; Morris, AP (1994) Chest and abdominal injuries caused by seat belt loading. *Accident Analysis and Prevention*, 26:1, pp. 11-26.

Hill, JR; Mackay, GM; Morris, AP, Smith, MT; Little, S (1992) Car occupant injury patterns with special reference to chest and abdominal injuries caused by seat belt loading. *Proceedings of the 1992 International IRCOBI Conference on the Biomechanics of Impacts*, pp. 357-372. IRCOBI, Bron, France.

Huelke, DF; Mackey, GM; Morris, AP (1993) *Intraabdominal injuries associated with lap-shoulder belt usage*. SAE Paper No. 930639. Society of Automotive Engineers, Warrendale, PA.

Leung, YC; Terriere, C; Lestrelin, D; Got, C; Guillon, F; Patel, A; Hureau, J (1982) Submarining injuries of 3-point belted occupants in frontal collisions – Description, mechanisms and protection. *Proceedings of the 26th Stapp Car Crash Conference*, pp. 173-205. Society of Automotive Engineers, Warrendale, PA.

Melvin, JW; Stalnaker, RL; Roberts, VL (1973) Impact injury mechanisms in abdominal organs. *Proceedings of the 17th Stapp Car Crash Conference*, pp. 115-126. Society of Automotive Engineers, Warrendale, PA.

Mertz, HJ (1984) *A procedure for normalizing impact response data*. SAE Paper No. 840884. Society of Automotive Engineers, Warrendale, PA.

Miller, MA (1989) The biomechanical response of the lower abdomen to belt restraint loading. *Journal of Trauma*, 29:11, 1571-1584.

Nusholtz, G; Kaiker P (1994) Abdominal response to steering wheel loading. *Proceedings of the 14th International Technical Conference on Enhanced Safety of Vehicles*, pp. 118-127. U.S. Department of Transportation, Washington, DC.

Ridella, SA; Viano, DC (1990) Determining tolerance to compression and viscous injury in frontal and lateral impacts. *Proceedings of the 34th Stapp Car Crash Conference*, pp. 349-356. Society of Automotive Engineers, Warrendale, PA.

Rouhana, SW; Jedrzejczak, EA; McCleary, JD (1990) Assessing submarining and abdominal injury risk in the Hybrid III family of dummies: Part II Development of the small female frangible abdomen. *Proceedings of the 34th Stapp Car Crash Conference*, pp. 145-173. Society of Automotive Engineers, Warrendale, PA.

Rouhana, SW; Ridella, SA; Viano, DC (1986) The effect of limiting impact force on abdominal injury: A preliminary study. *Proceedings of the 30th Stapp Car Crash Conference*, pp. 65-79. Society of Automotive Engineers, Warrendale, PA.

Rouhana, SW; Viano, DC; Jedrzejczak, EA; McCleary, JD (1989) Assessing submarrining and abdominal injury risk in the Hybrid III family of dummies. *Proceedings of the 33rd Stapp Car Crash Conference*, pp. 257-279. Society of Automotive Engineers, Warrendale, PA.

SAE J1460-1 Report (1995) *Human mechanical impact response characteristics-dynamic response of the human abdomen*. Society of Automotive Engineers, Warrendale, PA.

Stalnaker, RL; McElhaney, JH; Snyder, RG; Roberts, VL (1971) *Door crashworthiness criteria*. NTIS No. PB203721.

Stalnaker, RL; Ulman MS (1985) Abdominal trauma--Review, response, and criteria. *Proceedings of the 29th Stapp Car Crash Conference*, pp. 1-16. Society of Automotive Engineers, Warrendale, PA.

Trollope, ML; Stalnaker, RL; McElhaney, JH; Frey, CF (1973) The mechanism of injury in blunt abdominal trauma. *Journal of Trauma*, 13:11, 962-970.

Viano, DC; Lau, IV; Asbury C; King, AI; Begeman, PC (1989) Biomechanics of the human chest, abdomen, and pelvis in lateral impact. *The 33rd Annual Proceedings for the Advancement of Automotive Medicine*, pp. 367-382. AAAM, DesPlaines, ILL.

APPENDIX A

AUTOPSY RESULTS FROM RIGID-BAR IMPACTS GI13-GI18

Cadaver	Gender	Age	Stature (cm)	Mass (kg)	Test	MAIS
28682	Male	87	173	73	GI3	4
Configuration	Free-back, rigid-bar impact, 6 m/s range, midabdomen					
Region	**Injuries**					
Rib fx	Bilateral 7, 8, 9					
Diaphragm	Left lateral tear, 9 cm					
Liver	Vertical tear of right lobe, 7.5 cm anteriorly/9 cm posteriorly					
Intestine	Tear of cecum, 10 cm					

Cadaver	Gender	Age	Stature (cm)	Mass (kg)	Test	MAIS
28764	Female	93	165	58	GI4	4
Configuration	Free-back, rigid-bar impact, 6 m/s range, midabdomen					
Region	**Injuries**					
Rib fx	Bilateral 6, 7, 8, 9, 10					
Liver	Right capsule tear, 11 cm anteriorly Tear of left lobe, 3.5 cm posteriorly					

Cadaver	Gender	Age	Stature (cm)	Mass (kg)	Test	MAIS
28800	Female	65	164	61	GI5	4
Configuration	Free-back, rigid-bar impact, 6 m/s range, upper abdomen					
Region	**Injuries**					
Rib fx	Bilateral 2, 6, 7, 8, 9, 10; Individual left 5					
Liver	Oblique central tear, 5.5 cm Oblique tear of left lobe, 9 cm					

Cadaver	Gender	Age	Stature (cm)	Mass (kg)	Test	MAIS
28838	Male	85	165	91	GI6	3
Configuration	Free-back, rigid-bar impact, 6 m/s range, midabdomen					
Region	**Injuries**					
Rib fx	Bilateral 8, 9; Individual left 6, 7					
Diaphragm	Left lateral tear, 2.5 cm					
Liver	Vertical tear of inferior edge, 25 cm					
Spleen	Capsule tear, 12 cm					
Heart	Vertical tear of anterior right ventricle, 2cm Transverse tear of posterior left ventricle, 1.5 cm					
Other	Tear of the left R8/R9 intercostal space, 12 cm					

Cadaver	Gender	Age	Stature (cm)	Mass (kg)	Test	MAIS
28879	Male	74	181	77	GI7	3
Configuration	Free-back, rigid-bar impact, 9 m/s range, midabdomen					
Region	**Injuries**					
Rib fx	Bilateral 8, 9, 10; Left 7					

Cadaver	Gender	Age	Stature (cm)	Mass (kg)	Test	MAIS
28889	Male	71	182	64	GI8	4
Configuration	Free-back, rigid-bar impact, 9 m/s range, midabdomen					
Region	**Injuries**					
Rib fx	Bilateral 6, 7, 8, 9, 10; Individual left 5, right 3					
Liver	Tear of inferior edge, 3 cm Multiple lacerations of left lobe posteriorly (6x5.5 cm) Multiple lacerations of right lobe inferiorly (7.5x3.5 cm)					

Cadaver	Gender	Age	Stature (cm)	Mass (kg)	Test	MAIS
28942	Female	85	155	51	GI9	5
Configuration	Free-back, rigid-bar impact, 6 m/s range, midabdomen					
Region	**Injuries**					
Rib fx	Bilateral 2, 3, 4, 5, 6, 7, 8, 9, 10					
Liver	Vertical tear of right lobe of liver, 5.0 cm Transverse tear of right lobe of liver, 3.5 cm Transverse tear of right lobe of liver, 3.2 cm Multiple irregular tears of right lobe of liver posteriorly (3.5 cm x 2.5 cm)					
Spleen	Transverse tear of anterior edge, 2.2 cm					

Cadaver	Gender	Age	Stature (cm)	Mass (kg)	Test	MAIS
29084	Male	64	180	65	GI10	5
Configuration	Free-back, rigid-bar impact, 9 m/s range, upper abdomen					
Region	**Injuries**					
Rib fx	Bilateral 3, 4, 5, 6, 7, 8, 9; Individual left 5, 6, 8, 9, 10 Bilateral costal cartilage 7, 8					
Diaphragm	Left posterior tear, 4 cm Left posterior tear, 3.5 cm Separation from right lobe of liver, 7 cm					
Liver	Horizontal tear, 4.5 cm connecting to vertical tear, 3.5 cm Capsule tear Falciform ligament tear					
Spleen	Complete tear, 8 cm					
Other	Sternum fx between R3/R4 under mount					

Cadaver	Gender	Age	Stature (cm)	Mass (kg)	Test	MAIS

29115	Male	74	168	75	GI11	5
Configuration	Free-back, rigid-bar impact, 6 m/s range, upper abdomen					
Region	**Injuries**					
Rib fx	Bilateral 4, 5, 6, 7, 8, 9; Individual left 3, 11, right 7 Right costal cartilage 7					
Diaphragm	Left posterior tear, 4 cm Left posterior tear, 3.5 cm Separation from right lobe of liver, 7 cm					
Liver	Falciform ligament tear					
Spleen	Transfer tear, 7 cm, 1.2-cm deep					
Other	Sternum fx between R2/R3 above mount					

Cadaver	**Gender**	**Age**	**Stature (cm)**	**Mass (kg)**	**Test**	**MAIS**
29425	Male	80	175	88	GI12-18	4
Configuration	Fixed-back, rigid-bar impact, 3-9 m/s range, midabdomen					
Region	**Injuries**					
Rib fx	Bilateral 6, 7, 8, 9, 10, 11; Individual left 5, 10					
Other	Postmortem contusion (dried liquefied fat) anterior abdominal wall, 10x6.5 cm, 9 cm above umbilicus Postmortem contusion, 8 x 10 cm, at level of 5^{th}, 6^{th}, 7^{th} costal cartilage					

APPENDIX A

APPENDIX B

AUTOPSY RESULTS FROM SEATBELT TESTS CB1-CB6

Cadaver	Gender	Age	Stature (cm)	Mass (kg)	Test	MAIS
29311	Female	77	168	53	CB1/CB2	4
Configuration	Fixed-back and free-back seatbelt loading, midabdomen					
Region	**Injuries**					
Rib fx	Bilateral 7, 8, 9, 10; Individual right 2, 11, left 4, 5, 9, 10					

Cadaver	Gender	Age	Stature (cm)	Mass (kg)	Test	MAIS
29116	Male	78	170	52	CB3/CB4	3
Configuration	Free-back seatbelt loading, mid and lower abdomen					
Region	**Injuries**					
No injuries	No injuries					

Cadaver	Gender	Age	Stature (cm)	Mass (kg)	Test	MAIS
29131	Male	88	156	82	CB5/CB6	0
Configuration	Free-back seatbelt loading, mid and lower abdomen					
Region	**Injuries**					
No injuries	No injuries					

APPENDIX B

APPENDIX C

AUTOPSY RESULTS FROM PASSENGER AIRBAG AND SURROGATE AIRBAG TESTS AA1-AA3, AS1-AS6

Cadaver	Gender	Age	Stature (cm)	Mass (kg)	Test	MAIS
29613	Male	83	160	73	AA1	4
Configuration	Free-back, midmount standard passenger airbag, midabdomen contact					
Region	**Injuries**					
Rib fx	Bilateral 2, 3, 4, 5, 6, 7, 8					
Diaphragm	Right lateral tear, 8.5 cm					
Liver	Transverse tear of visceral surface at midline, 2.5 cm Tear of anterior hilum, 1.5 cm Interrupted tear of left lobe at diaphragmatic attachment, 3 cm Separation of gall bladder bed, 2 cm					
Intestine	Tear of transverse colon serosa, 12 cm					
Mesentery	Multiple tears, 4 cm, 2.5 cm, 2.5 cm, 5 cm					
Peritoneum	Tear right inguinal oblique, 12 cm Tear right posterior lower quadrant, 10 cm Tear left descending mesocolon, 6.5 cm Tear left lower quadrant oblique 6.5 cm					
Heart	Tear of pericardial sac, 8.5 cm					
Other	Sternum fx between R4/R5 Tear of the parietal plura, left intercostal space, 7.5 cm Intervertebral disk separation, T12/L1					

Cadaver	Gender	Age	Stature (cm)	Mass (kg)	Test	MAIS
29739	Male	64	166	64	AA2	4
Configuration	Free-back, midmount next-generation passenger airbag, midabdomen contact					
Region	**Injuries**					
Rib fx	Bilateral 4, 5, 6, 7, 8, 9; Individual left 3, 10 Bilateral costal cartilage, 6; Right 3					
Liver	Vertical tear of anterior surface left of midline, 13 cm, 2-cm deep Vertical tear of inferior diaphragmatic surface of right lobe, 3.5 cm, 5.5 cm into gall bladder bed Superficial vertical tears anterior surface of right lobe, 2.5 cm upper, 2 cm lower, 5 cm lateral					
Spleen	Superficial tear, 4 cm					
Intestine	Tear of transverse colon, 4 cm complete					
Mesentery	Multiple tears, 4 cm, 2.5 cm, 2.5 cm, 5 cm					
Other	Sternum fx between R4/R5					

Cadaver	Gender	Age	Stature (cm)	Mass (kg)	Test	MAIS
29787	Female	79	169	64	AA3	3
Configuration	Free-back, midmount next-generation passenger airbag, midabdomen 5 cm space					
Region	**Injuries**					
Rib fx	Individual left 6, 7, 8, 9, 10					
Diaphragm	Left diagonal tear, 8 cm					
Spleen	Capsular tear of diaphragmatic surface, 5 cm					
Other	Sternum fx between R2/R3 (partial)					

Cadaver	Gender	Age	Stature (cm)	Mass (kg)	Test	MAIS
29490	Female	68	163	57	AS1-4	2
Configuration	Free-back and fixed-back surrogate airbag impacts, midabdomen					
Region	**Injuries**					
Liver	Transverse tear posterior left lobe 4 cm from free edge/11 cm from midline, 6 cm (0.9-cm deep) Transverse tear posterior left lobe 6.5 cm from free edge/11 cm from midline, 6 cm (1.2-cm deep) Vertical tear below insertion of Teres ligament, 3 cm (0.8-cm deep) Vertical tear anterior left lobe 6 cm from free edge/3.5 cm from midline, 2 cm (1.5-cm deep) Diagonal tear anterior right lobe 4 cm from free edge/6.5 cm from midline, 7 cm (1.8-cm deep) Vertical tear anterior right lobe 6 cm from free edge/11.5 cm from midline, 1 cm (0.2-cm deep) Vertical tear anterior right lobe 6 cm from free edge/13 cm from midline, 4.5 cm (0.7-cm deep)					

Cadaver	Gender	Age	Stature (cm)	Mass (kg)	Test	MAIS
29566	Male	86	173	79	AS5	1
Configuration	Fixed-back surrogate airbag impact, midabdomen					
Region	**Injuries**					
Other	Postmortem contusion of the abdominal wall 4 cm below the umbilicus, 15x5 cm					

Cadaver	Gender	Age	Stature (cm)	Mass (kg)	Test	MAIS
29491	Male	72	178	81	AS6	2
Configuration	Free-back and fixed-back surrogate airbag impacts, midabdomen					
Region	**Injuries**					
Rib fx	Bilateral 10, 11; Individual right 12 (severe osteoporosis)					
Liver	Capsular tear left side of gall bladder bed, 2 x 1 cm Diagonal tear posterior right lobe at inferior edge of gall bladder bed, 2.5 cm (0.5-cm deep)					

APPENDIX D

ESTIMATION OF REACTION LOADS DURING AIRBAG-ABDOMEN INTERACTION

Five tests (HA1-5) were conducted using midmount passenger airbags and two heavy bags (punching bags) strapped together to form one 91-kg mass. The objectives were to examine the effect of the module door on the reaction loads measured by load cells mounted behind the airbag, and to examine the differences in reaction load measurement for contact and 5-cm spacing conditions. The results of these tests show that the module door has negligible effect on reaction load for this airbag system. The results also show that a potentially better estimate of load experienced by the abdomen can be obtained by conducting the deployments with the abdomen in contact with the airbag module. When the airbag is not initially in contact with the abdomen, the airbag quickly deployed around the abdomen rather than into it. Also, an initial gap between the airbag and abdomen resulted in reaction loads prior to contact with the abdomen. Both of these phenomena produced reaction loads that are influenced predominantly by the inertia of the rapidly deploying airbag fabric instead of due to forces applied to the abdomen. These tests suggested a possible method of improving the estimate of abdominal loading by subtracting the unloaded ("free") reaction-load response of the airbag from the reaction loads measured during a test where the airbag module was in direct contact with the abdomen at the time of deployment. The results of these tests also lead to conducting a subsequent test with a cadaver using a contact configuration and no module door. During these tests it was found that this particular airbag prototype reached speeds of 80 m/s during unimpeded deployment.

Figure D-1 shows the reaction load measured for airbag test AA2, and the unloaded (nothing in front of the deploying airbag) "free-response" of the same type of airbag used for AA2. The initial slopes of the curves are aligned. The free-response force-time curve was subtracted from the measured reaction load-time history. The reaction load-time history and the adjusted reaction load-time history are shown in Figure D-2, along with the abdominal penetration from test AA2. Adjusting the reaction load in this way has the effect of removing the forces generated by the rapidly accelerating airbag fabric and gasses. The adjusted load and abdominal penetration begin at nearly the same time, whereas the unadjusted load begins much before the abdominal penetration.

Figure D-3 compares the adjusted load-penetration response for test AA2, to the newly developed surrogate airbag corridor. Although the load from AA2 extends substantially beyond the corridor as the airbag inflates and interacts with the entire abdomen and much of the thorax, comparison of the initial stiffness is quite good. This suggests that this method of adjusting airbag reaction loads for abdominal contact conditions may have some validity, and reinforces the idea that the surrogate airbag device closely approximates the initial phase of such a deployment. However, a significant amount of additional testing is required to prove the validity of this technique.

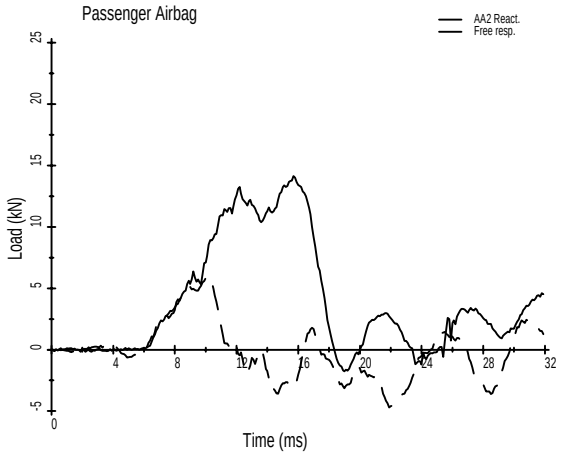

FIGURE D-1. Representative passenger airbag deployment reaction load (Test AA2), with and without a subject positioned in front of the airbag (free response).

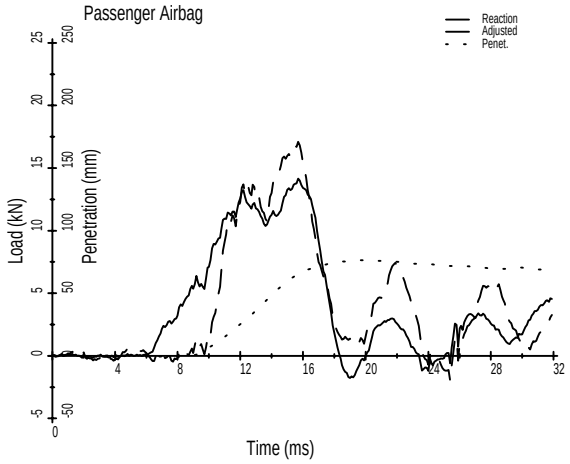

FIGURE D-2. Representative reaction load (Test AA2) and "corrected" reaction load (load minus free response), and cadaver abdominal penetration (Test AA2).

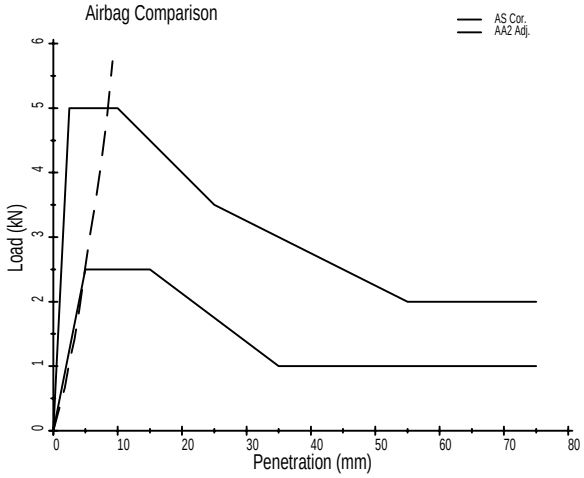

FIGURE D-3. Corrected AA2 load-penetration response compared to the surrogate airbag corridor.